STUDIES ON
FLUIDIZATION IN TAPERED VESSELS

A DISSERTATION
Submitted in partial fulfilment of the
requirements for the award of the Degree
of
MASTER OF ENGINEERING
in
CHEMICAL ENGINEERING
(EQUIPMENT & PLANT DESIGN)

by

ASHOK KUMAR

DEPARTMENT OF CHEMICAL ENGINEERING
UNIVERSITY OF ROORKEE
ROORKEE
September, 1978

C E R T I F I C A T E

Certified that the thesis entitled 'FLUIDIZATION IN TAPERED VESSELS' which is being submitted by Shri Ashok Kumar in partial fulfilment of the requirements for the award of the degree of MASTER OF ENGINEERING IN CHEMICAL ENGINEERING (Equipment and Plant Design) of the University of Roorkee, Roorkee is a record of candidate's own work carried out by him under the supervision and guidance of the undersigned. The matter embodied in this thesis has not been submitted for the award of any other degree or diploma.

This is further to certify that he has worked for a period of about Eight months from January 5, 1978 for preparing this thesis at this University.

(YOGESH CHANDRA)
Reader

(N.GOPAL KRISHNA)
Professor and Head
Department of Chemical Engineering
University of Roorkee, Roorkee.

Dated: Sept. 26, 1978.

ABSTRACT

Studies in gas-solid fluidisation have been conducted in tapered vessels with circular cross section using glass-beads, crushed bauxite, baryte and calcite of particle sizes ranging from 460 to 977 microns. Tapered vessels of cone angles 20°, 30°, 45° and 90° were used. Pressure drop data were obtained in the fixed bed region, at the onset of fluidisation and in the expanded bed zone. Pressure peak which is characteristic of tapered vessels, has been observed. The correlations for pressure peak and minimum fluidising velocity have been proposed as

$$\left[\frac{D_p \rho_g Q_{mf}}{\mu_g}\right] = 0.1359 \left[\frac{P_g(\rho_s - \rho_g) g D_p^3 \rho_g^3}{\mu_g^2}\right]^{0.613} \left[\tan\frac{\alpha}{2}\right]^{0.93} \left[\frac{L}{D_o}\right]^{1.20}$$

Minimum fluidising velocity in a tapered vessel can be predicted within a deviation of $\pm 20\%$ and for pressure peak as

$$\left(\frac{\Delta P}{\Delta P_{net}}\right) = 0.102 \left(\frac{D}{D_o}\right)^{-0.94} \left(\tan\frac{\alpha}{2}\right)^{-0.80} \left(Rop_{mf}\right)^{0.51}$$

It was found that nearly 90% data vary between the range of $\pm$ 20%.

Effect of mechanical stirrer was studied in fluidisation in tapered vessels. Fluidization characteristics like minimum fluidising velocity and pressure peak were observed to be affected by the presence of mechanical stirrer. The power required for particle separation was observed to be reduced when stirrer was used. Dimensionless correlation

is proposed for predicting the minimum fluidizing velocity in tapered beds with stirrer

$$\left[\frac{D_p \rho_g G_{mf}}{\mu_g}\right] = 0.3119 \left[\frac{\rho_g(\rho_p-\rho_g)\, g\, D_p^3\, \rho_g^3}{\mu_g^2}\right]^{0.163} \left[\tan\frac{\alpha}{2}\right]^{0.008} \left[\frac{h}{L}\right]^{0.23} \left[\frac{R^2 \Pi \rho_g}{\mu_g}\right]^{-0.103}$$

which can predict minimum fluidizing velocities well within ± 20% deviation from those of experimental values. The following correlation is proposed for predicting the pressure peak in tapered beds with stirrer

$$\left(\frac{\Delta P}{\Delta P_{max}}\right) = 0.139 \left[\frac{\Pi}{D_0}\right]^{-0.90} \left[\tan\frac{\alpha}{2}\right]^{-0.57} \left[Re_{mf}\right]^{0.180} \left[\frac{h}{L}\right]^{-0.41} \left[\frac{R^2 \Pi \rho_g}{\mu_g}\right]^{-0.088}$$

Theoretical values predicted were compared with the experimental data and deviation was found to be ± 20% .

ACKNOWLEDGEMENTS

The author wishes to express his deep sense of gratitude and indebtedness to Dr.N.Gopal Krishna, Professor and Head and Shri Yogesh Chandra, Reader, Chemical Engineering Department, University of Roorkee, Roorkee, for their constant guidance, interest and encouragement at all stages of the work presented in this thesis.

My sincere thanks are due to Dr.N.J.Rao, Reader, Chemical Engineering Department for his inspiration and valuable suggestions during the preparation of this thesis.

My thanks are also due to staff of various laboratories and fabrication section for their help and cooperation. I would like to thank Shri C.P.Mathur of Fluid Particles Mechanics Lab. for his help during experimentation.

Last but not the least I am thankful to all those who have helped me during the course of this work.

C O N T E N T S

NOMENCLATURE

d_p	Particle diameter, cm
D	Bed diameter at top of packed section, cm
D_o	Bed diameter at distributor, cm
G	Acceleration due to gravity, cm/sec^2
G_o	Gravitational constant
h	Depth of the stirrer in the bed, cm
L	Height of the fixed bed, cm
n or N	Speed of stirrer, rpm
P	Length of the stirrer blade, cm
$\triangle P$	Pressure drop across the bed, gm/cm^2
R	Radial distance from the apex of the cone to the top of the bed, cm
R_o	Radial distance from the apex of the cone to the top of the bed, cm
Re_{mf}	Reynolds number at minimum fluidizing conditions
U_{mf}	Minimum superficial fluidizing velocity, cm/sec
W_{net}	Buoyant weight of material in the bed, gms
α	Apex angle degrees
ϵ	Bed porosity
ρ_o	Density of solid material, gm/cm^3
ρ_g	Density of fluid (air), gm/cm^3
μ_f	Fluid viscosity, poise
$\triangle \pi$	Pressure peak

CHAPTER-I

LITERATURE REVIEW

C H A P T E R - I

LITERATURE REVIEW

1.1 Introduction to Fluidization Phenomenon

Fluidization is the operation by which fine solids are transformed into a fluid like state through contact with a gas or liquid.

Phenomenon of fluidization can be explained by passing a fluid upward through a bed of find particles. At a low flow rate, fluid merely percolates through the void spaces between stationary particles. This is a fixed bed.

With increase in flow rate, particles move apart and few are seen to vibrate and move about in restricted regions. This is the expanded bed.

At a still higher velocity a point is reached, when the particles are all just suspended in the upward flowing gas or liquid. At this point the frictional force between a particle and fluid counterbalances the weight of the particle, the vertical component of the compressive force between adjacent particles disappears, and the pressure drop through any section of the bed about equals the weight of fluid and particles in that section. The bed is considered to be just fluidized and is referred to as an incipiently fluidized bed or a bed at minimum fluidization.

In liquid solid systems an increase in flow rate above minimum fluidization usually results in a smooth, progressive expansion of the bed. Gross flow instabilities are damped

is small in diameter contains a deep bed of solids, the bubbles may grow until they fill the entire cross-section of the vessel. Successive bubbles then travel up the vessel, separated by the slugs of the solid particles. Operation is erratic and unstable.

1.2 Advantages and Disadvantages of Fluidisation for Industrial Operations

The fluidised bed has both desirable and undesirable characteristics. These can be brought out as follows:

1.2.1 Advantages

1) The smooth, liquid like flow of particles allows continuously automatically controlled operations with ease of handling.

2) The rapid mixing of solids leads to nearly isothermal conditions throughout the reactor or vessel, hence the operation can be controlled simply and reliably.

3) The circulation of solids between two fluidised beds makes it possible to transport the vast quantities of heat produced or needed in large reactors.

4) It is suited to large scale operations.

5) Heat and mass transfer rates between gas and particles are high when compared with other modes of contacting.

6) The rate of heat transfer between a fluidised bed and an immersed object is high, hence heat exchangers with in fluidised beds require relatively small surface area.

1.2.2. Disadvantages

1) The difficulty to describe the flow of gas, because of its large deviations from plug flow and the bypassing of solids by bubbles, represents an inefficient contacting system.

2) Friable solids are pulverised and entrained by the gas, they then must be replaced.

3) Erosion of pipes and vessels from abrasion by particles can be serious.

4) For non-catalytic operations at high temperatures, the agglomeration and sintering of fine particles can necessitate a lowering in temperature of operation, reducing the reaction rate considerably.

1.3 Application of Fluidization

Fluidization has been put to many applications in petroleum, chemical and metallurgical industries as given below:

1) Fluidised beds provide a more efficient, convenient and economical way for transportation, drying and heating.

2) It is widely used for mixing the powdery . . materials

intimately by circulation in the storage bins.

3) Fluidised beds have been used extensively for heat exchange, in both physical operations and chemical processes because of their unique ability to rapidly transport heat and maintain uniform temperature.

4) The technique is used for coating of plastic materials on metal surfaces.

5) Fluidised beds have been used for drying and sizing of powdery materials.

6) It is also used for particle growth and condensation of sublimate materials.

7) Fluidised beds have been frequently applied for absorption purposes.

8) A number of synthetic reactions are carried out in the fluidised bed. The main reason for choosing the fluidised bed in preference to the fixed bed for these solid catalysed gas phase reactions is the demand for strict temperature control of the reaction zone.

9) Many chemical compounds are prepared in the fluidised bed only.

10) The breakdown of hydrocarbons into lower molecular weight materials (cracking reactions) and their synthesis into low molecular weight materials (reforming reactions) are carried only in the fluidised beds for having - (a) better control of temperature

(these are exothermic reaction) (b) carbon deposits are removed, (c) larger quantities are handled successfully.

11) These beds are used in thermal cracking.

12) The applications are made in the carbonization and gasification of coal.

13) The use has been made in the calcining clinkering and drying of clay materials.

14) It is used in the roasting of ores.

1.4 Fluidization in Cylindrical Vessels with Constant Area of Cross Section

A typical variation of pressure drop with superficial velocity in cylindrical vessel is shown in Fig. 1.1 where the logarithm of the pressure drop is plotted against the logarithm of fluid velocity. The straightline from A to B represents the variation of the pressure drop through the bed with fluid velocity during the period of fixed bed operation when no motion of the particles occurs. Fluid merely percolates through the void spaces between stationary particles and the pressure drop is given by Kozeny-Carman equation. Eventually the pressure drop equals the force of gravity on the particles (point B). Bed has become unstable now and a minor movement and readjustment of the particles in the bed begin to take place to offer the maximum cross sectional area for flow. Bed expands slightly with the grains still in contact. The change in the structure of the

bed produces a deviation from the simple relationship between the pressure drop and velocity shown in the section A to B. Instability of the bed continues as the velocity is increased, until at point C the loosest arrangement of particles in contact is established. With any further increase in the velocity of flow, some of the particles in the bed are no longer in permanent contact with one another and become continuously agitated. This point 'C' is known as the point of incipient fluidization. At this point of fluidization, the bed begins to expand with increasing fluid velocity thus more and more particles loosing contact with others. At point 'D' fluidization is complete and all the particles are in motion. From point 'C' to 'D' there is sudden though slight fall in the pressure drop due to unlocking of particles from each other. Further increase in fluid velocity beyond point 'D' causes slight increase in pressure drop which is required to overcome the increase in frictional losses between fluid, suspended solids and walls of the container. Particles move more and more vigorously, swirling about and travelling in random directions. The contents of the tube strongly resemble a boiling liquid.

The linear velocity of the fluid between the particles is much higher than the velocity in the space above the bed consequently nearly all the particles drop out of the fluid above the bed. Even with vigorous fluidization only the smallest grains are entrained in the fluid and carried away. As fluid velocity is further increased the porosity of the bed increases causing the bed to expand. Entrainment

becomes appreciable, then severe, then complete. At point 'E' all the particles have been entrained in the fluid, the porosity approaches unity, and the bed as such has ceased to exist. The phenomenon then becomes that of the simultaneous flow of two phases. From point 'D' to 'E' and beyond pressure drop rises with fluid velocity very slowly.

1.5 Comparison between Fluidization in Cylindrical and Tapered Vessels

When fluidization is carried out in the vessel of constant cross section, solid mixing rate in longitudinal direction is quite severe in case of gas-solid beds. This will result in to the attrition of particles, a phenomenon which should be avoided in certain cases. Due to attrition particles become smaller and smaller in size and as the linear velocity remains same in cylindrical vessel, a flow rate fixed for a particular size of particles will cause entrainment of smaller particles. In case of reactions like cracking or reforming in fluidized beds, the solids used is generally the costly catalyst and therefore it is important to avoid attrition.

The back mixing of solids, as created by severe solids mixing rate is supposed to be reduced if fluidization is either carried out in long narrow tube with high L/D ratios or in multistages. If fluidization is carried out in deep beds with higher L/D ratios, it is quite non-uniform. Since in such beds pressure drop is quite substantial and being a compressible fluid gas goes on expanding as it passes through

the bed thus there is a consequent rise in its velocity. When the upper portion of the bed is made to fluidise satisfactorily, lower portion of the bed is not fluidised at all while when the gas velocity at the base corresponds to U_{mf} value i.e. bottom is made to fluidize satisfactorily, the upper part of the bed is slugging badly. This is serious specially for uniformly sized particles where it is difficult to fluidise the bed at all.

If fluidization is carried out in tapered/conical vessels with such a taper that superficial gas velocity is more or less constant around U_{mf} value as the gas rises up through the bed, the whole bed can be fluidised uniformly throughout its height. This is only true for deep bed of dense materials or with uniformly sized coarse/dense materials. Solids mixing rate which was severe in cylindrical beds is reduced in such vessels, still retaining other desirable important properties of the fluidised bed. This may be possible because of the major portion of the gas which flows through the bed as large practically solid-free-gas bubbles while the solids are suspended by a relatively slow moving gas.

Another advantage of tapered vessels is that mixed sized particles can be fluidised simultaneously, the fines or lighter being at the top while the coarser or dense at the bottom with intermediates in between.

1.6 Fluidization in Tapered Vessels

When fluidization is carried out in a conical apparatus

tapering downward, there is a considerable pressure peak at the limit of stability. This peak is much larger than pressure at the onset of fluidisation in a vessel with constant cross section and is due to the conical form of the bed. In some experiments the pressure drop before the onset of fluidisation was two to three times greater than the value established after the limit of stability. This phenomenon was explained by the observation that in conical vessels the bed passes in to the fluidized state only after attainment of fluidization in upper portions. Since at this time the gas velocities in the lower and middle parts of the bed are considerably greater than the critical fluidization velocities, the pressure drop in the stationary bed portions increases rapidly as compared to that at the limit of stability in a cylindrical bed of the same height. Immediately beyond the limit of stability the pressure drop falls to approximately the usual theoritical value, equal to the product of the bed density and its height regardless of the bed configuration.

As the fluid velocity is further increased the pressure drop does not remain constant but in contrast to the cylindrical bed, begins to fall. The reason[10] being that as the fractional voidage 'ε' increases, the bed height increases slowly than its volume such that the product $L(1-\varepsilon)$ goes on decreasing.

Experiments have revealed that in conical vessels the point of incipient fluidisation is not as clear cut as in cylindrical vessels. Further, as the upward flow of fluid

through the fixed bed of particles in a conical vessel is increased, a compacting effect is noted. This effect is seen well below the point of incipient fluidisation. The explanation appears to be that the particles near the bottom of the bed experience a substantial upward drag force, due to relatively large velocity of the fluid near the bottom of the bed. The upward drag force will be greater than the force of gravity on the particles. At the same time, the velocity near the top of the bed is relatively low, so the force of gravity on particles near the top of the bed is greater than the upward drag force exerted on them by the fluid. The resultant force on the particles near the bottom is upward and on the particles near the top is downward. The bed height reaches a minimum value due to this compaction effect and a minimum observed porosity is thus realised.

1.7 Fluidisation of Solids by Gas Stream

In case of gas fluidisation solids mixing rate in vertical direction is quite severe in cylindrical vessels. Drotz[1] and Rowe[2] stated that the mixing rate increases with increasing fluid velocity. Most of the mixing of solids in the fluidized bed occurs by the bulk movement of the solid material. Such bulk movements are generally associated with eddies in liquid fluidised beds and with bubbles in gas fluidized beds. This severe backmixing in longitudinal direction causes back mixing of solids in the bed. Levey et al[3] while studying the residence time distribution of solid particles in a continuous gas-solids fluidised bed observed

that solids behave approximately as the contents of a continuously stirred tank or perfectly mixed vessel. Spread of residence time is very wide indeed. This wide range may be reduced if fluidization is to be carried out either in multistages[4] with a narrow range of solids residence time in each with overall countercurrent flow of gas and solids or to make the bed very deep in relation to its diameter in order to make mixing of the upper and lower regions of the bed more difficult. This, however, causes non-uniformity of bed loading to poor quality of fluidization.

If deep beds are employed in cylindrical vessels the pressure drop between bottom and top of the bed, which is needed for the gas flow to occur through the packed bed and to overcome the resistance offered by the solids and thus fluidize the bed, becomes substantial. The gas velocity increases considerably due to the gas expansion as gas passes through the bed from bottom to top. This means that if the gas velocity is only made sufficient to give normal fluidising conditions in the upper regions of the bed, the base of the bed will be completely stagnant. If the gas velocity is increased until fluidization occurs immediately above the support plate at the bottom of the bed, then the bed is violently agitated at the top, and the solids may be carried away.

It was originally suggested by Ohme and Furukawa[5] for liquid fluidized beds, that a possible solution to the problem of smooth operation of deep beds would be to increase

the bed cross-sectional area upwardly through the bed so that increase in gas volume could be accomodated i.e. to construct a bed tapering towards its base. The first such bed was constructed and operated by Lovey et al (1950)[3] for the conversion of uranium oxide to uranium Fluoride by fluidization with hydrogen Fluoride gas mixed with Nitrogen as a diluent to moderate the reaction and carry away the heat. Spheriodally shaped UO_3 particles in size range 20-40 mesh were fluidized in 4-5" cylindrical tubes and for bed heights above two feet. Fluidization was highly uniform with violent bed eruptions and inefficient contacting of the fluid. Fluidization was observed to begin at the upper surface of the bed and proceeded downward through the bed as the inlet gas velocity was raised and when the gas velocity was sufficient to fluidise the bed completely, the upper portion of the bed was slugging. Since the superficial gas velocity increases considerably along the bed owing to the expansion of the gas (the pressure drop being approximately 1.75 psi/ft) the bubble volume increases steadily along the bed, and thus deeper the bed and higher the particle density or size, the greater is the tendency of the bed to slug. In deep beds a much higher gas velocity is required to fluidise the whole bed, than that for a shallow bed. To compensate for the gas expansion and thus to have constant superficial gas velocity along the bed, a suitable tapered tube was employed. The angle of taper for the ideally fluidised bed was calculated out for conical vessel as follows

$$\alpha = \tan^{-1} (a_b \rho_D / 2 P_b)$$

Here a_b is the distance normal to the longitudinal axis of the column between tapered sides. ρ_D is the bulk density of the bed and P_b is the pressure at the inlet of the bed.

In such beds it was noted that pressure drop-flow rate curves are like those ordinarily encountered in fluidized beds. All the properties such as flow-ability of the bed and good heat and mass transfer were retained and the bed expansion was reduced, gas bubble formation was largely suppressed and most important of all, the amount of mixing between the upper and lower regions of the bed was reduced. It was noted that at velocities substantially above the minimum, bubbles do appear but they do not coalesce and in many cases disappear before reaching the upper surface.

According to Romero and Johanson[6] the reduced rate of mixing of solids is caused by operating close to the minimum fluidizing velocity.

Sutherland[7] carried out mixing rate experiments using a tapered bed of copper shot, sized between 30-52 mesh. Nickel spheres of the same size and density acted as a tracer material which were added (about 1% of the bed weight) from the top while the bed was under just fluidization state and then increasing the gas velocity to the desired values. Qualitatively, the curves of Nickel concentration against time for various probe locations showed that vertical solid mixing rate was greatly reduced in the tapered beds. It

tapered fluidised beds of rectangular cross-section. Gas velocities up to 110% above the minimum fluidising velocity and bed height to diameter ratios of 8 and 16 to 1 were employed. It was noted that at gas velocities close to minimum fluidising velocity axial solids mixing rate was quite low.

1.8 Pressure Drop in Conical/Tapered Vessels

At the minimum fluidising velocity the bed is acting as a fluid and the pressure drop is calculated by

$$\Delta P = L(1-\varepsilon)(\rho_p - \rho_g)\, G/G_0 = \frac{W_{bed}}{A_{avg}}$$

Here L is bed height, W the bed weight and A_{avg}, the average cross-sectional area of the bed.

Gel'perin[10] derived the following theoretical expression for pressure peak, ΔP assuming that the gas motion was quite laminar in the bed and fluidising gas was uniformly distributed over the bed cross-section throughout the bed height.

$$\Delta P_{Theo} = \frac{D_0}{2\tan(\frac{\beta}{2})}\left(\frac{D}{D_0} - 1\right)\left(K U_{1-\varepsilon}\frac{D}{D_0} - \rho_{gas}\right)$$

where $U_{1-\varepsilon}$ is superficial fluid velocity at minimum fluidisation and K is the constant in the equation, relating the resistance of the fixed bed and the fluid velocity as,

$$\Delta P = K U_g H_{bed}$$

H_{sta} and $\rho_{s\,ta}$ are the height and bulk density respectively of the stationary bed and U_2 is superficial fluid velocity at the base.

Another theoretical equation as derived by Gel'perin et al[11], valid for laminar flow is, for fixed bed pressure drop,

$$\Delta P = K U_0 (D/D_0 - 1)\, 2 \tan \alpha/2$$

The coefficient K is given as

$$K = C \mu/2 D_p^2$$

The value of constant C was not given by the authors. Basakov and Gel'perin[11] presented the following equation

$$\Delta P = C_1 A \frac{R_0}{R} (R-R_0) U_0 + C_2 B \left(\frac{R_0}{3R^3}\right) (R^3-R_0^3) U_0^2$$

The coefficient C_1 and C_2 are the proposed values of Ergun that is, $C_1 = 150$ and $C_2 = 1.75$,

$$A = (\mu/\alpha_0 D_p^2)(1-\varepsilon^2)/\varepsilon^3 \text{ and } B = (\rho_2/\alpha_0 D_p)(1-\varepsilon)/\varepsilon^3$$

Actually the assumption for uniform distribution of gas is far from practice. For this purpose they proposed[10]

$$\Delta P = F (D/D_0, \tan \alpha/2)$$

which is true for a single gas solid-system.

The recent experimental studies made by Parkins[12] has revealed that conical or tapered vessel data can be correlated

by equation of Ergakov if new values of coefficients C_1 and C_2 were substituted for the cylindrical vessel coefficients, even where the apex angle is small. They substituted axial distance Z for radial distance R and $\varphi_s D_p$ for D_p, thus introducing a particle shape factor. Constant C_1 and C_2 are strongly dependent on the geometry of the bed. As pointed out by Barkas the pressure drop to be used above is ΔP_f, only due to frictional losses in the bed and is given by the relation

$$\Delta P_f = \Delta P_{Gross} - \Delta P_{static}$$

i.e. subtracting from the Gross value the 'static head value' for the bed. This fact can be verified from Bernoullie's equation.

Studies[15] were conducted for air-solids fluidization in the tapered vessel with circular cross section. A correlation for the pressure peak was proposed as

$$\Delta n_{expt} = 2.59 \, (D/d_0)^{2.55} \, (\tan \alpha/2)^{-1.19}$$

Δn is pressure peak, D is the dia of the upper limit of the bed and d_0 is the dia of lower limit of column in cms, α is the cone angle in degrees.

In liquid fluidization studies in tapered vessels with taper ranging from 10 to 120°,[14] coarse size solid particles (Glass beads, Quartz and Calcite) have beenused for studying the effect of physical properties of the material, bed weight and cone angle on fluidization characteristics. Following

dimensionless correlation was proposed for pressure peak,

$$\left(\frac{\Delta P}{\Delta P}\right) = 1.02\times10^{-3} \left(\frac{H}{D_0}\right)^{1.63} \left(\tan\frac{\theta}{2}\right)^{-1.25} \left(\frac{D_p G_{mf}}{\mu}\right)^{0.712}$$

It was observed that smooth fluidization occured only in lower cone angles i.e. 10, 15 and 20°. In 30 and 45° cones particle movement was similar to that observed in spouted beds. In over tapered vessels of cone angles greater than 45° and upto 120° mixing of solids was confined to the central part of the bed only with thick particle layer remaining stationary at the vessel wall.

Studies[15] were conducted in gas-solid fluidization in tapered vessels using spherical glass beads and crushed particles bauxite and calcite and cone angles ranging from 10° to 90°. Gas solid contact was observed to be more efficient with larger particle sizes and smaller cone angles (10° to 30°). For smaller sized particles and larger cone angles the fluidization was limited to a central core with layers of particles remaining stationary near the walls. Slugging was predominant in smaller angle cones while in larger angle cones it was completely absent. A correlation was obtained as

$$\left(\frac{\Delta H}{\Delta P_{net}}\right) = 3.48\times10^{-2} \left(D/D_0\right)^{0.497} \left(\tan\frac{\theta}{2}\right)^{-0.08} \left(R_{opmf}\right)^{0.426}$$

1.9 Object of the Present Work

In a cylindrical vessel, cross sectional area of flow is constant throughout and the entire bed fluidises at the

same time. Pressure drop before fluidisation i.e. in fixed bed region increases with fluid velocity and after fluidisation, it becomes almost constant. In a tapered vessel, area of cross section increases from bottom to the top and thus the linear velocity of fluid decreases in the upward direction. A bed of solid particles in a tapered vessel is said to be in fluidising state when the entire bed is fluidised. But it has been observed that when the lower part of the bed is in fluidising state, the upper part still remains in fixed bed condition and pressure drop increases with increase in air flow rate. Pressure drop continues to rise till the entire bed gets fluidised and pressure drop values are quite higher in tapered beds. A pressure peak i.e. maximum pressure drop value is also observed in case of tapered vessel. Therefore, power requirements for pumping will be substantially high in such cases.

If the upper part of the bed is slightly disturbed by some method keeping the lower part of the bed in fluidising state, the entire bed can be fluidised at lower air flow rate and thus pressure drop and pressure peak values may be reduced. One of such methods is to make use of stirrer. The present studies include the use of a stirrer for disturbing the upper part of the bed and to study its effect on air flow rate, pressure drop and pressure peak values. A comparative study has been made on power consumption and power saving with stirrer.

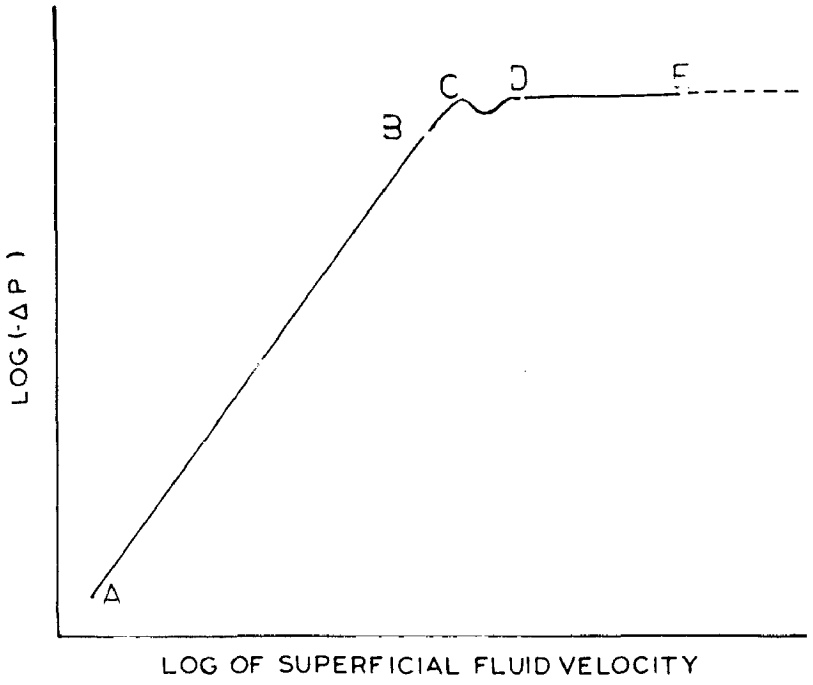

FIG. 1·1 PRESSURE DROP VS FLOW RATE CURVE IN A CYLINDRICAL VESSEL

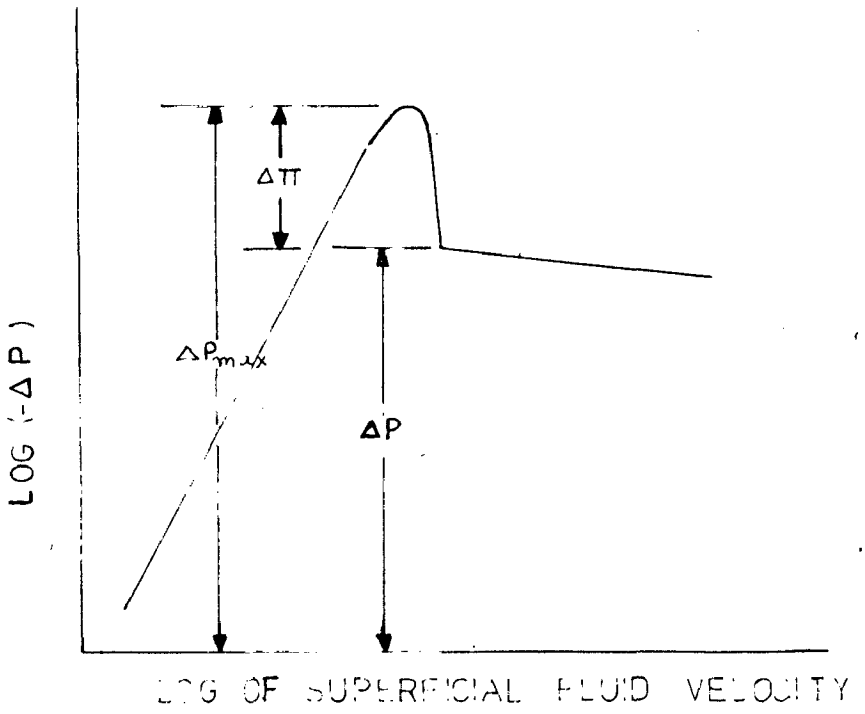

FIG 1·2 PRESSURE DROP VS FLOW RATE CURVE IN A TAPERED VESSEL

was also shown that this effect is found only with deep beds of dense materials and only at flow rates less than 30% above the minimum fluidizing velocity to bed heights greater than 2.0 feet. Sutherland also observed like Levey et al[3] that particle movements and bubbling in untapered beds began at the top of the bed as the air rate was increased and that by the time particle movement was observed at the base, the top was slugging violently. In tapered beds, it was observed that the fluidization at lower velocities was more even with bubbles appearing in the lower as well as in the upper part of the bed. Once the flow rate reached 1.2-1.3 times of U_{mf}, however, the whole bed began to slug and appeared very similar to the corresponding non-tapered beds. In contrast to cylindrical beds, a more precise value of U_{mf} was obtained for tapered beds. Thus main effect of tapering would appear to be the stabilising of the just fluidized state throughout the depth of the bed.

Later work of Sutherland and Rowe[8] was directed at elucidating the mixing mechanism. A bed of copper shots was overlaid with a Nickel shot layer and fluidised for varying periods. It was concluded that without bubbles in the bed there was no mixing and the range of flow rates in which the bed was fluidised but bubbles were absent was very narrow. Only in this range could the bed be operated as a continuous plug flow reactor.

Littman[9] also compared the solids mixing rates for dense particles (-140 + 200 mesh copper) in straight and

CHAPTER-II

EXPERIMENTAL SET-UP AND PROCEDURE

CHAPTER - II

EXPERIMENTAL SET-UP AND PROCEDURE

2.1 Experimental Set-up

The experimental set-up used for the study of the fluidization in tapered vessels consists mainly of a tapered fluidizing vessel, rotameter and manometer. The air inlet cone and calming section are used to get uniform distribution of air while entering the column. The schematic diagram of the experimental set up is shown in Fig. 2.1. Plate 2.1 shows the photograph of the experimental assembly.

2.1.1 Calming Section and Air Inlet Cone

The calming section has been provided at the bottom portion of the tapered column to have uniform distribution of air. Raschig rings were filled in a section of 4.0 cms diameter to check the channeling of the inlet air. The air inlet is an inverted conical section with 12 mm bottom diameter and 4.0 cms top diameter. The total height of conical section is 10 cms. For the line fittings 12 mm mild steel socket is welded at the bottom part and a 10 cms diameter flange at the top portion. Four holes with 10 mm diameter have been drilled in the flange at 7.0 cm pitch circle diameter. Wire mesh is provided to support the raschig rings at the junction of the air inlet cone and calming section. Both air inlet cone and calming section are shown in Fig.2.2.

2.1.2 Distributor or Grid Plate

The quality of bubbling fluidisation is strongly influenced by the type of gas distributor used. For few air inlet openings the bed density fluctuates appreciably at all flow rates (20 to 50% of mean value), though more severely at high flow rates the bed density varies with height and gas channeling becomes severe. For many air inlet openings the fluctuation in bed density is negligible at low air flow rates but again becomes appreciable at high flow rates and becomes uniform throughout. Also, the bubbles are smaller, and air-solid contacting is more intimate with less channeling tendencies:

Contacting is superior when consolidated porous media or plates with many small orifices are used. The grid plate used in the experiment is shown in Fig.2.3. The holes are drilled in an area of 4.0 cms diameter. The thickness of the plate is 5 mm. The total diameter of the plate is 10.0 cms. The details of the plate are as follows

Material	-	Aluminium
Thickness	-	5 m.m.
Holes size	-	1.5 m.m.
Pitch	-	4.5 m.m.

2.1.3 Flow Measurement Device

The flow rate of air was measured with the help of rotameter which gives the flow rate in normal litres per hour. Two rotameters were used to cover the entire flow

range of air. The lighter particles and the smaller bed heights need only lesser flow rates while the heavier particles and larger bed heights require higher air flow rates. Rotameters having the flow range 0 to 12000 and 0 - 35000 MLPH were used.

2.1.4 Tapered Columns

The tapered column is the main part of the apparatus. The taper angles of the columns taken for the experiment are 20°, 30°, 45° and 90°. The bottom diameter of the column has been chosen arbitrarily as 4.0 cms. This diameter equals the diameter of the calming section. The 10 cms flange is welded at the bottom of the column for the necessary fittings. In order to observe the fluidization visually in the tapered column, the transparent perspex slit of 25 m.m. width has been fixed in the column. Plate 2.2 shows the photograph of the tapered columns of different cone angles.

2.2 Stirring

The main part of the present set up is an electrically driven stirrer. This is used to disturb the bed to see its effect on air flow rate and pressure drop value. The stirrer used is very simple in construction. This is located in the centre of the fluidising vessel and its position can be changed in upward and downward direction by moving it on its shaft. It has two flat blades. The speed of the stirrer is adjusted by the variac transformer. An ammeter and

voltmeter were employed in the line to note the current and voltage for power computation. A voltage stabilizer is used to eliminate the voltage fluctuations. Plate 2.3 shows the photograph of the stirrer used. The stirrer is shown in Fig. 2.4 and its specifications are given below:

Length of the shaft	=	505 m.m.
Diameter of the shaft	=	7 m.m.
Type and number of blades	=	flat, two
Length of a blade	=	33 m.m.
Width of a blade	=	12 m.m.
Thickness of a blade	=	2 m.m.
Maximum speed of stirrers	=	120 rpm
H.P.	=	1/20
Current	=	0.6 amp
Voltmeter range	=	0 - 300 volt
Ammeter range	=	0 - 0.5 amp and
		0 - 1 amp

2.3 Operating Procedure

The air drawn from the compressor and regulated through a surge tank at the required pressure, is supplied to the fluidizing column at a uniform pressure. The fluctuations caused by the compressor were eliminated completely by using surge tank. The air is fed to the main equipment through a pressure regulator which gives the constant air supply. This air from the pressure regulator is passed through the rotameter, where the air flow rate is measured. This measured air is then fed to the main fluidizing column. In between the

air inlet cone and the main column the calming section has been provided which ensures the proper distribution of the air through the bed. The Raschig ring packing have been provided in the calming section. At the top of the calming section the grid plate and a brass wire cloth are fixed. Thus before passing through the column the air is properly distributed. The stirrer was fixed at the top of the fluidizing column. The stirrer can be moved in upward and downward directions. The pressure difference for the bed is measured with the help of manometer. The pressure difference is directly measured as the difference of cms of water. Thus we, ΔP (cms of water) = ΔP (gms/cm^2), directly get the pressure difference in gm/cm^2.

2.4 Calibration of Rotameter

The rotameters were pre-calibrated with the help of dry gas flow meter. The air at different flow rates through the rotameter indicates the flow in litres per hour. The same air from the rotameter exit is allowed to pass through the gas flow meter. The gas flow meter gives its actual readings according to the air flowrate. Sufficient data have been taken at different flow rates and both the rotameters are thus calibrated using standard gas flow meter. The calibration curves are shown in Fig. 2.5 and Fig. 2.6.

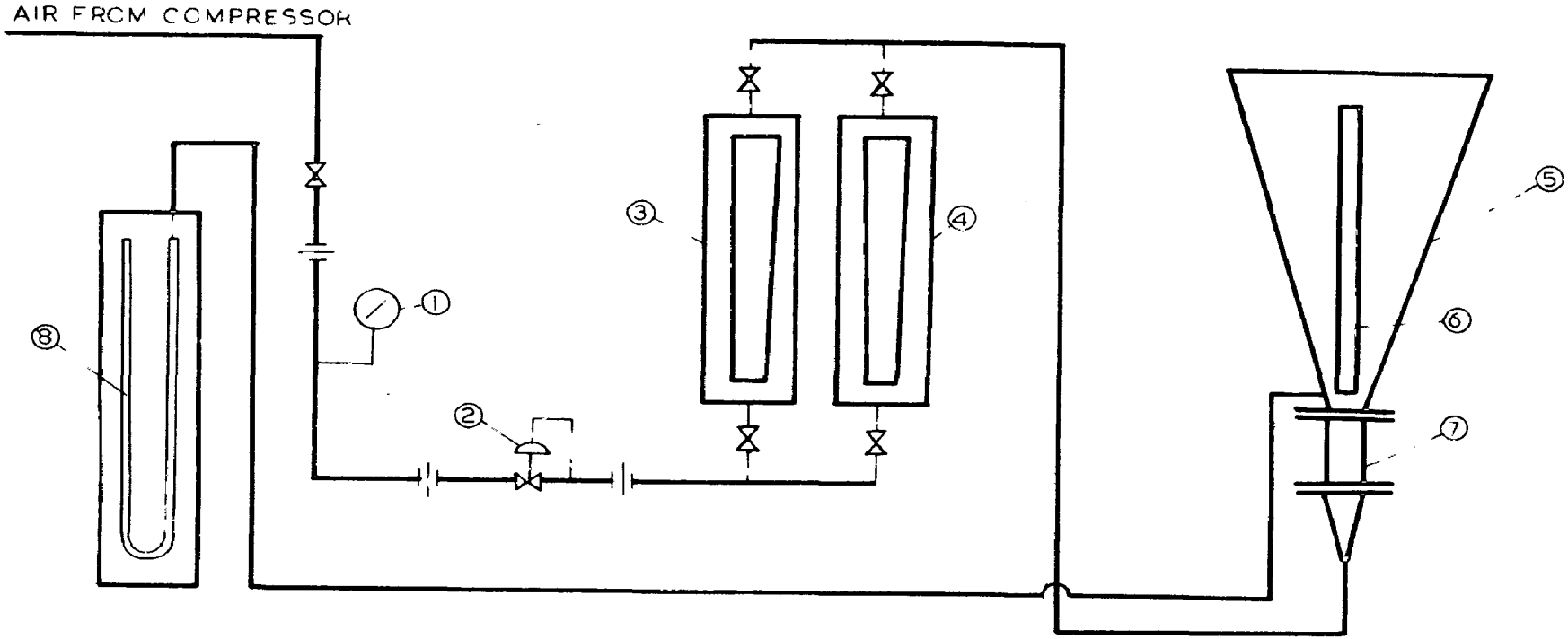

1 - PRESSURE GAUGE
2 - PRESSURE REGULATOR
3,4 - ROTAMETERS
5 - FLUIDIZING COLUMN
6 - PERSPEX SLIT
7 - CALMING SECTON
8 - MANOMETER

FIG. 2.1 SCHEMATIC DIAGRAM OF EXPERIMENTAL SET UP

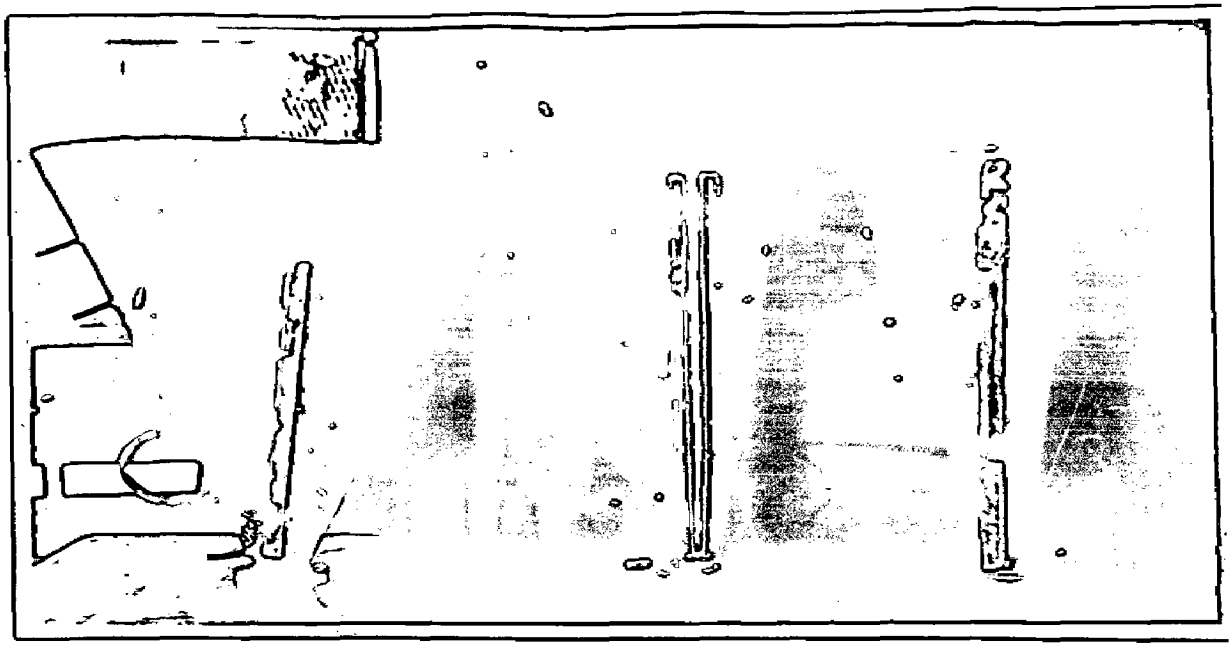

PLATE 2.2 FLUIDIZING COLUMNS

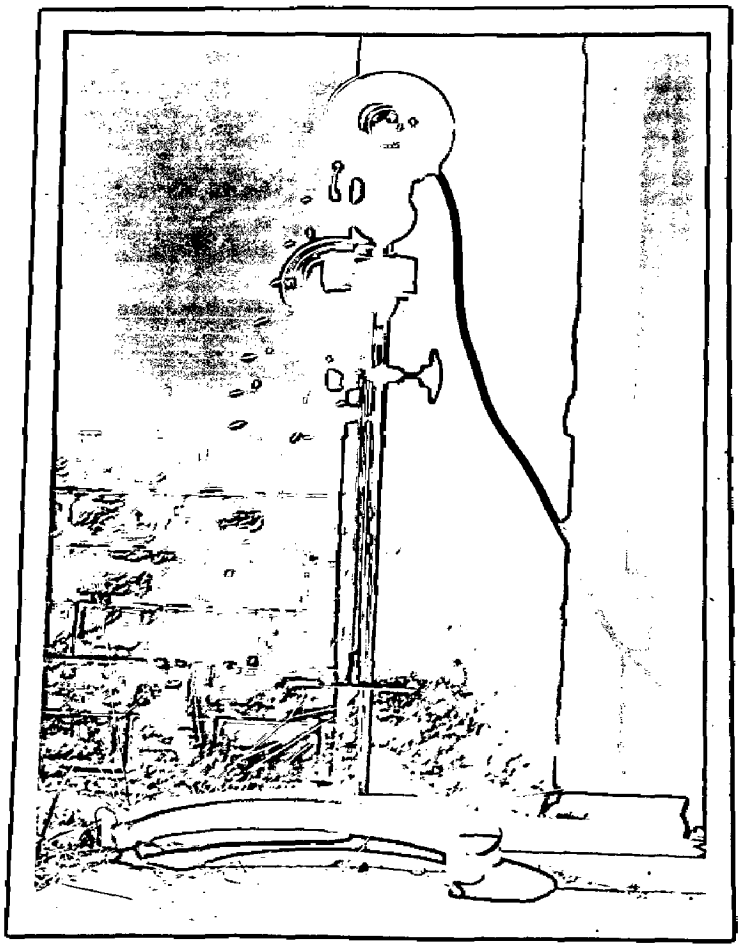

PLATE 2.3 STIRRER

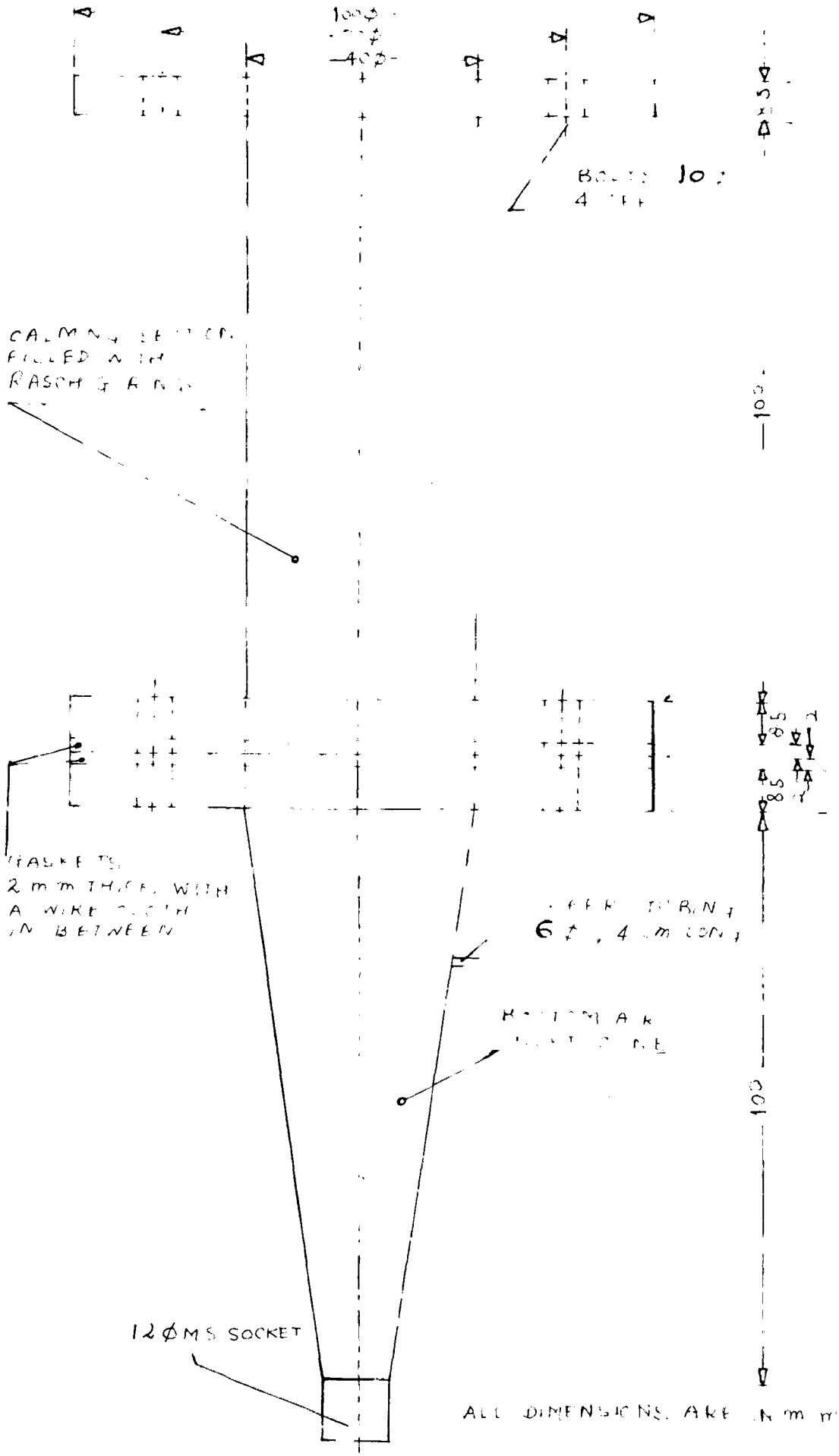

FIG 2.2 DETAILS OF CALMING SECTION AND AIR INLET CONE

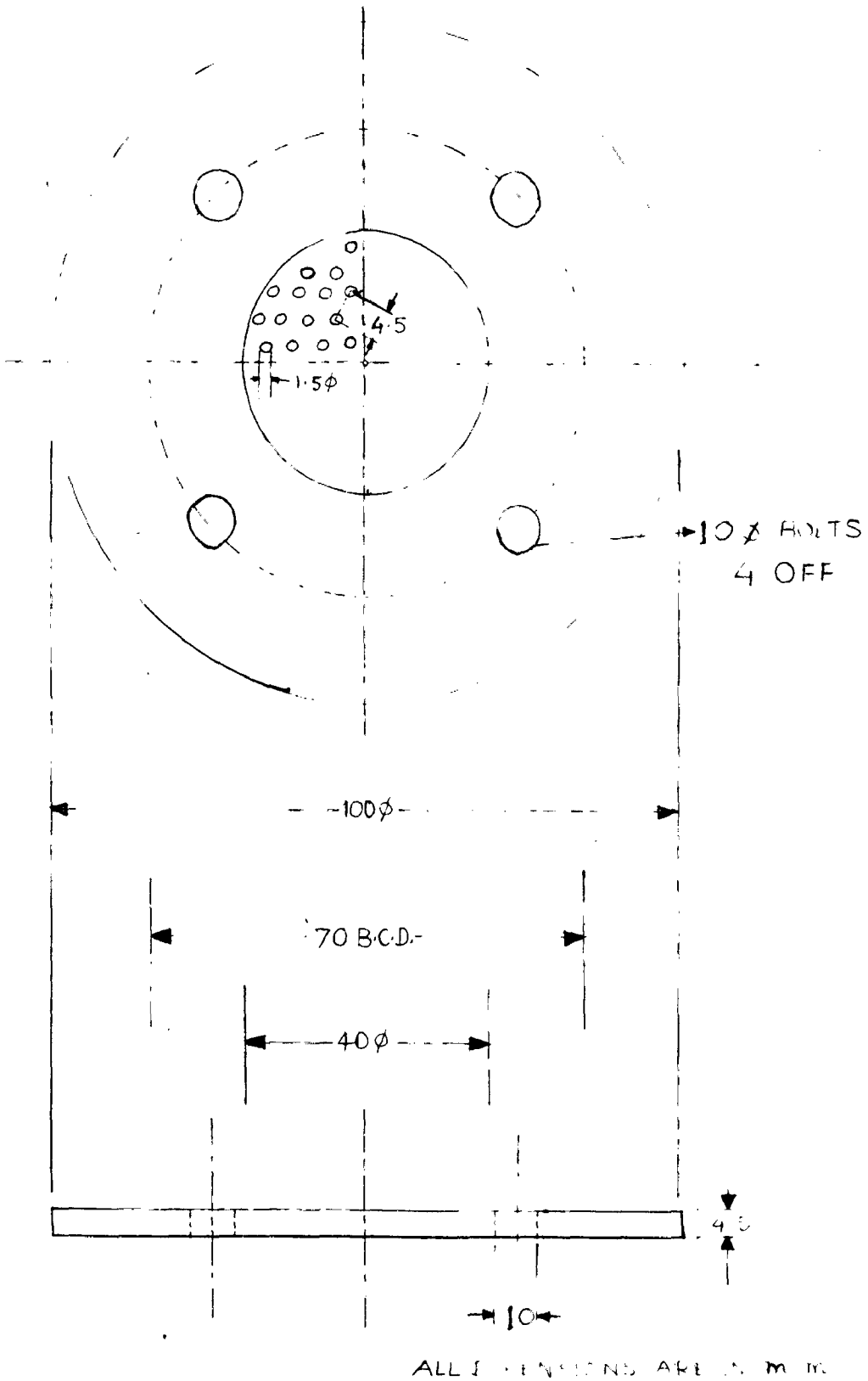

FIG 2.3 DETAILS OF GRID PLATE

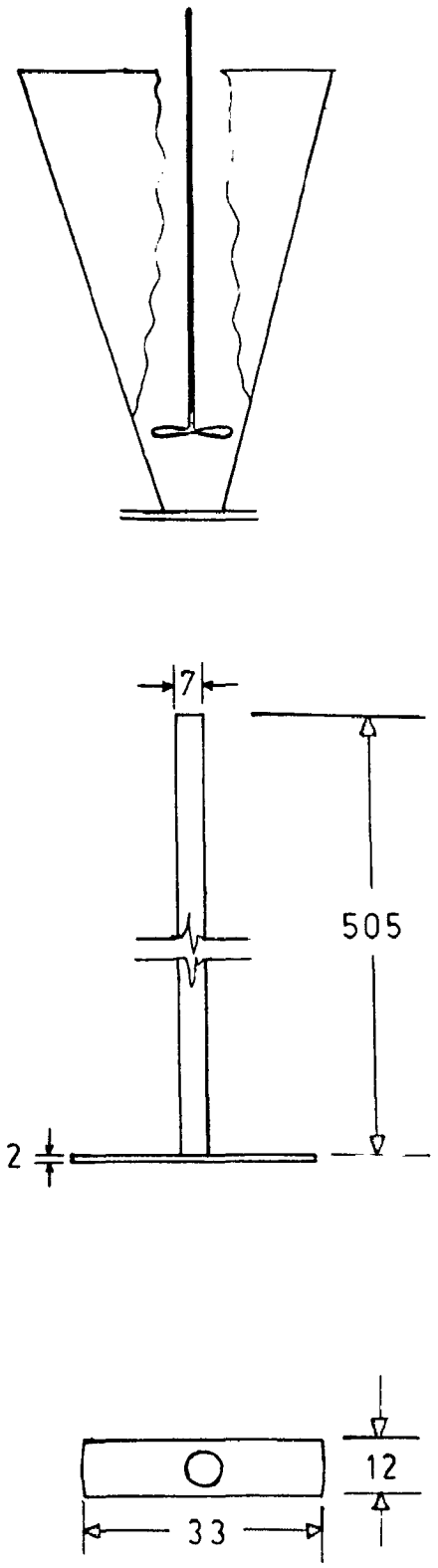

All dimensions are in mm.

FIG 2.4 STIRRER

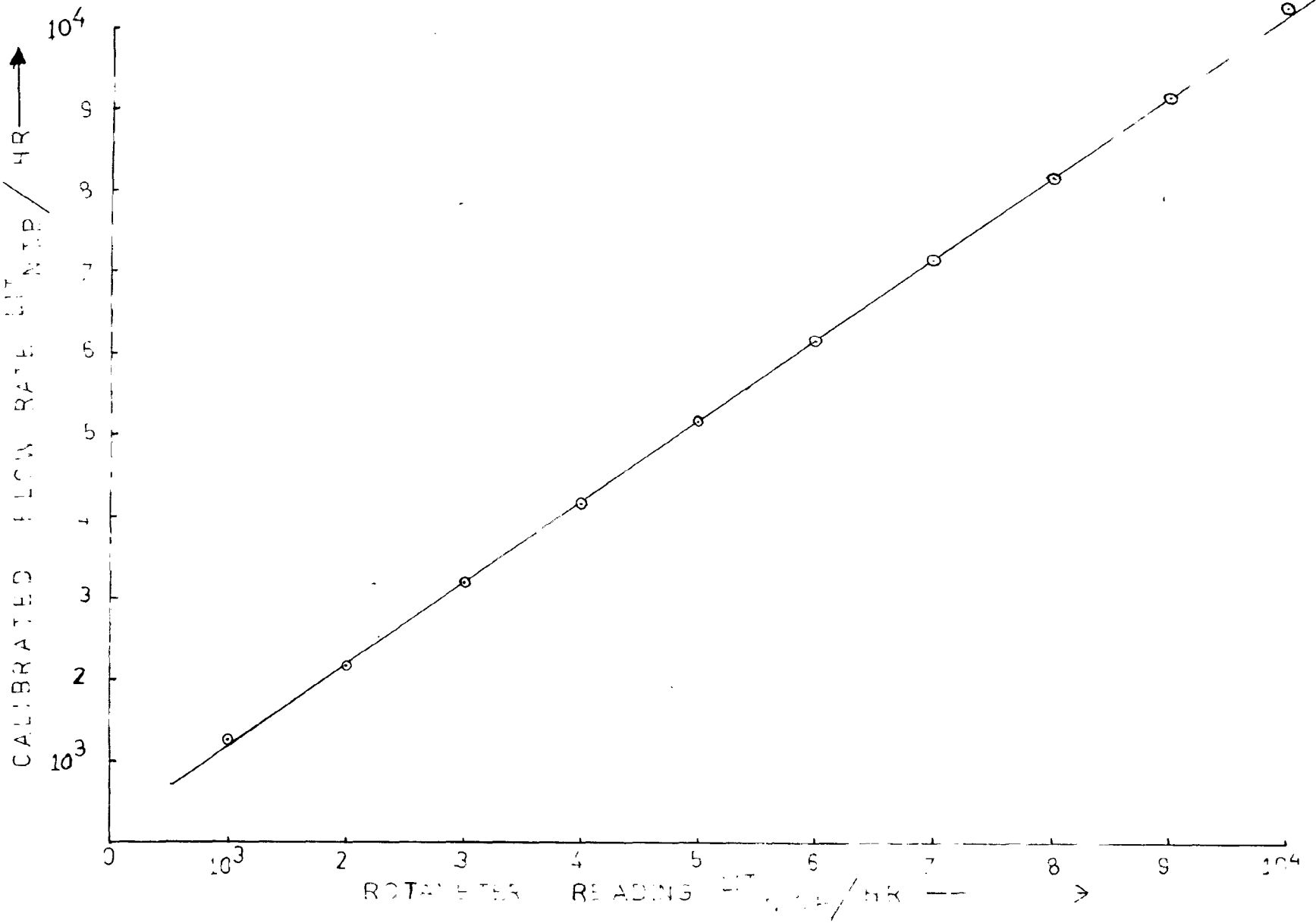

FIG. 2.5 CALIBRATION OF ROTAMETER (RANGE 0-12500 NL PH)

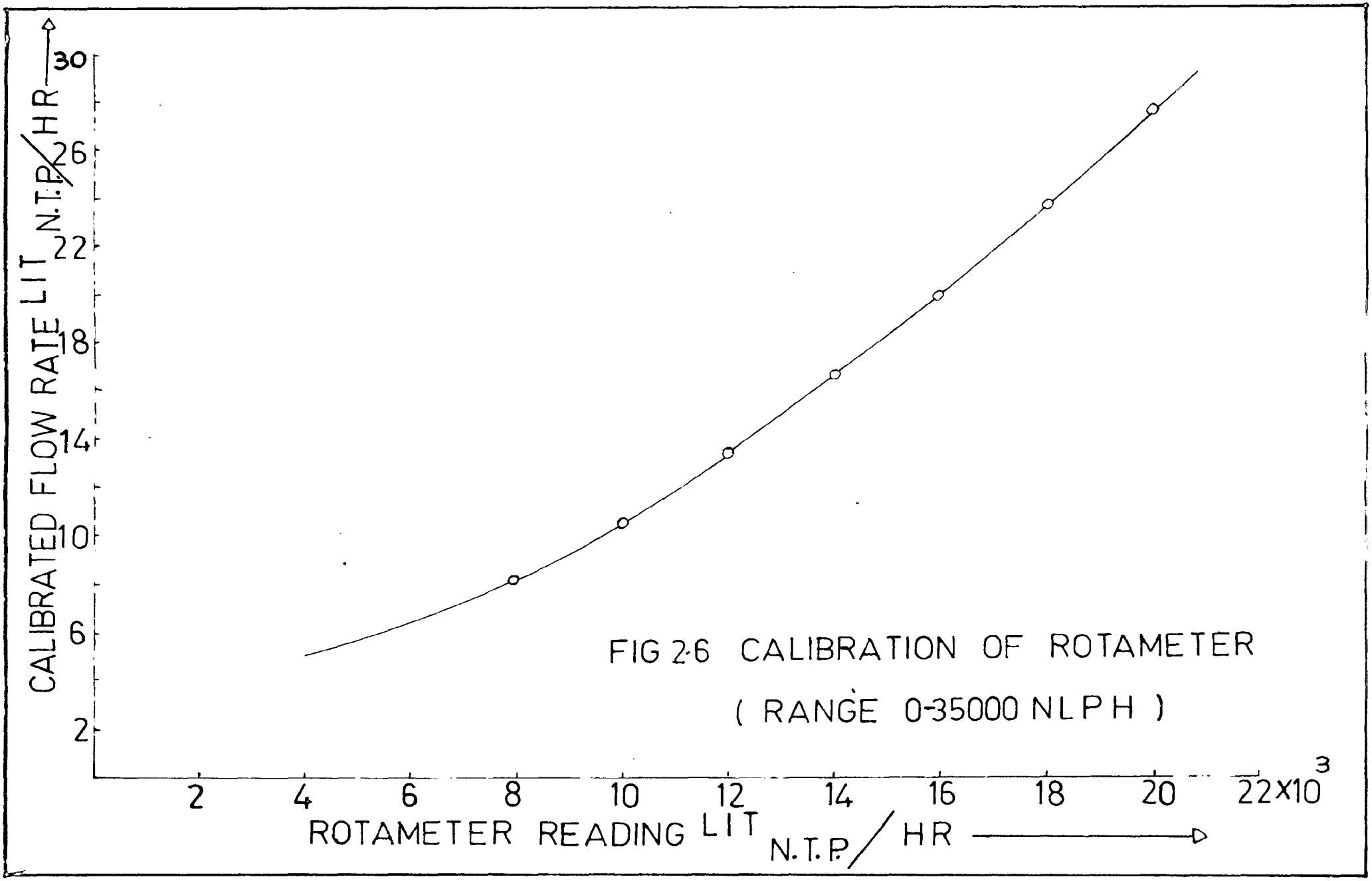

FIG 2·6 CALIBRATION OF ROTAMETER

(RANGE 0-35000 NLPH)

CHAPTER-III

FLUIDIZATION IN TAPERED VESSELS (RESULTS AND DISCUSSION)

CHAPTER - III

FLUIDIZATION IN TAPERED VESSELS

The pressure drop and air flow rate data are obtained for glass-beads, bauxite, calcite and baryte in tapered vessels of varying cone angles. The parameters studied include particle size, particle density, bed height and cone angle. The data obtained are given in Appendix-I in Table 1 to Table 23 and are shown in Fig. 3.1 to Fig. 3.6.

RESULTS AND DISCUSSION →

3.1 Effect of Particle Diameter

Fig. 3.1 and 3.2 show the variation of pressure drop with air flow rate for glass beads and baryte respectively in the size ranging from 460 microns to 977 microns in a tapered vessel of 45° cone angle keeping the weight of the material as 1 Kg in all cases. It is observed that for the same material and bed weight, minimum fluidizing velocity increased with particle size as observed in case of a cylindrical vessel. It was also observed that pressure peak value increased with the particle size both in the case of glass-beads and baryte as well. However, it was more steep in case of baryte for the same size of particles compared to glass-beads.

3.2 Effect of Particle Density

Fig. 3.3 is the plot of variation of pressure drop with air flow rate for different materials in tapered vessel of 45° cone angle for a constant bed weight and particle size. It is observed that pressure peak value increased with particle

flow rate in tapered vessels of cone angles 20°, 30°, 45° and 90° for same weight of material in the bed for glass-beads. It is observed from the figure that with increase in cone angle, pressure drop reduced. Pressure peak values also were noted to be reduced in larger angles of cones. This reduction in pressure drop and pressure peak is caused by the fluidisation of only a limited part of the bed, confined to the central portion in the tapered vessel. The solids near the wall remains stationary even at high air flow rates. However, the minimum fluidizing velocity decreases as the cone angle decreased.

3.5 Quality of Fluidisation in Vessels of Different Cone Angles

Fluidisation is observed to be more uniform in tapered vessels of lower cone angles. In higher angle cones, the bed behaves like a spouted bed. Solids move down along the walls and rise up in the central portion just like a fountain of particles. The particles on falling, form a heap which is convex upwards. But once the angle of cone falls below the value of angle of repose of solid particles, they have little tendency to slide down. In 90° cone the fluidisation is limited to the central portion only. In tapered vessels of lower cone angles, slugging is more pronounced and it reduces with increase in cone angles but in lower cone angles, whole of the bed is in a state of fluidisation. Similar phenomenon has been observed by the previous workers also. Taking all above factors in to consideration the fluidisation in a tapered vessel of 45° cone angle is found

to be quite uniform. The studies have been carried out with the cone angle of 45°.

3.6 Correlations Proposed

Minimum fluidizing velocity for any fluid-solids system will depend upon physical characteristics of solids viz. ρ_s, D_p, ϕ_s and ϵ, physical characteristics of fluid viz. ρ_f, μ_f and geometry of the vessel i.e. tan α. The correlation for minimum fluidizing velocity in tapered vessel will therefore basically have all the factors governing minimum fluidizing velocity in cylindrical vessel and the geometry which differentiates the tapered vessel from a cylindrical vessel. Thus a dimensionless correlation of the type

$$(Re_p)_{mf} = K \left[\frac{\rho_f (\rho_s - \rho_f) D_p^3 \phi_s^3 G}{\mu_f^2}\right]^a (\tan \tfrac{\alpha}{2})^b \left(\frac{L}{D_o}\right)^c \ldots (3.1)$$

may be proposed.

Based on experimental data, the program for evaluating the values of the exponents a, b and constant K was run on computer IBM 1620 (Appendix II) and the following correlation is obtained.

$$\left(\frac{D_p \phi_s G_{mf}}{\mu_f}\right) = 0.1359 \left[\frac{\rho_f(\rho_s - \rho_f) D_p^3 \phi_s^3 G}{\mu_f^2}\right]^{0.61} [\tan \tfrac{\alpha}{2}]^{0.93} \left[\frac{L}{D_o}\right]^{1.} \ldots (3.2)$$

The computed values of the minimum fluidizing velocities were compared with experimental values and more than 80% data were found to be within a deviation of ±3% as

shown in Fig. 3.7. From the correlation, it is evident that as the taper angle increases, fluidization tends towards non-uniformity.

The following correlation is proposed for predicting the pressure peak

$$\left(\frac{\Delta P}{\Delta P_{net}}\right) = 0.102 \left(\frac{D}{D_e}\right)^{-0.94} \left(\tan \frac{\alpha}{2}\right)^{-0.8} \left(Re_{mf}\right)^{0.31} \quad \ldots (3.3)$$

The computed values of pressure peak were observed to lie well within ± 20% deviation from those of experimental values as shown in Fig. 3.8.

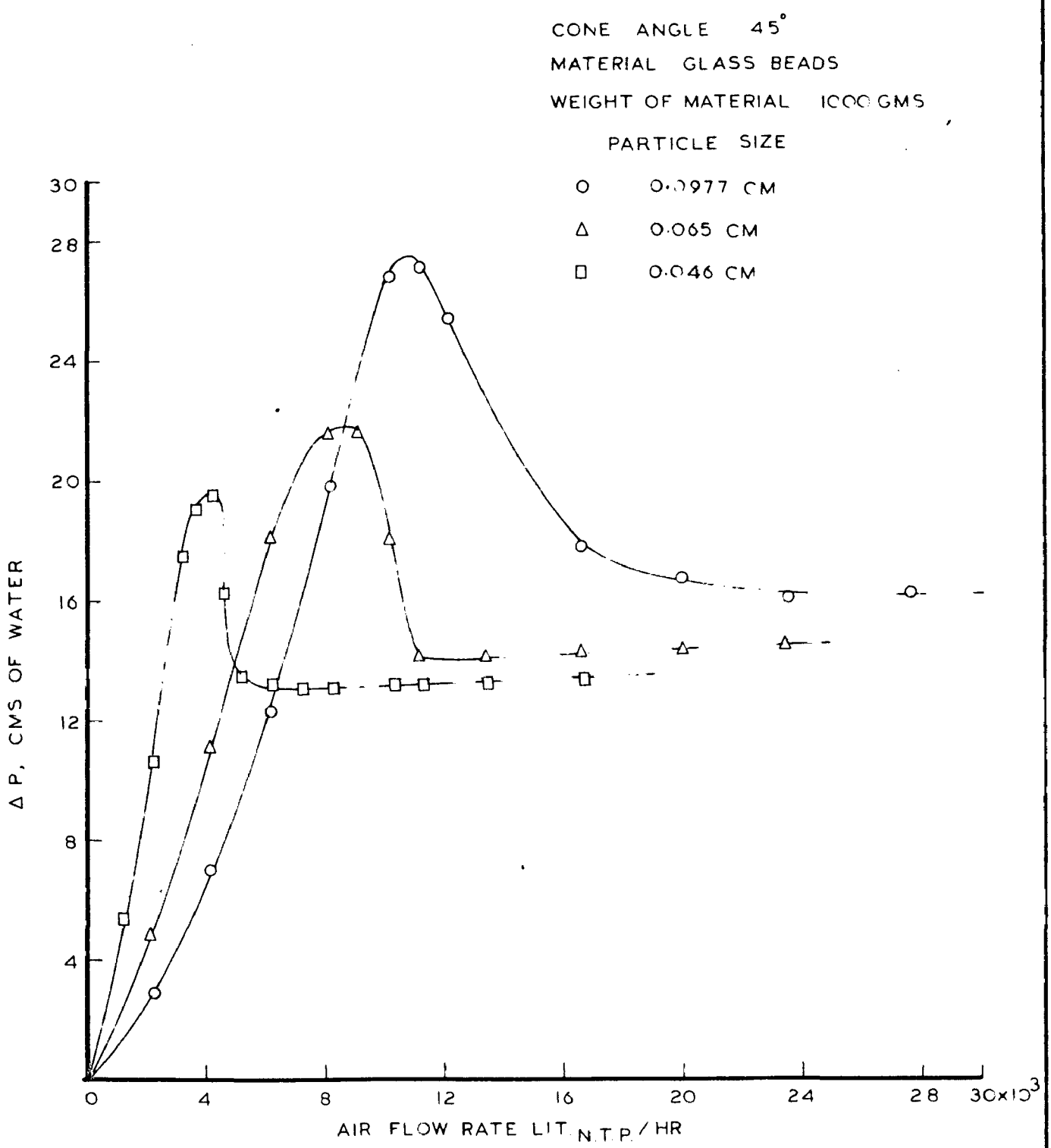

FIG. 3·1 VARIATION OF Δ P WITH AIR FLOW RATE FOR DIFFERENT SIZES OF PARTICLES OF GLASS BEADS

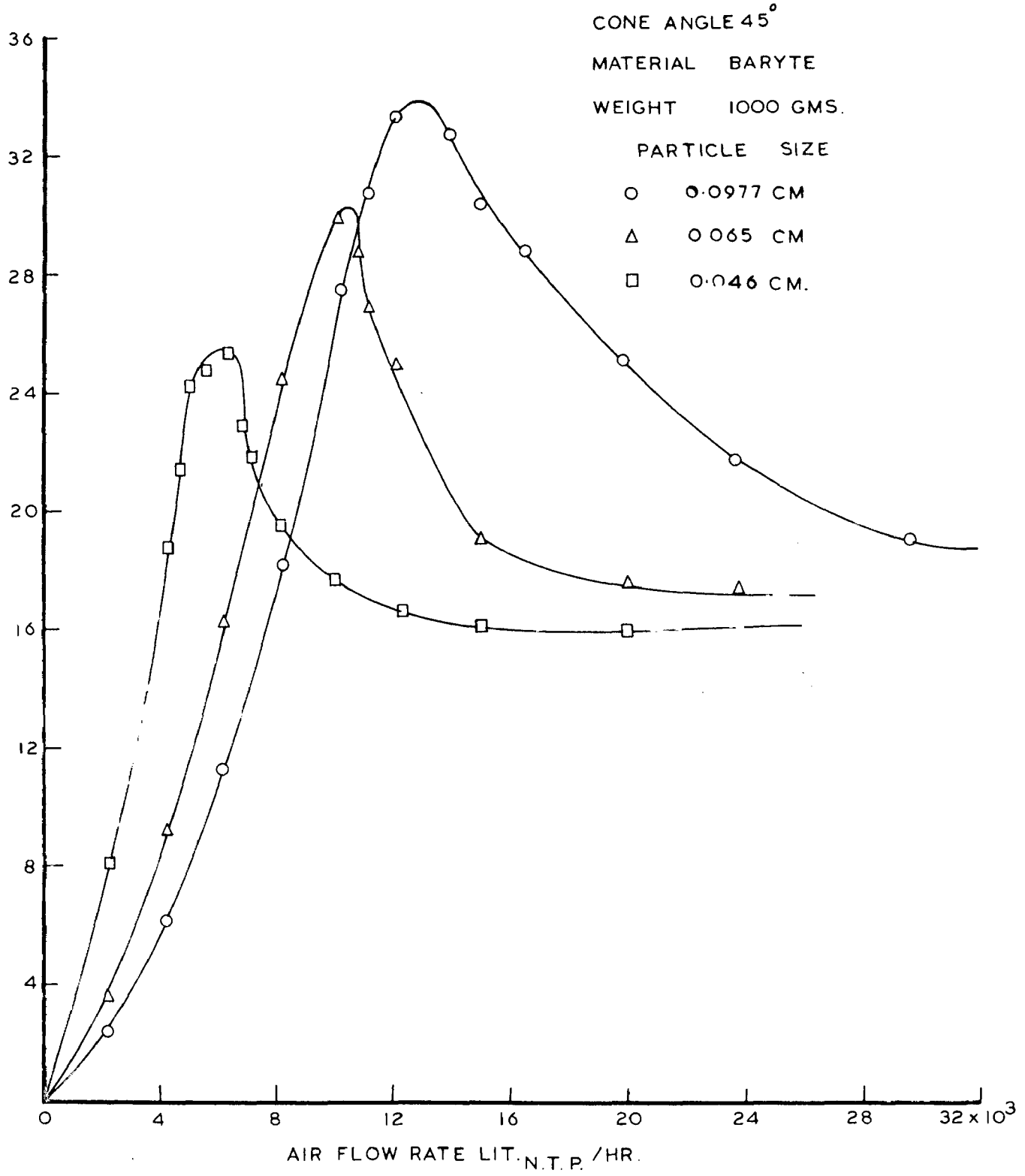

FIG. 3·2 VARIATION OF ΔP WITH AIR FLOW RATE FOR DIFFERENT SIZES OF PARTICLES OF BARYTE

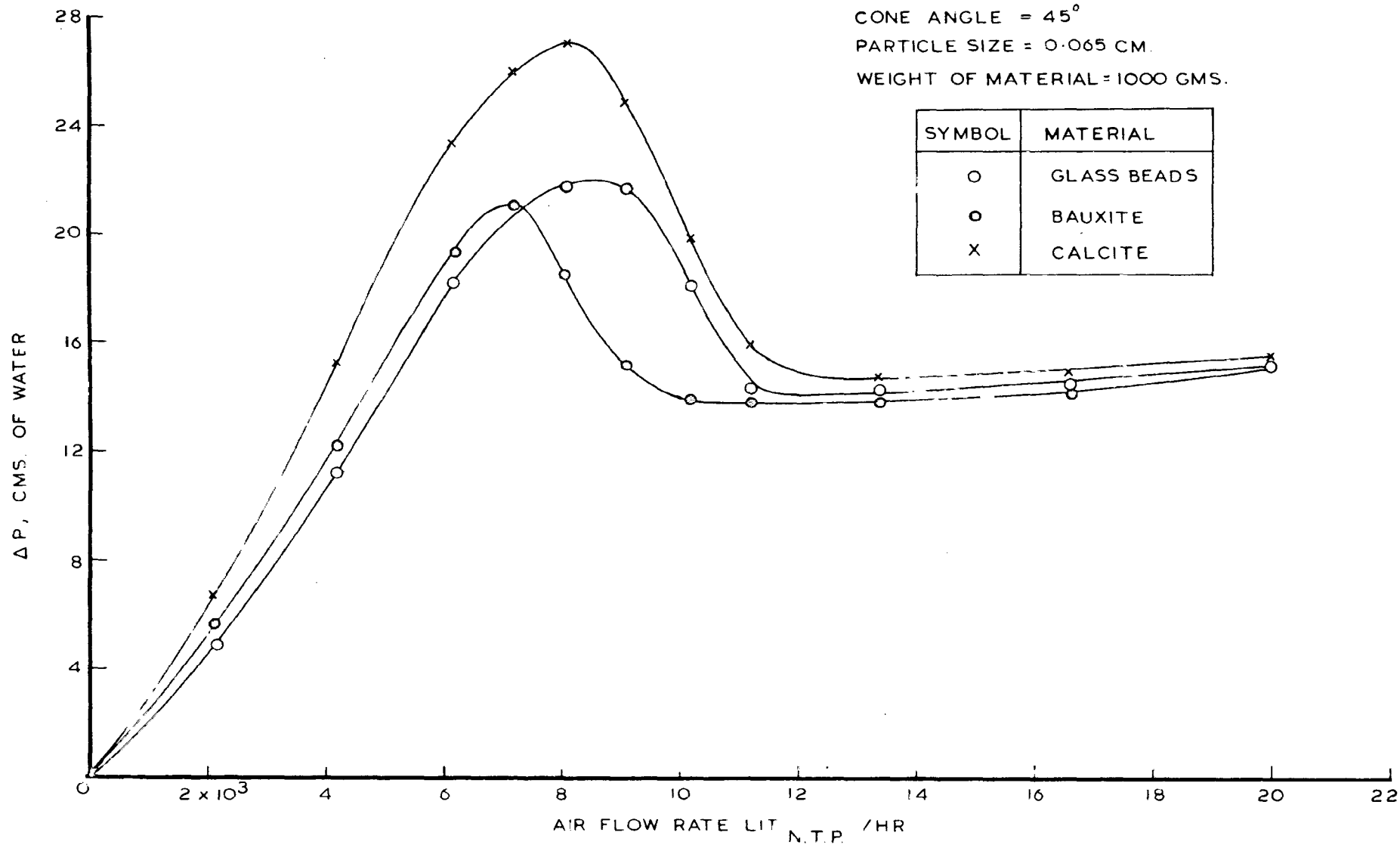

FIG 3·3 VARIATION OF Δ P WITH AIR FLOW RATE FOR DIFFERENT MATERIALS OF SAME SIZE.

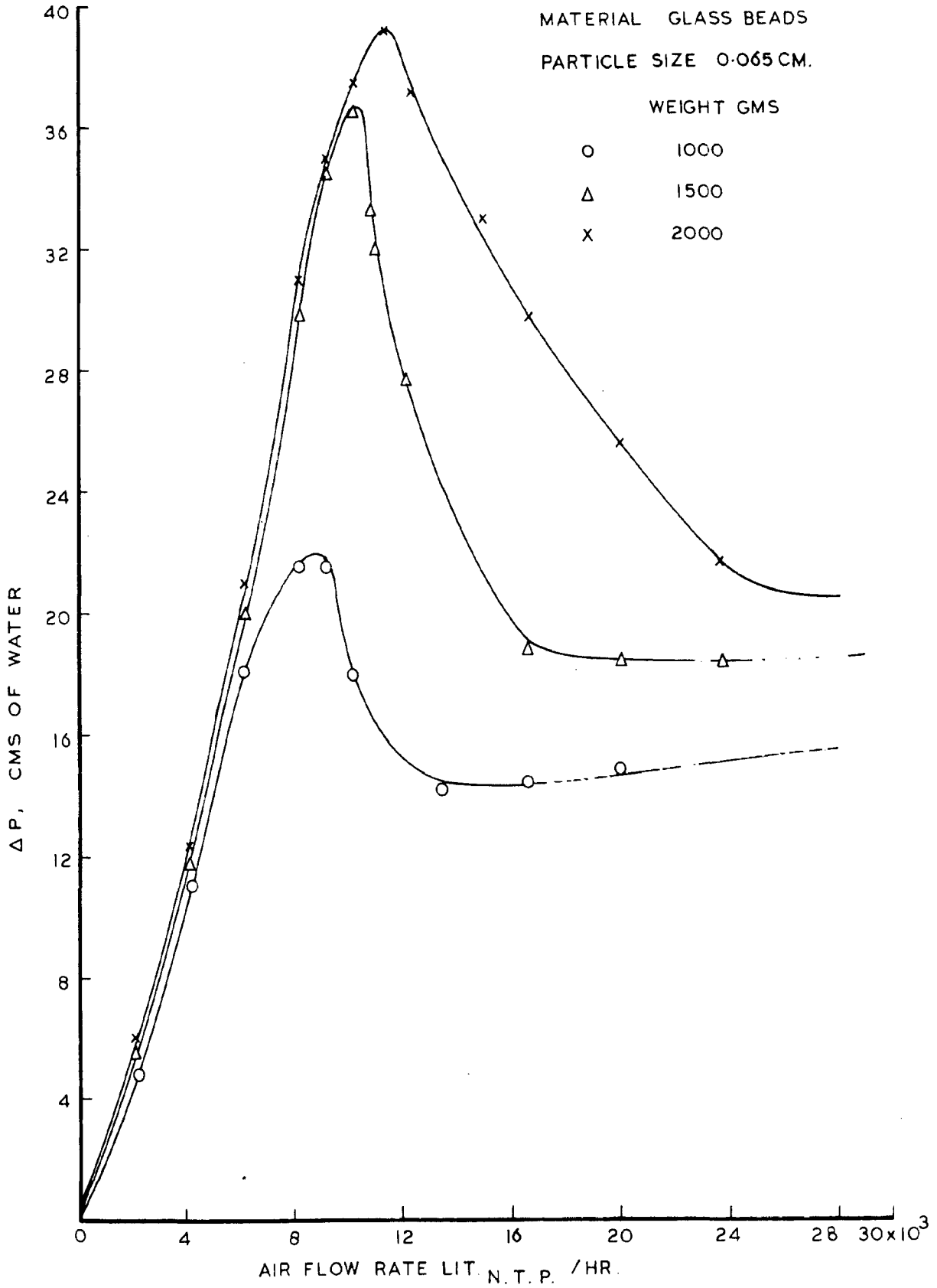

FIG. 3·4 VARIATION OF ΔP WITH AIR FLOW RATE FOR DIFFERENT BED HEIGHTS OF GLASS BEADS

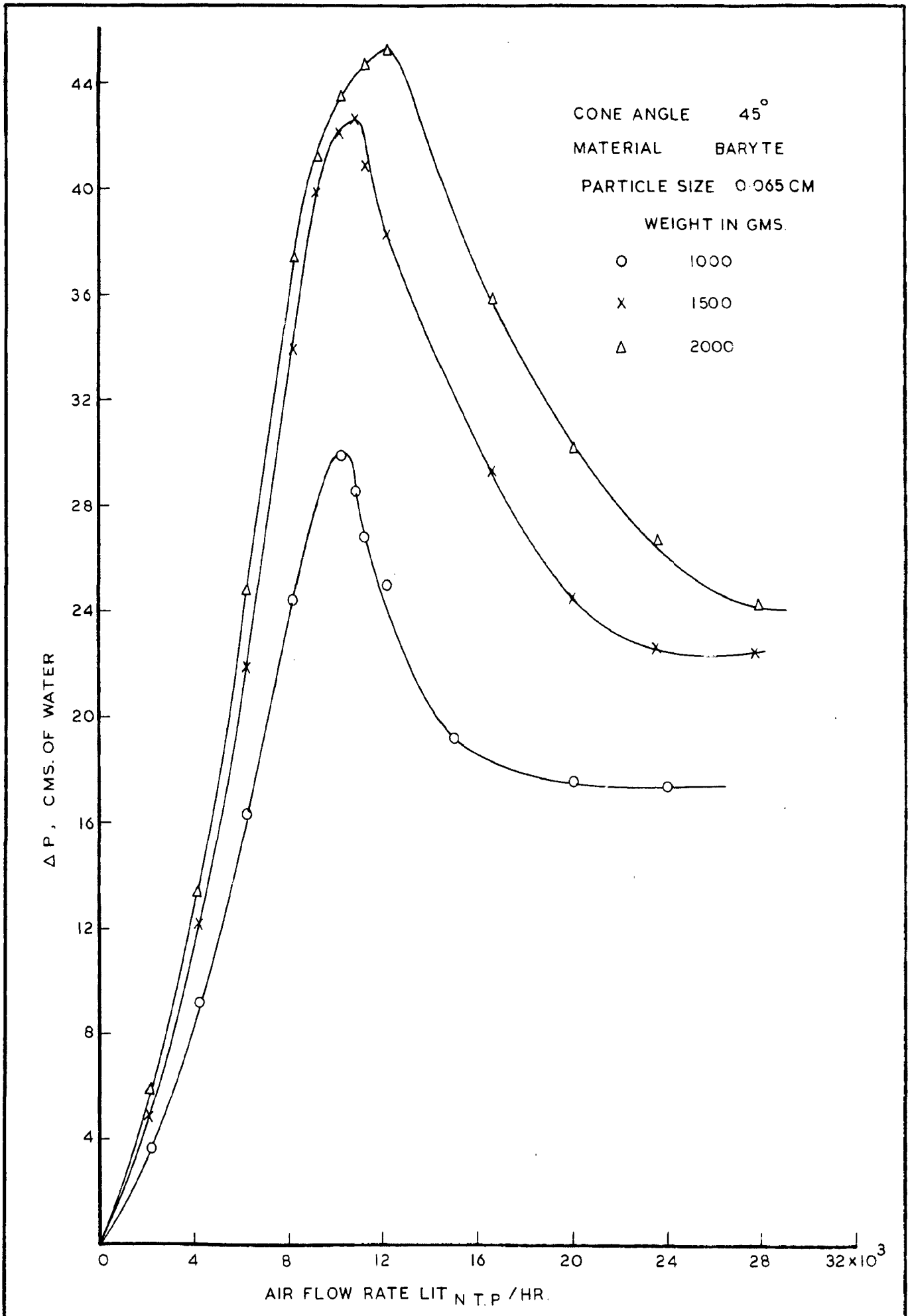

FIG. 3·5 VARIATION OF Δ P WITH AIR FLOW RATE FOR DEFFERENT BED HEIGHTS OF BARYTE

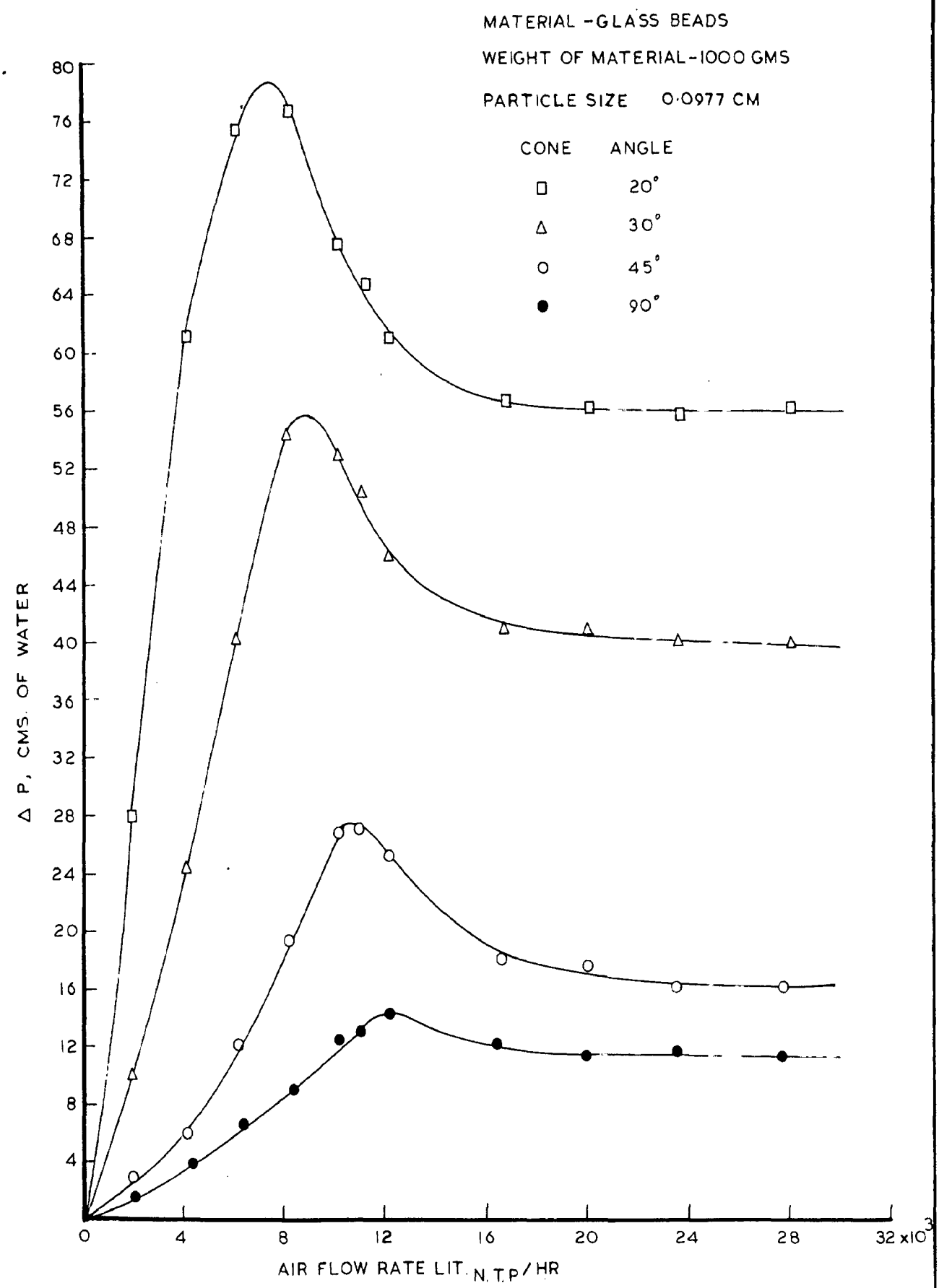

FIG. 3·6 VARIATION OF ΔP WITH AIR FLOW RATE FOR DIFFERENT CONE ANGLE USING GLASS BEADS

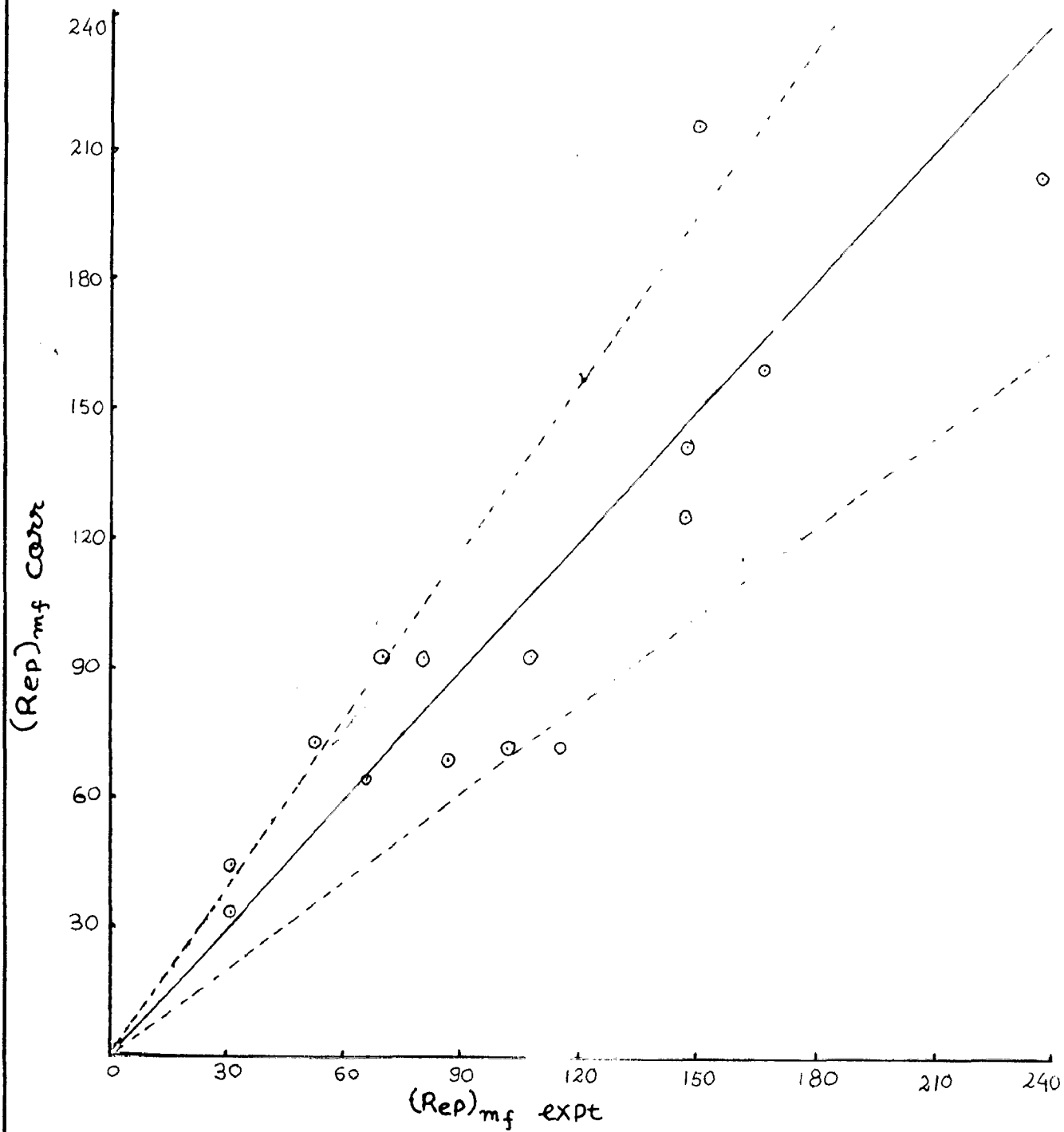

FIG 3.7 PLOT BETWEEN CORRELATED AND EXPERIMENTAL VALUES OF $(Rep)_{mf}$

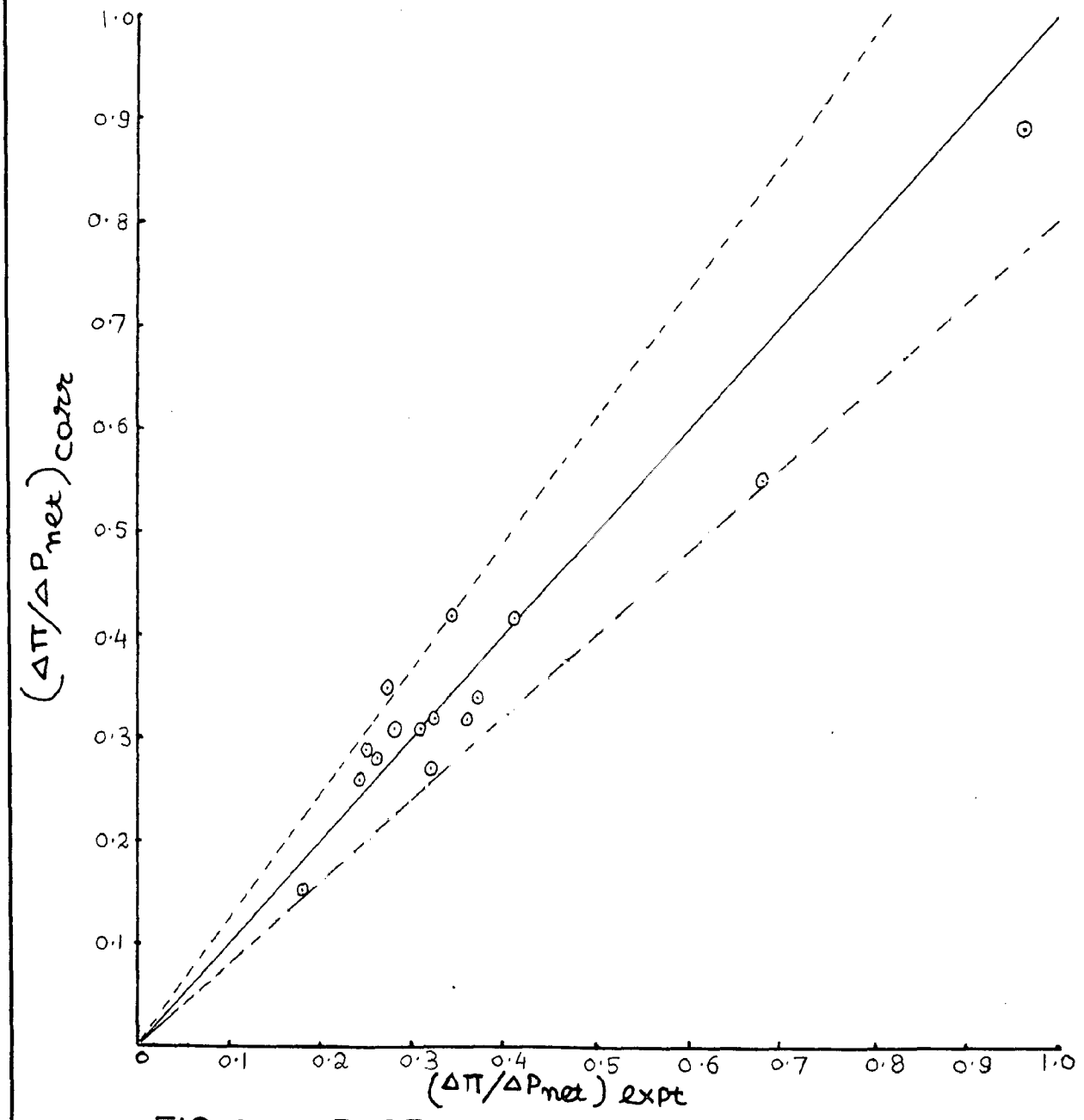

FIG 3.8 PLOT BETWEEN CORRELATED AND EXPERIMENTAL VALUES OF $\left(\frac{\Delta\Pi}{\Delta P_{net}}\right)$

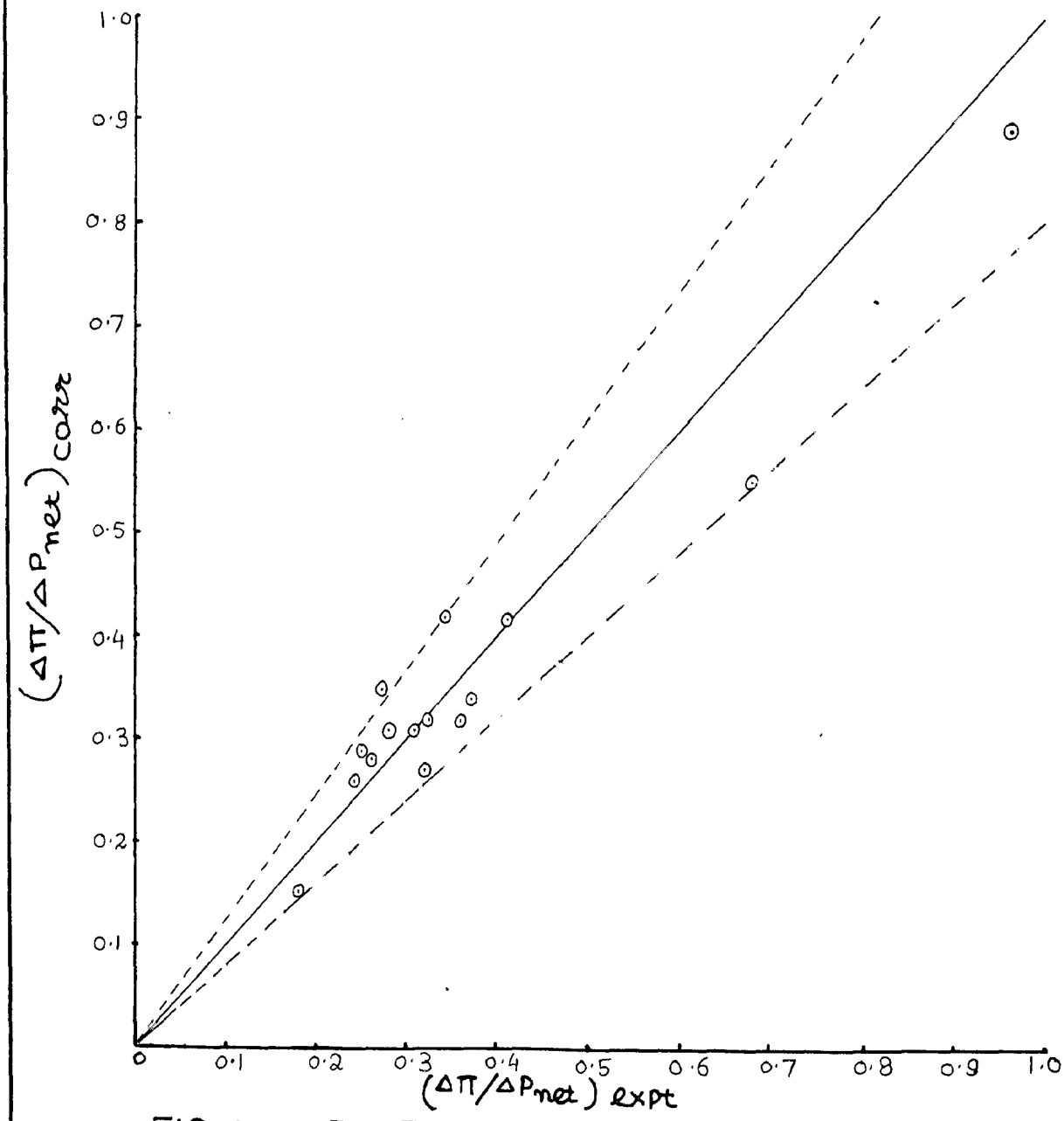

FIG 3.8 PLOT BETWEEN CORRELATED AND EXPERIMENTAL VALUES OF $\left(\frac{\Delta\Pi}{\Delta P_{net}}\right)$

CHAPTER-IV

FLUIDIZATION STUDIES IN TAPERED VESSELS WITH STIRRER (RESULTS AND DISCUSSION)

C H A P T E R - IV

FLUIDIZATION STUDIES IN TAPERED VESSELS WITH STIRRER

The pressure drop and air flow rate data are obtained for glass-beads and baryte in tapered vessels of varying cone angles using a stirrer. The experimental set up same as shown in chapter II The parameters studied include particle size, particle density, bed height, cone angle, speed of stirrer and depth of stirrer in the bed. The data obtained are given in Appendix I in Table 1 to 23 and are shown in Fig 4.1 to 4.16.

RESULTS AND DISCUSSION →

4.1 Effect of Particle Diameter

In Fig. 4.1 pressure drop is plotted against air flow rate for glass beads of size ranging from 460 microns to 977 microns in a tapered vessel of cone angle 45° with stirrer. Fig. 4.2 to 4.4 show the variation in pressure drop with air flow rate for glass-beads of size 460, 650 and 977 microns respectively in a tapered vessel of 45° cone angle with and without stirrer, keeping the weight of material as 1 Kg in all cases. Similarly Fig. 4.5 shows the variation in pressure drop with air flow rate for baryte of size ranging from 460 microns to 977 microns in a tapered vessel of cone angle 45° with stirrer. In Fig. 4.6 to 4.8 pressure drop is plotted against air flow rate for baryte of size 460, 650 and 977 microns respectively in a tapered vessel of 45° cone angle with and without stirrer , keeping the weight of material as 1 Kg in all cases.

It is observed from Fig. 4.1 and 4.5 that pressure peak values were reduced in cases where stirrer was used. Also variation in pressure peak values with particle size was decreased and the air flow rates for fluidization were reduced in beds with stirrer. It is seen from Fig. 4.2 to 4.4 for glass-beads and Fig. 4.6 to 4.9 for baryte that variation of pressure drop with air flow rate with stirrer, followed the same trend as that obtained in the tapered beds without stirrer. But it is clear from all these plots that the pressure peak and minimum air flow rate for fluidization were much reduced in case of beds with stirrer. In the beginning, in fixed bed region, the pressure drop is almost equal to that of the bed without stirrer. However, pressure drop was much reduced in the neighbourhood of minimum fluidizing condition. It is because at this stage the lower part of the bed was fluidized and the upper part was disturbed by the stirrer and thus the entire bed was fluidised at a lower air flow rates. The pressure peak which was quite substantial in beds without stirrer, reduced sharply in beds with stirrer. If air flow rate is increased beyond minimum fluidizing condition, pressure drop was still lower in beds with stirrer, However, stirrer was not found to be of much use at very high air flow rates. Pressure drop values become almost equal at very high air flow rates in the beds with and without stirrer.

Therefore, stirrer is found to be more useful at the minimum fluidizing condition or just in its neighbourhood. The

use of stirrer is not recommended in the fixed bed region and also for air flow rates much higher than the minimum fluidising conditions.

4.2 Effect of Particle Density

In Fig. 4.9 pressure drop is plotted against air flow rate for different materials of same size in tapered vessel of 45° cone angle for a constant bed weight, constant speed of stirrer and constant depth of stirrer in the bed in all cases. It is observed that variation of pressure drop with air flow rate with stirrer followed the same trend as that obtained in the tapered beds without stirrer. Though pressure peak value increased with particle density but these values were lower than that obtained in beds without stirrer. It is also noted that the minimum fluidizing velocity was more for non-spherical particles than that for spherical particles. But these values of air flow rate for minimum fluidisation in beds with stirrer were again lower than in the case of beds without stirrer. Here also, the stirrer is found to be more useful at the minimum fluidizing condition or just in its neighbourhood. The use of stirrer is not found suitable either in fixed bed region or for the air flow rates which are very high as compared to the minimum fluidizing velocity condition.

4.3 Effect of Bed Height

In Fig. 4.10 and 4.11 pressure drop is plotted against air flow rate for glass beads and baryte of particle size

of 650 micron respectively for different bed heights keeping speed of stirrer and depth of stirrer in the bed as constant in all the cases. It is observed from these figures that nature of the plots remained the same as it was in the beds without stirrer. For the same particles, pressure drop, pressure peak and minimum fluidizing velocity values increased with bed height. This increase in pressure drop is justified by the fact that at onset of fluidization the pressure drop is equal to the net weight of particles in the bed and thus the pressure drop increased. A bed in tapered vessel is in a fluidized state when the entire bed gets fluidized. Hence as the bed height increases, more air flow rate is required to fluidize the whole bed. This is the reason that minimum fluidizing velocity increased with the bed height.

But pressure drop, pressure peak and air flow rate for minimum fluidizing conditions were found to be much reduced in beds with stirrer as compared to the beds of particles without stirrer. The stirrer was found to be quite effective at the minimum fluidizing condition and just in its neighbourhood.

4.4 Effect of Cone Angle

In Fig. 4.12 pressure drop is plotted against air flow rate in tapered vessels of cone angles 20°, 30°, 45°, and 90° for same weight of material in the bed for glass-beads keeping stirrer speed and depth of stirrer in the bed as constant in all cases. It is observed that the trend of

the variation of pressure drop was similar to that in the beds without stirrer, with increase in cone angle, pressure drop was reduced. Pressure peak values also were found to be reduced in larger cone angles. But these values of pressure drop and pressure peak were lower than that in beds without stirrer.

4.5 Effect of Depth of Stirrer in the Bed

Fig. 4.13 and 4.14 show the variation of pressure drop with air flow rate for glass-beads and baryte respectively of size of 650 micron for varying depths of the bed keeping weight of the bed and stirrer speed constant. It is observed from the plots that in fixed bed region, pressure drop was almost same in all the cases for the same particles. Pressure peak and minimum fluidizing velocity values were found to be reduced as the depth of stirrer in the bed increased. At very high air flow rates, pressure drop values were again same. The important factor in this case is the ratio of the depth of stirrer in the bed to the bed depth itself. If this ratio is very small, only the upper layer of the bed will be influenced by stirrer and rest of the bed will remain almost stagnant. The proper choice of this ratio will always be useful.

4.6 Effect of Speed of Stirrer

In Fig. 4.15 and 4.16 pressure drop is plotted against air flow rate for glass-beads and baryte of size of 650 micron respectively for varying speed of stirrer keeping the weight

of material and depth of stirrer in the bed constant in all cases. It is observed from the plots that pressure drop in fixed bed region, was constant irrespective of speed for a particular material. The pressure peak and air flow rate values for minimum fluidization were reduced for higher speed of stirrer. But there was no significant decrease in their values. At very high air flow rates the pressure drop was again found to be steady for all the cases. Only in the neighbourhood of minimum fluidizing condition, the higher speed of stirrer was found to be useful.

4.7 Power Saving With Stirrer

Particles in a packed bed in contact with each other can be separated in a fluidizing column either by passing fluid across the bed or by agitating the bed with mechanical stirrer or by both. Energy requirements will be higher if air is used to achieve the separation and movement of particles in a packed bed. When mechanical stirrer is used in the bed, the fluidization characteristics like pressure drop, minimum fluidizing velocity are expected to be different from those of the bed without stirrer. Table 4.1 shows the comparison of air flow rate for minimum fluidization with and without stirrer, in tapered vessel of 45^{0} cone angle. Air flow rate required to achieve the onset of fluidization is observed to be lower in beds with stirrer compared to that of the beds without stirrer. Similar observations are made with regard to pressure peak which shows a decreasing tendency when stirrer is used in the bed as shown in Table 4.2.

The power required for achieving the unlocking of particles in tapered vessel is observed to be lower when mechanical stirrer is used. Table 4.3 shows the comparison of the power requirements at the onset of fluidisation in tapered vessels with and without stirrer. It is observed that the percentage saving in power increases with increase in particle size and bed height for a given material.

In the fixed bed region, the pressure drop in beds with stirrer is observed to be lower than that in beds without stirrer, however, the change in pressure drop is not significant. At the onset of fluidizing conditions the pressure drop in beds with stirrer is found to be much lower as compared to the beds without stirrer. At very high air flow rates of air the change in pressure drop in the beds with and without stirrer again becomes very small. Therefore, the stirrer is found to be more useful at the onset of fluidization and its neighbourhood.

4.8 Correlations Proposed

Minimum fluidizing velocity for a fluid-solid system with stirrer will depend upon the physical characteristics for the tapered vessel and will include the physical characteristics of the stirrer. The following correlation is proposed for predicting the minimum fluidizing velocity in tapered vessels with stirrer

$$\left[\frac{D_p \varphi_n G_{mf}}{\mu_f}\right] = 0.3119 \left[\frac{\rho_f (\rho_s - \rho_f) g D_p^3 \varphi_n^3}{\mu_f^2}\right]^{0.163} \left[\tan\frac{\alpha}{2}\right]^{0.008} \left[\frac{h}{L}\right]^{0.23} \left[\frac{D^2 N \rho}{\mu_f}\right]^{-0.103} \quad \ldots (4.1)$$

The predicted values of minimum fluidizing velocities were found to be well within ± 20% deviation from those of experimental values and is shown in Fig. 4.17.

The following correlation is proposed for predicting the pressure peak in tapered beds with stirrer.

$$\left(\frac{\Delta P}{\Delta P_{not}}\right) = 0.139 \left[Rep_{mf}\right]^{0.18} \left[\tan\frac{\alpha}{2}\right]^{-0.57} \left[\frac{D^2 N \rho}{\mu}\right]^{-0.088} \left[\frac{h}{L}\right]^{-0.41} \left[\frac{D}{D_0}\right]^{-0.90} \quad \ldots (4.2)$$

Theoretical values predicted were compared with the experimental data and deviation was found to be ±20% as shown in Fig. 4.18.

TABLE-4.1

Comparison of Air Flow Rate for Minimum Fluidization
With And Without Stirrer In Tapered Vessel
Of 45° Cone Angle

Material	Particle diameter Dp, microns	Speed of stirrer n, rpm	Depth of stirrer in the bed, h, m.m.	Height of fixed bed L, m.m.	Air flow rate for minimum fluidization without stirrer LIT/Hr N.T.P.	Air flow rate for minimum fluidization with stirrer LIT/H.R N.T.P.	Percentage decrease in Air flow rate
Glass-Beads	977	40	20	78.5	12200	11200	8.20
	650	40	20	74.0	10200	9180	10.00
	460	40	20	71.2	4600	4160	9.57
Baryte	977	40	20	74.0	15000	15000	-
	650	40	20	68.5	10800	10200	5.56
	460	40	20	65.6	6720	6170	8.18
Bauxite	650	40	20	95.2	8150	8150	-
Calcite	650	40	20	68.0	9180	8150	11.22
Glass-Beads	650	40	20	93.0	10800	10200	5.56
	650	40	20	115.0	12200	12200	-
Baryte	650	40	20	85.0	11200	10800	3.57
	650	40	20	102.0	16600	12200	26.51
Glass-Beads	650	40	40	115.0	12200	10200	16.39
	650	40	60	115.0	12200	10200	16.39
Baryte	650	40	40	102.0	16600	11200	32.53
	650	40	60	102.0	16600	10200	38.55
Glass-Beads	650	20	40	115.0	14200	11200	8.20
	650	80	40	115.0	12200	9180	24.75
Baryte	650	20	40	102.0	16600	12200	26.51
	650	80	40	102.0	16600	11200	32.53

TABLE-4.2

Comparison Of Pressure-Peak With And Without Stirrer In Tapered Vessel Of 45° Cone Angle

Material	Particle diameter D_p, microns	Speed of stirrer n, rpm	Depth of stirrer in the bed h, m.m.	Height of fixed bed L.H.M.	Pressure peak without stirrer cms of Water	Pressure Peak with stirrer cms of Water	Percentage Decrease in pressure peak
Glass-Beads	977	40	20	78.5	27.1	20.5	24.35
	650	40	20	74.0	21.8	19.8	9.17
	460	40	20	71.2	19.5	18.4	5.64
Daryte	977	40	20	74.0	33.4	23.7	29.04
	650	40	20	68.5	29.9	21.8	27.09
	460	40	20	65.6	25.4	21.4	15.75
Dauxite	650	40	20	95.2	21.0	18.4	12.38
Calcite	650	40	20	68	26.0	22.0	15.38
Glass-Beads	650	40	20	93	36.5	30.2	17.26
	650	40	20	115	39.2	35.0	10.71
Daryte	650	40	20	85	42.6	32.4	23.94
	650	40	20	102	45.2	38.6	14.60
Glass-Beads	650	40	40	115	39.2	30.4	22.45
	650	40	60	115	39.2	27.2	30.61
Daryte	650	40	40	102	45.2	31.8	29.65
	650	40	60	102	45.2	27.8	44.39
Glass-Beads	650	20	40	115	39.2	31.6	19.39
	650	80	40	115	39.2	27.6	29.59
Daryte	650	20	40	102	45.2	33.1	26.77
	650	80	40	102	45.2	28.2	37.61

TABLE-4.3

Comparison of Power-Required With And Without Stirrer At Minimum Fluidizing Conditions in A Tapered Vessel of 45° Cone Angle

Material	Particle diameter Dp, micron	Speed of stirrer n, rpm	Depth of stirrer in the bed, h m.m.	Height of fixed bed L, m.m.	Air flow rate for minimum fluidization without stirrer	Air flow rate for minimum fluidization with stirrer	Percentage decrease in Air flow rate
Glass-Beads	977	40	20	78.5	8.99	6.25	30.48
	650	40	20	74.0	6.05	4.94	18.35
	460	40	20	71.2	2.44	2.08	14.75
Daryte	977	40	20	74.0	13.63	8.90	34.70
	650	40	20	68.5	8.78	6.05	31.09
	460	40	20	65.6	4.64	3.59	22.63
Bauxite	650	40	20	95.2	4.66	4.08	12.45
Calcite	650	40	20	68.0	6.50	4.88	24.92
Glass-Beads	650	40	20	93	10.72	8.38	21.83
	650	40	20	115	13.00	11.61	10.69
Daryte	650	40	20	85	12.93	9.52	26.66
	650	40	20	102	20.40	10.71	47.50
Glass-Beads	650	40	40	115	13.00	8.43	35.15
	650	40	60	115	13.00	7.55	41.92
Daryte	650	40	40	102	20.40	9.69	52.50
	650	40	60	102	20.40	7.71	62.21
Glass-Beads	650	20	40	115	13.00	9.63	25.92
	650	60	40	115	13.00	6.89	47.00
Daryte	650	20	40	102	20.40	10.93	46.18
	650	60	40	102	20.40	8.59	57.89

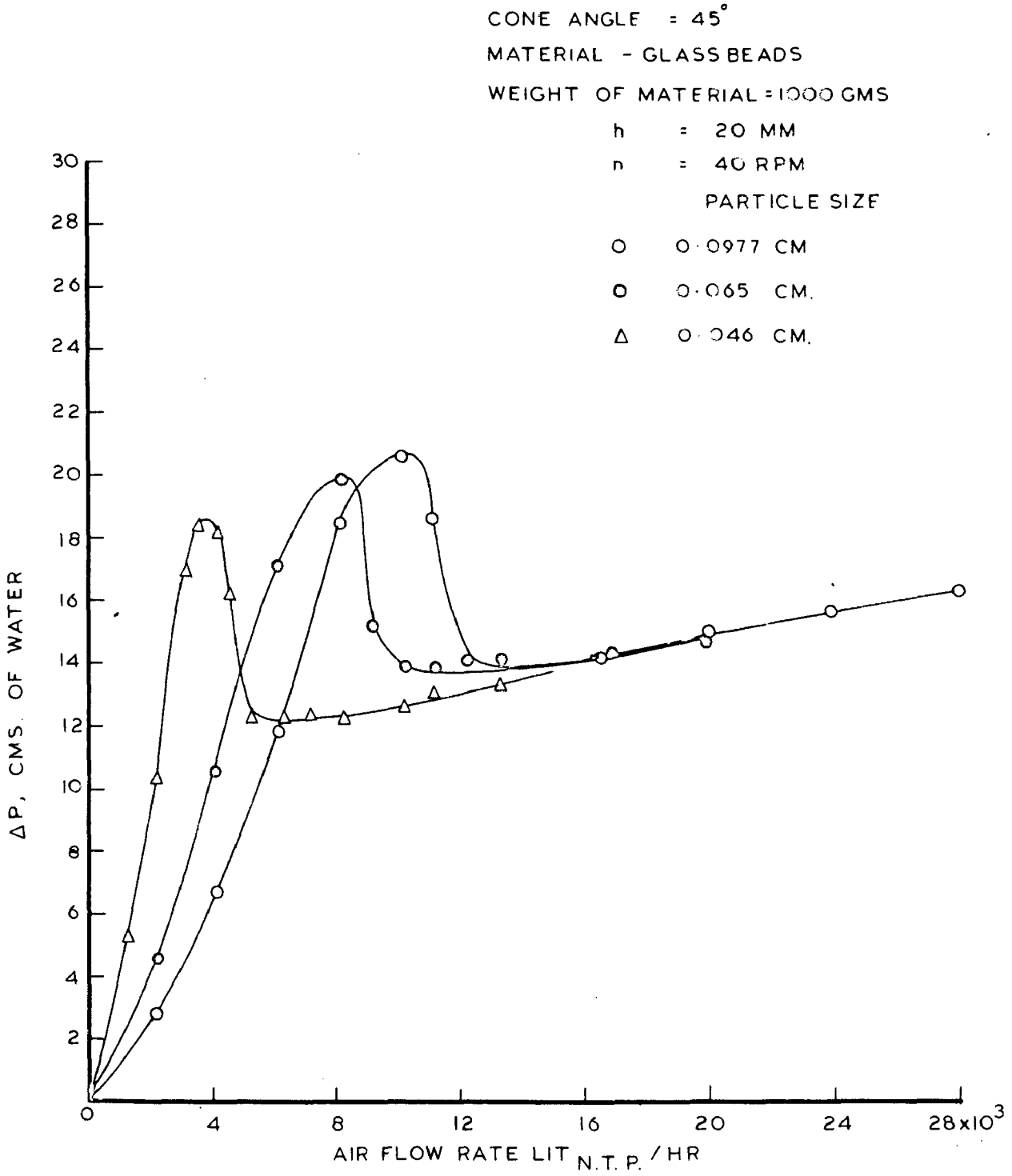

FIG. 4.1 VARIATION OF ΔP WITH AIR FLOW RATE WITH STIRRER FOR DIFFERENT SIZES OF GLASS-BEADS

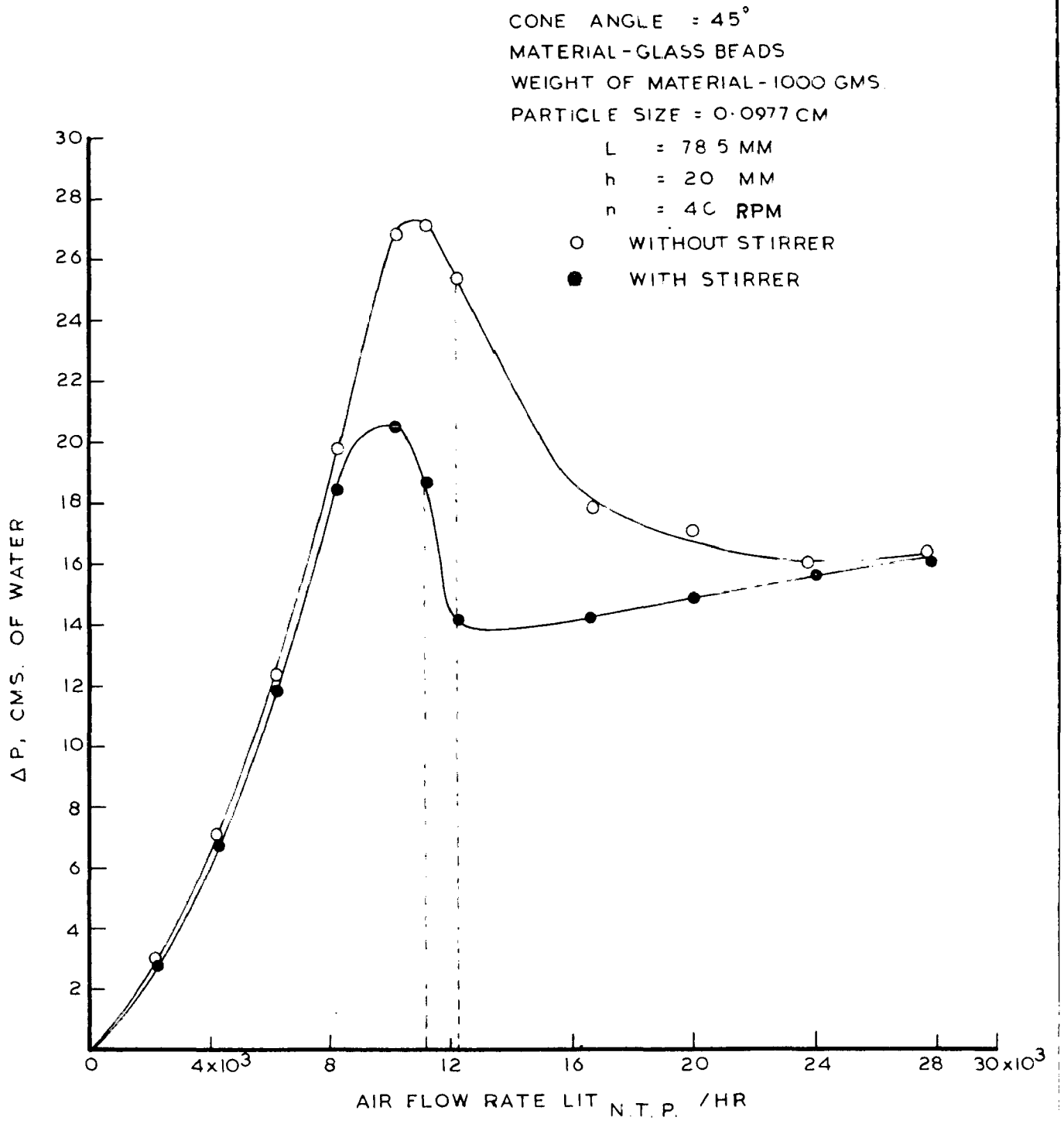

FIG. 4·2 VARIATION OF ΔP WITH AIR FLOW RATE WITH AND WITHOUT STIRRER FOR GLASS BEADS

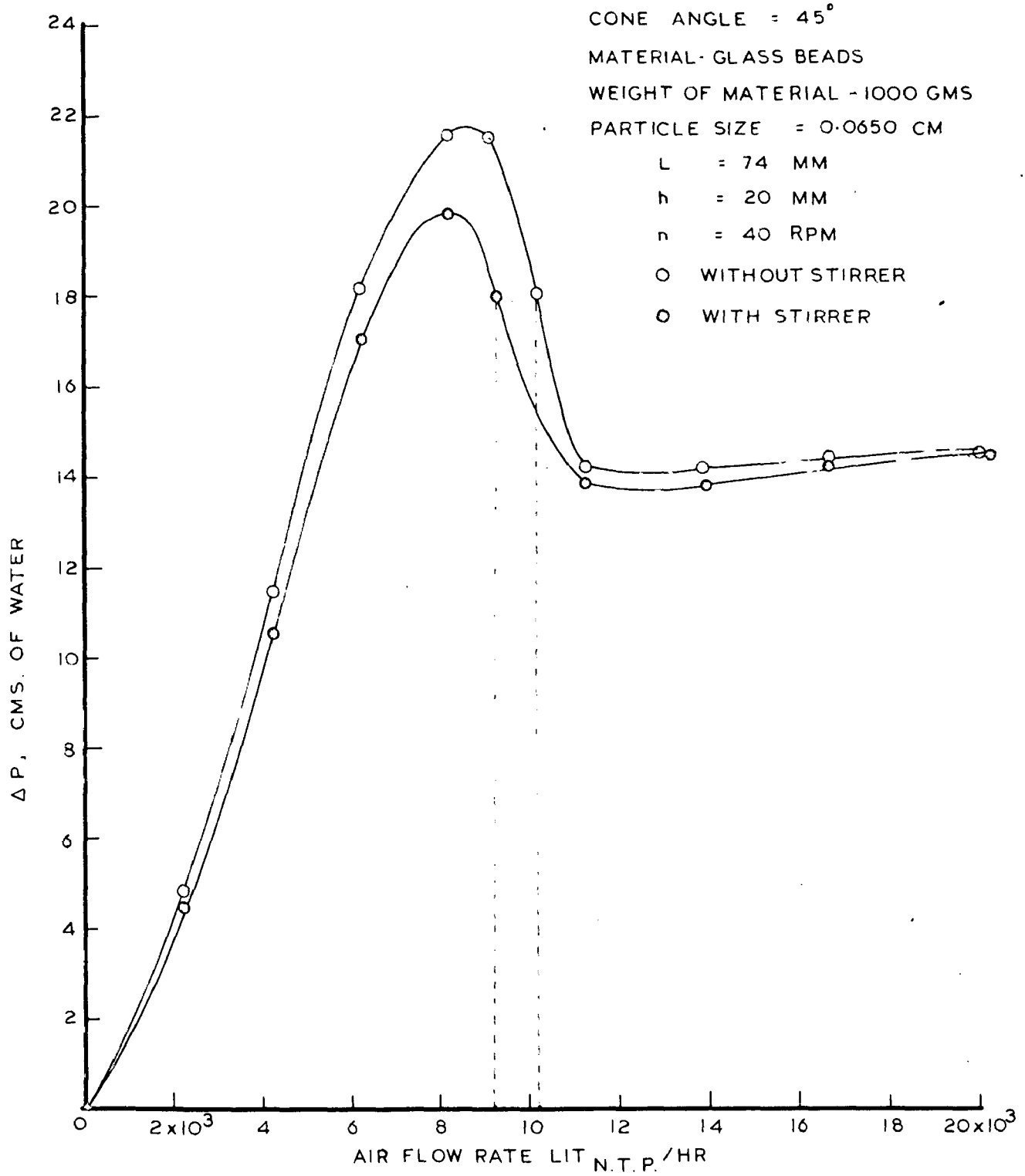

FIG. 4·3 VARIATION OF ΔP WITH AIR FLOW RATE WITH AND WITHOUT STIRRER FOR GLASS BEADS

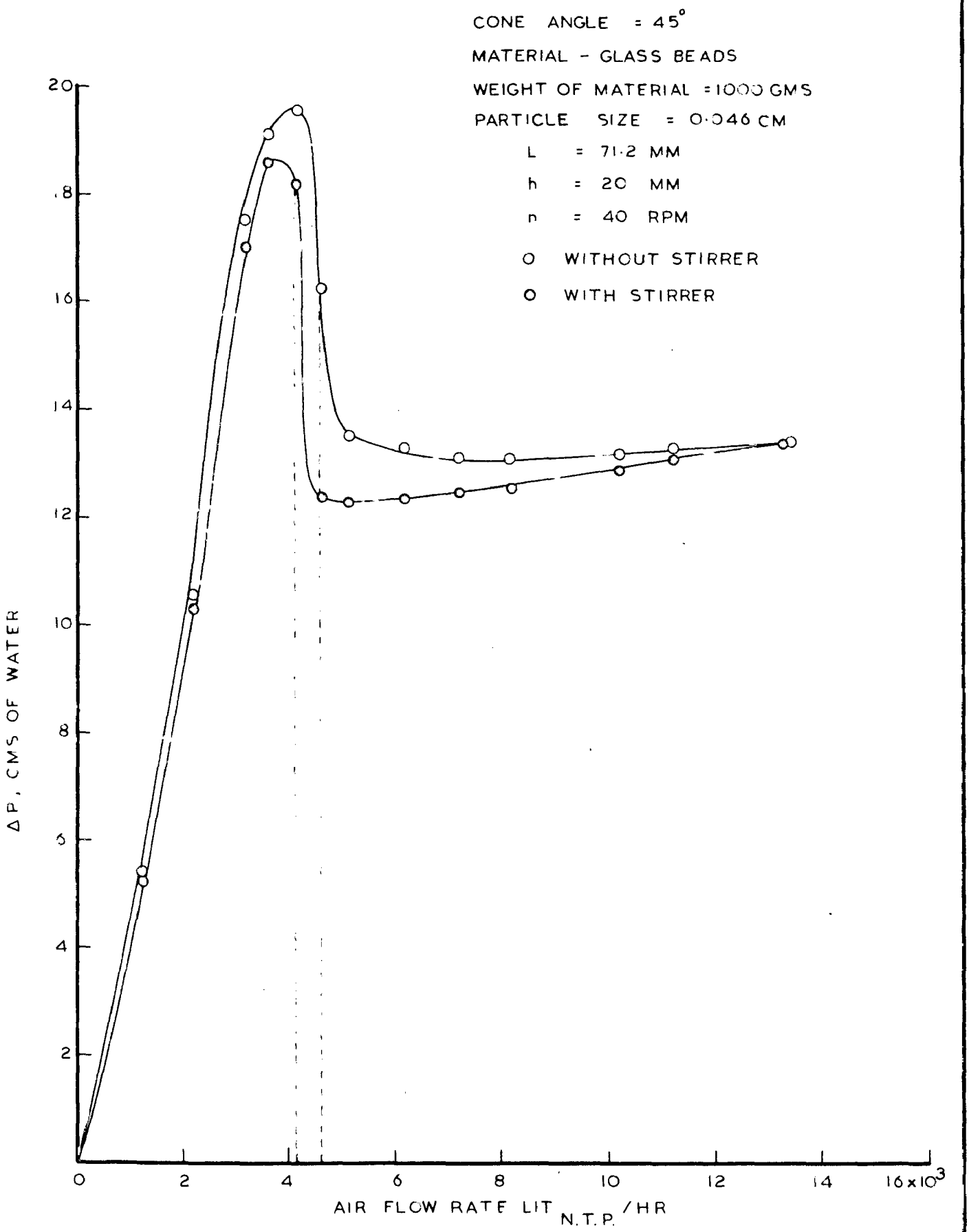

FIG. 4·4 VARIATION OF ΔP WITH AIR FLOW RATE WITH AND WITHOUT STIRRER FOR GLASS BEADS

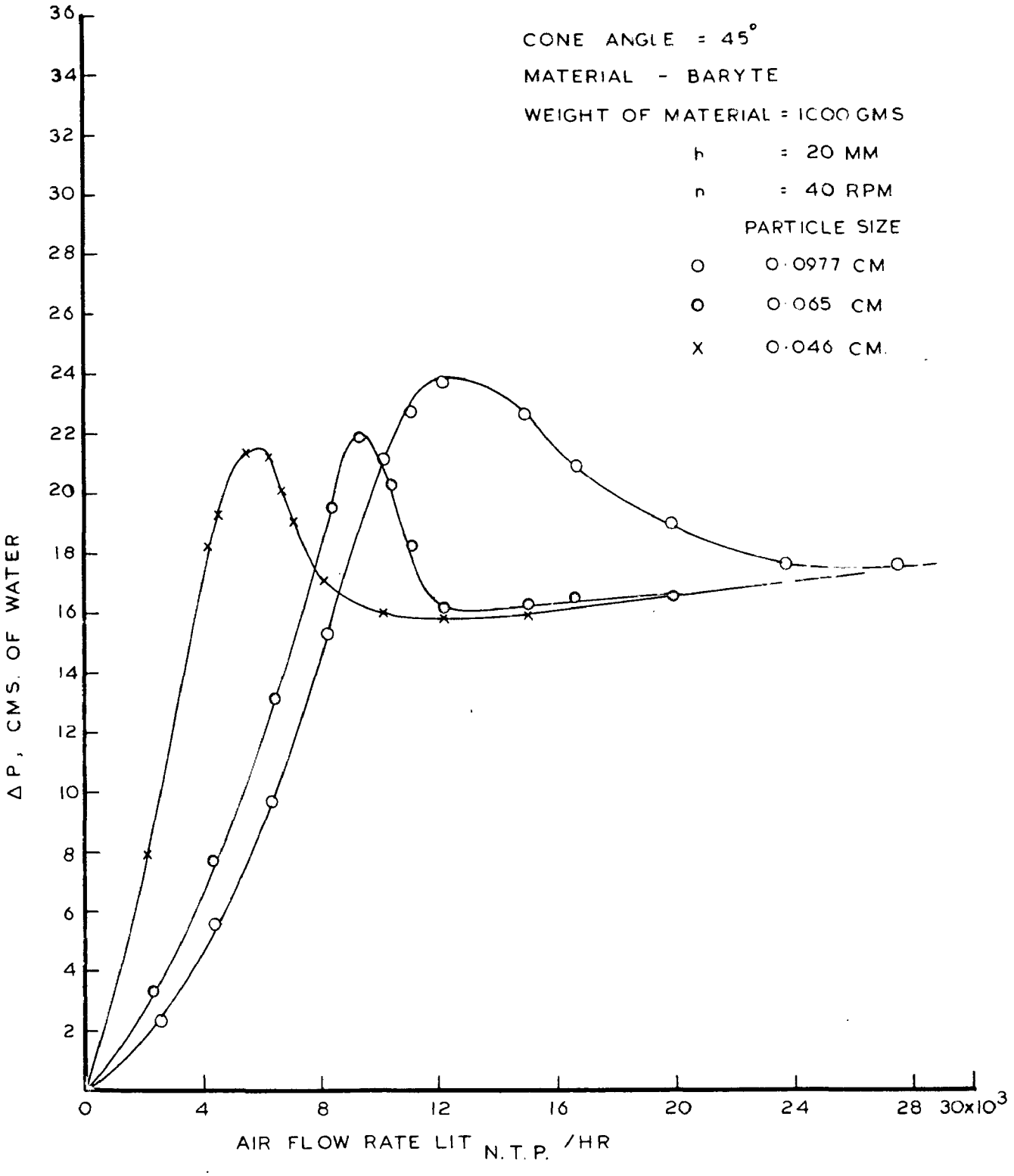

FIG. 4·5 VARIATION OF ΔP WITH AIR FLOW RATE WITH STIRRER FOR DIFFERENT SIZES OF BARYTE

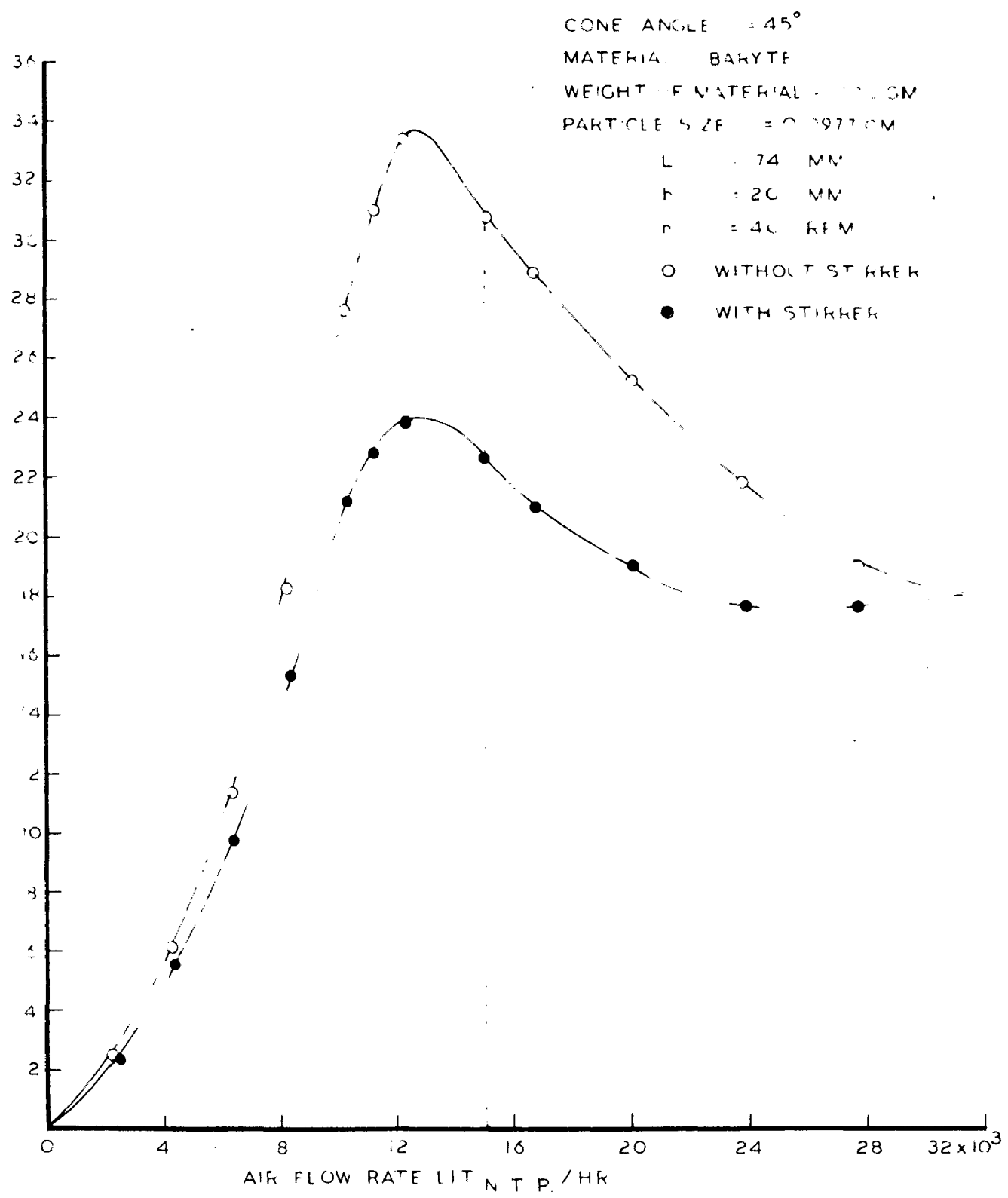

FIG 4·6 VARIATION OF ΔP WITH AIR FLOW RATE WITH AND WITHOUT STIRRER FOR BARYTE

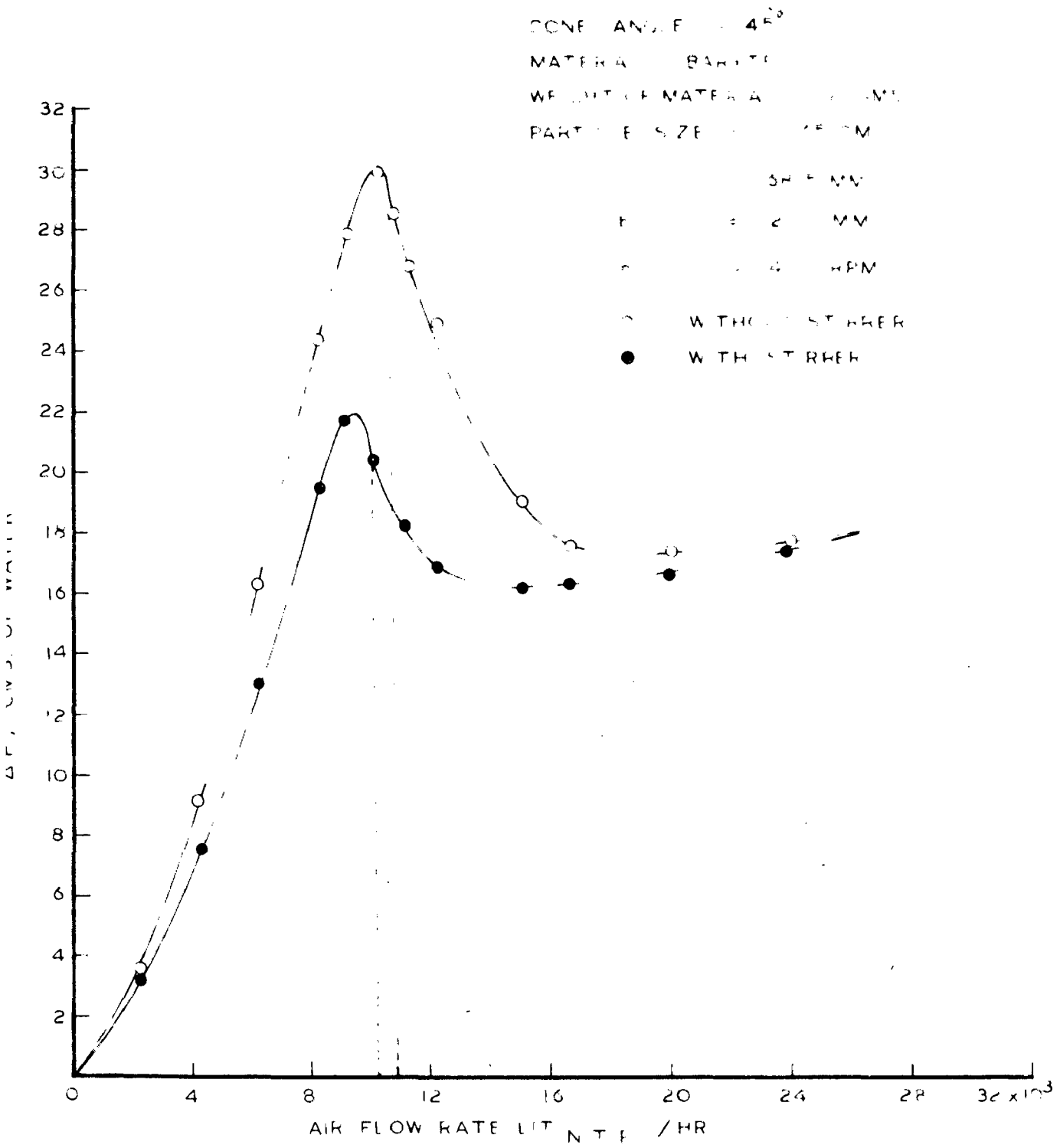

FIG 4·7 VARIATION OF ΔP WITH AIR FLOW RATE WITH AND WITHOUT STIRRER FOR BARYTE

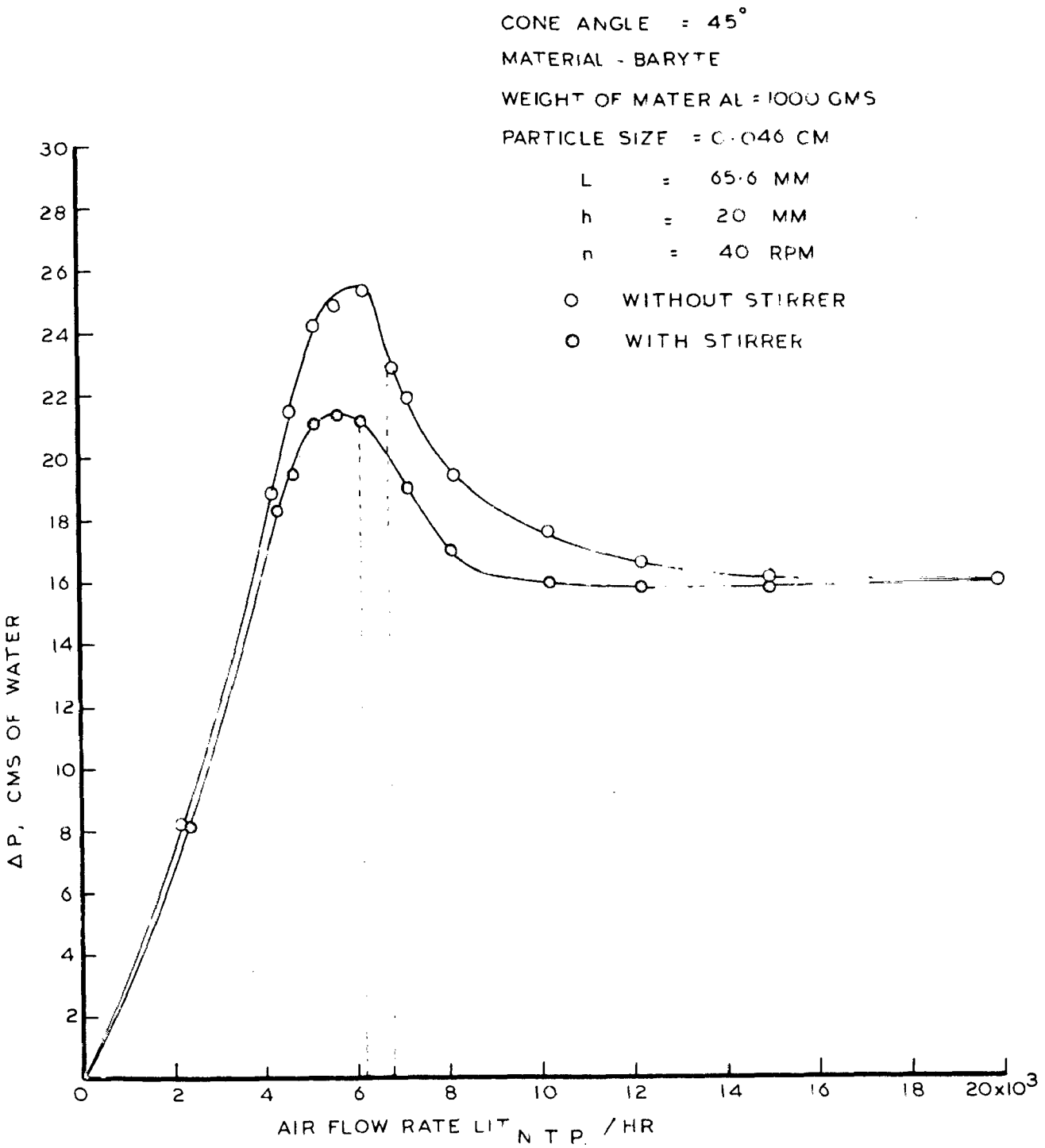

FIG. 4·8 VARIATION OF ΔP WITH AIR FLOW RATE WITH AND WITHOUT STIRRER FOR BARYTE

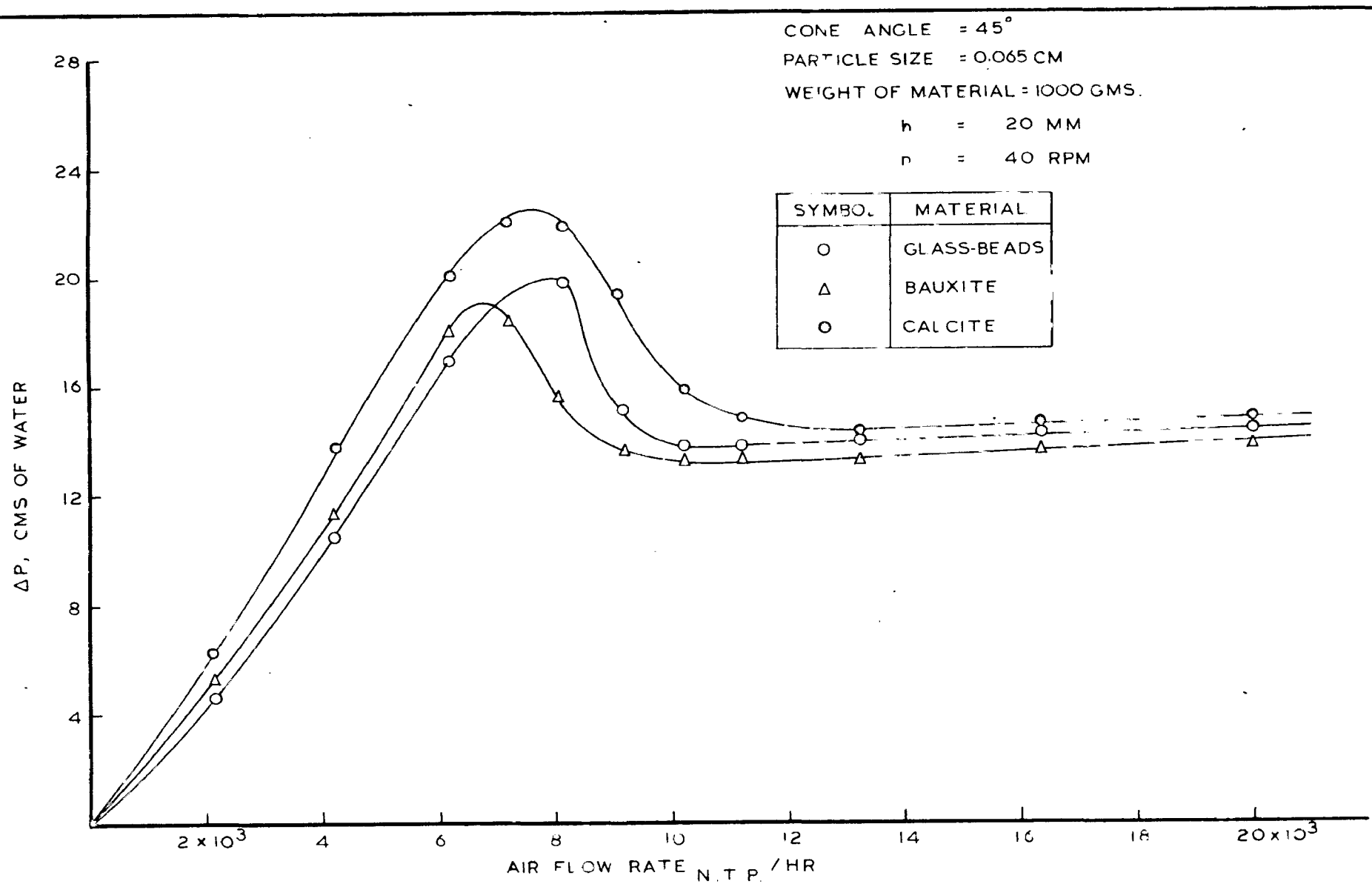

FIG. 4·9 VARIATION OF ΔP WITH AIR FLOW RATE FOR DIFFERENT MATERIALS OF SAME SIZE USING STIRRER

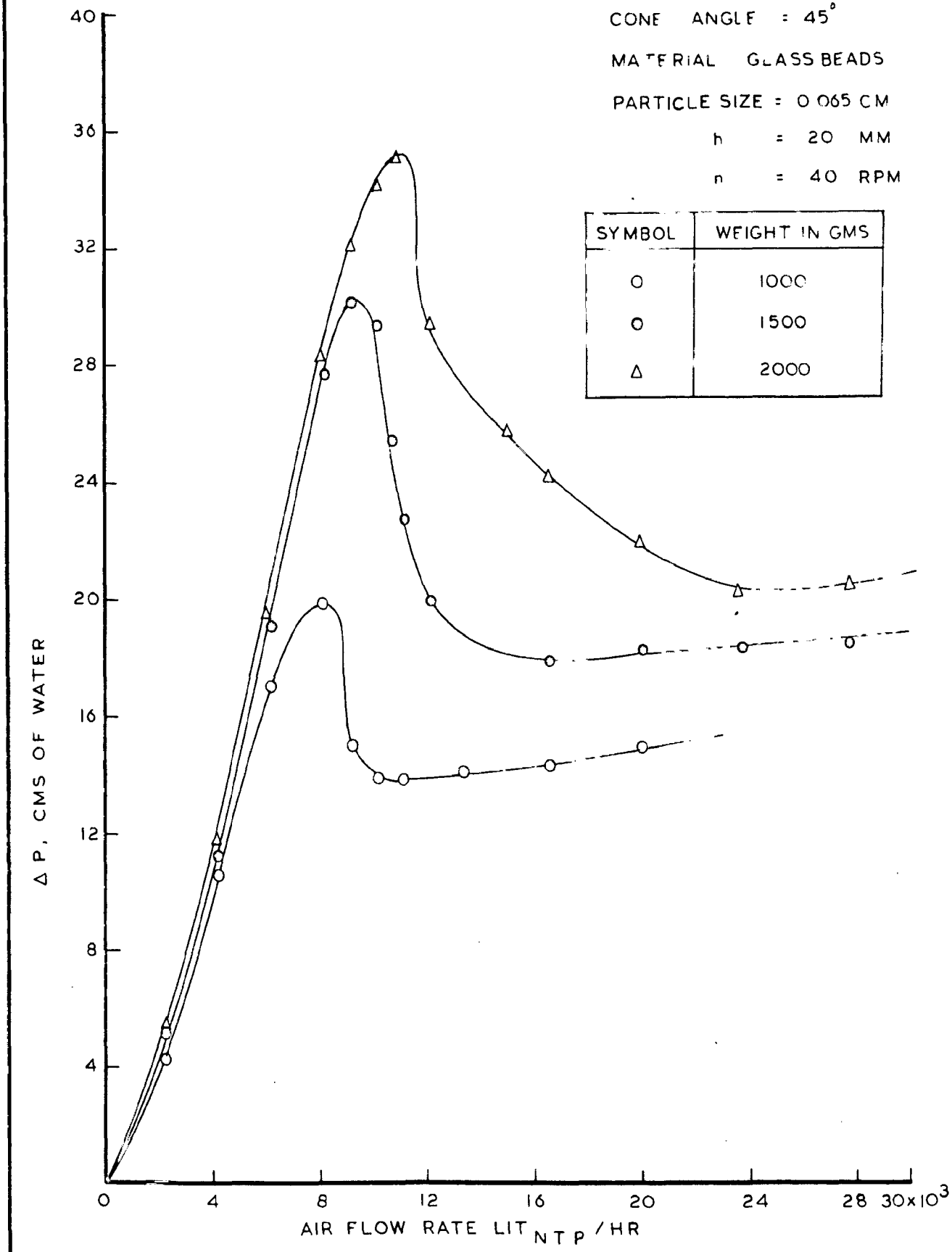

FIG. 4.10 VARIATION OF Δ P WITH AIR FLOW RATE FOR DIFFERET BED HEIGHTS OF GLASS BEADSUSING STIRRER

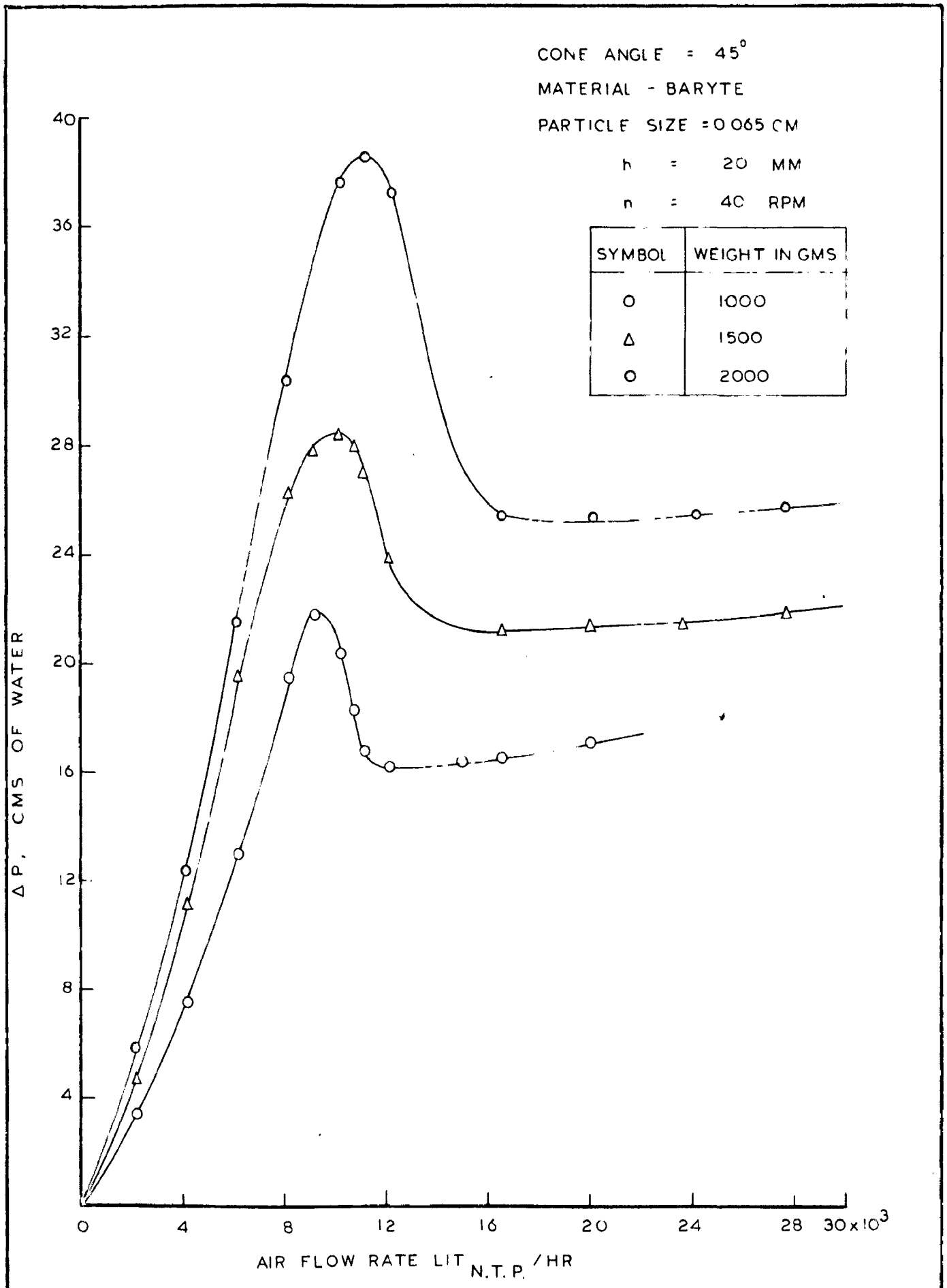

FIG. 4·11 VARIATION OF Δ P WITH AIR FLOW RATE FOR DIFFERENT BED HEIGHTS OF BARYTE USING STIRRER.

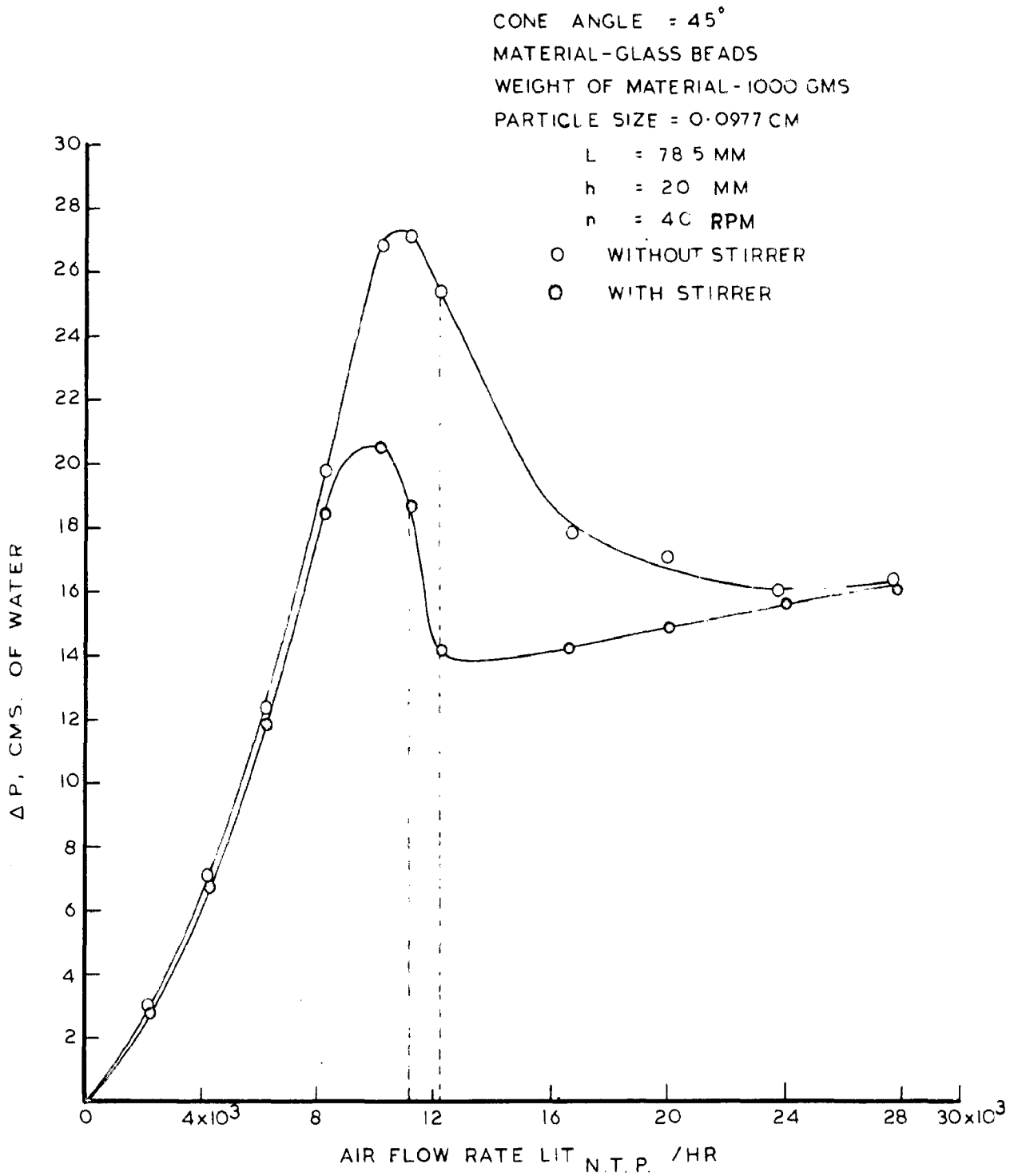

FIG. 4·2 VARIATION OF ΔP WITH AIR FLOW RATE WITH AND WITHOUT STIRRER FOR GLASS BEADS

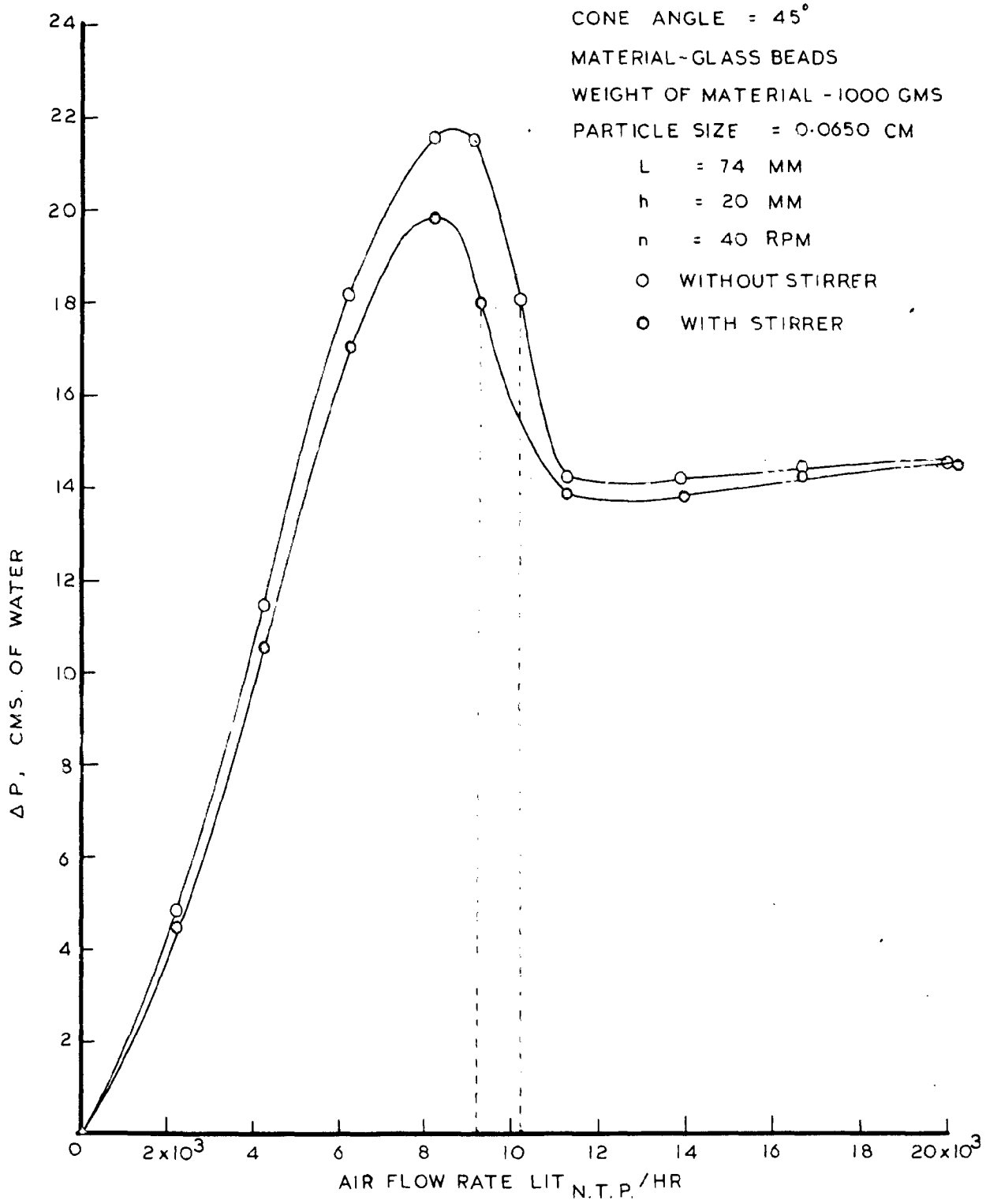

FIG 4·3 VARIATION OF ΔP WITH AIR FLOW RATE WITH AND WITHOUT STIRRER FOR GLASS BEADS

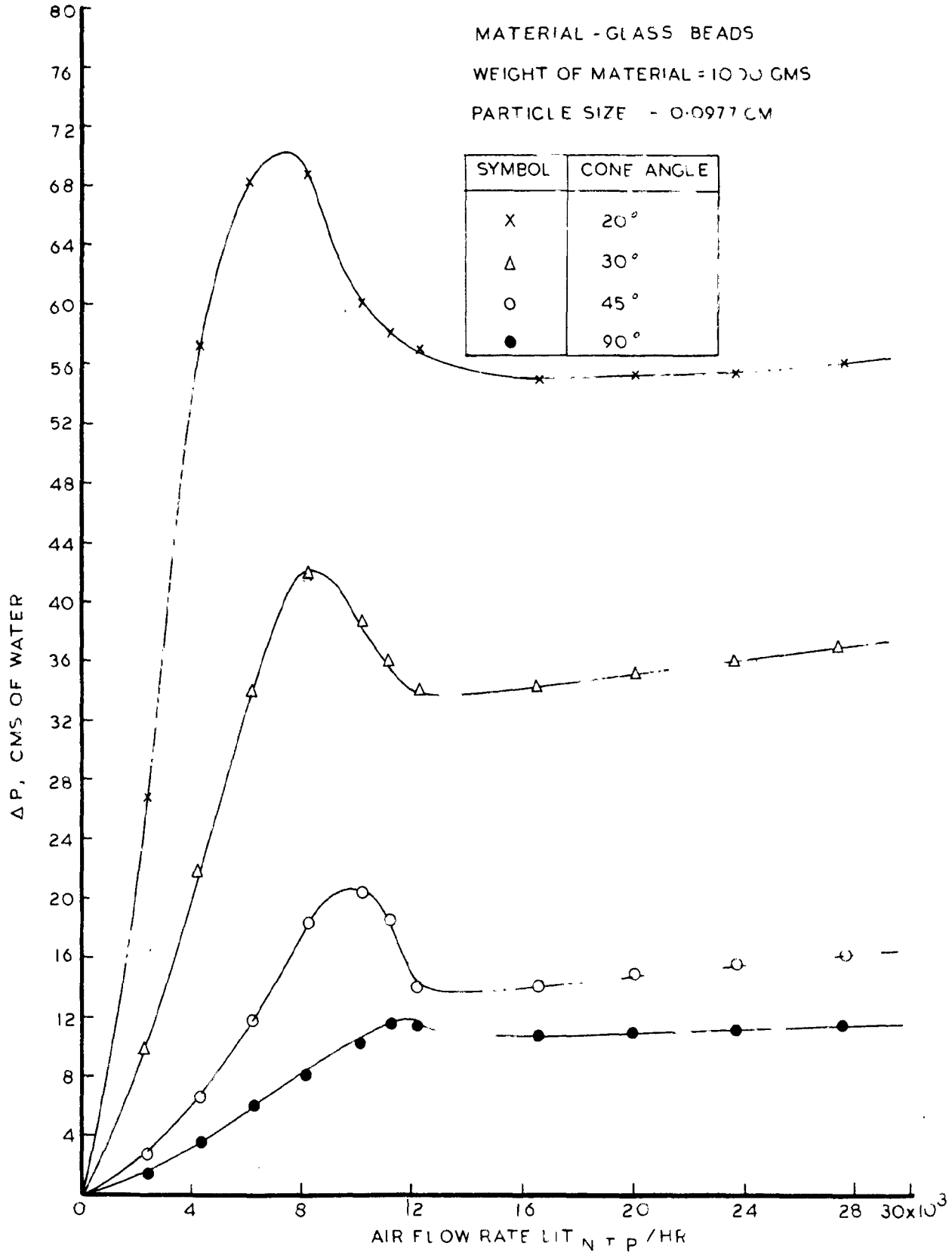

FIG. 4·12 VARIATION OF ΔP WITH AIR FLOW RATE FOR DIFFERENT CONE ANGLES FOR GLASS BEADS USING STIRRER

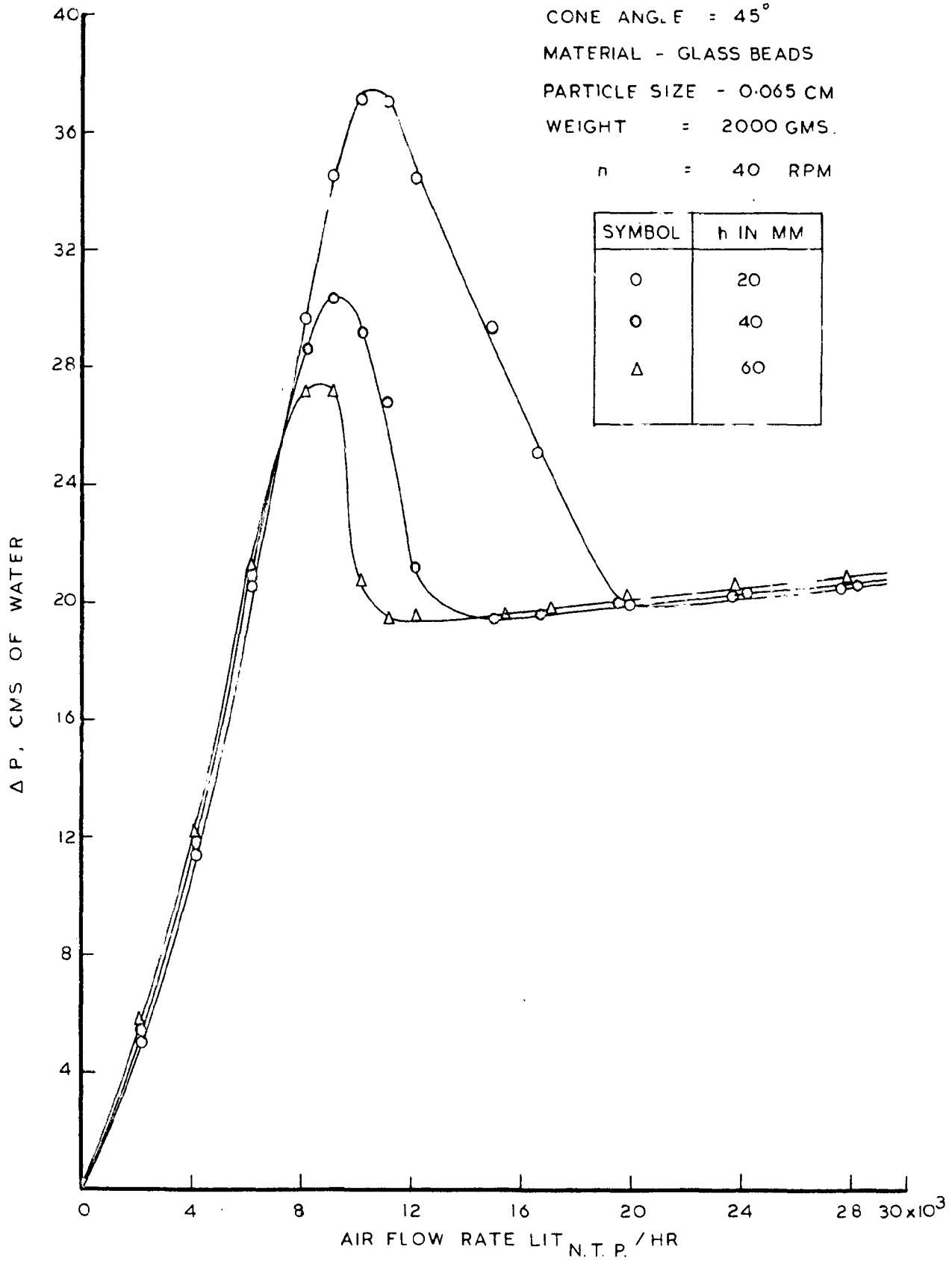

FIG. 4·13 VARIATION OF Δ P WITH AIR FLOW RATE FOR DIFFERENT DEPTHS OF STIRRER IN THE BED FOR GLASS BEADS

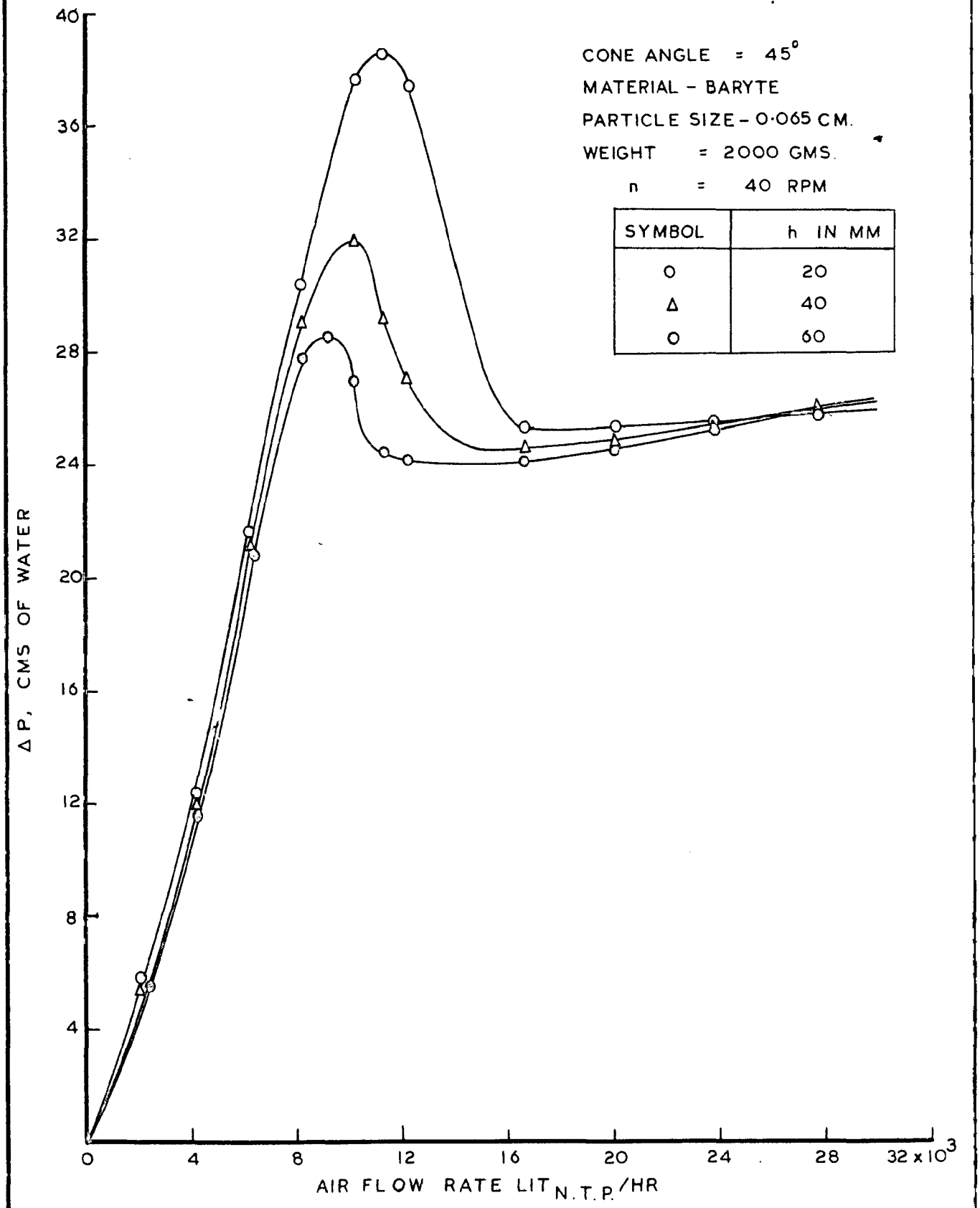

FIG. 4·14 VARIATION OF ΔP WITH AIR FLOW RATE FOR DIFFERENT DEPTHS OF STIRRER IN THE BED FOR BARYTE

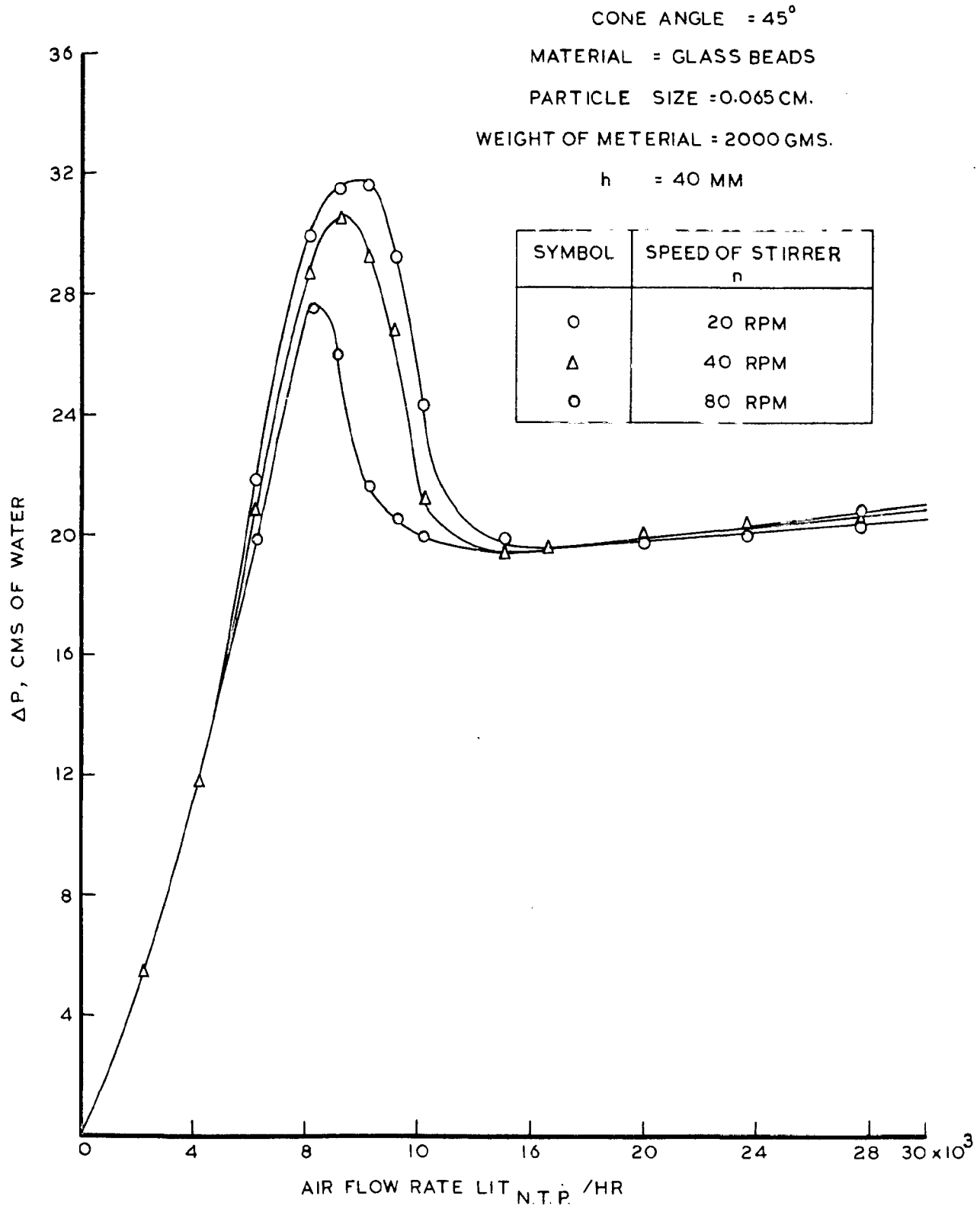

FIG. 4·15 VARIATION OF Δ P WITH AIR FLOW RATE BY VARYING THE STIRRER SPEED FOR GLASS BEADS

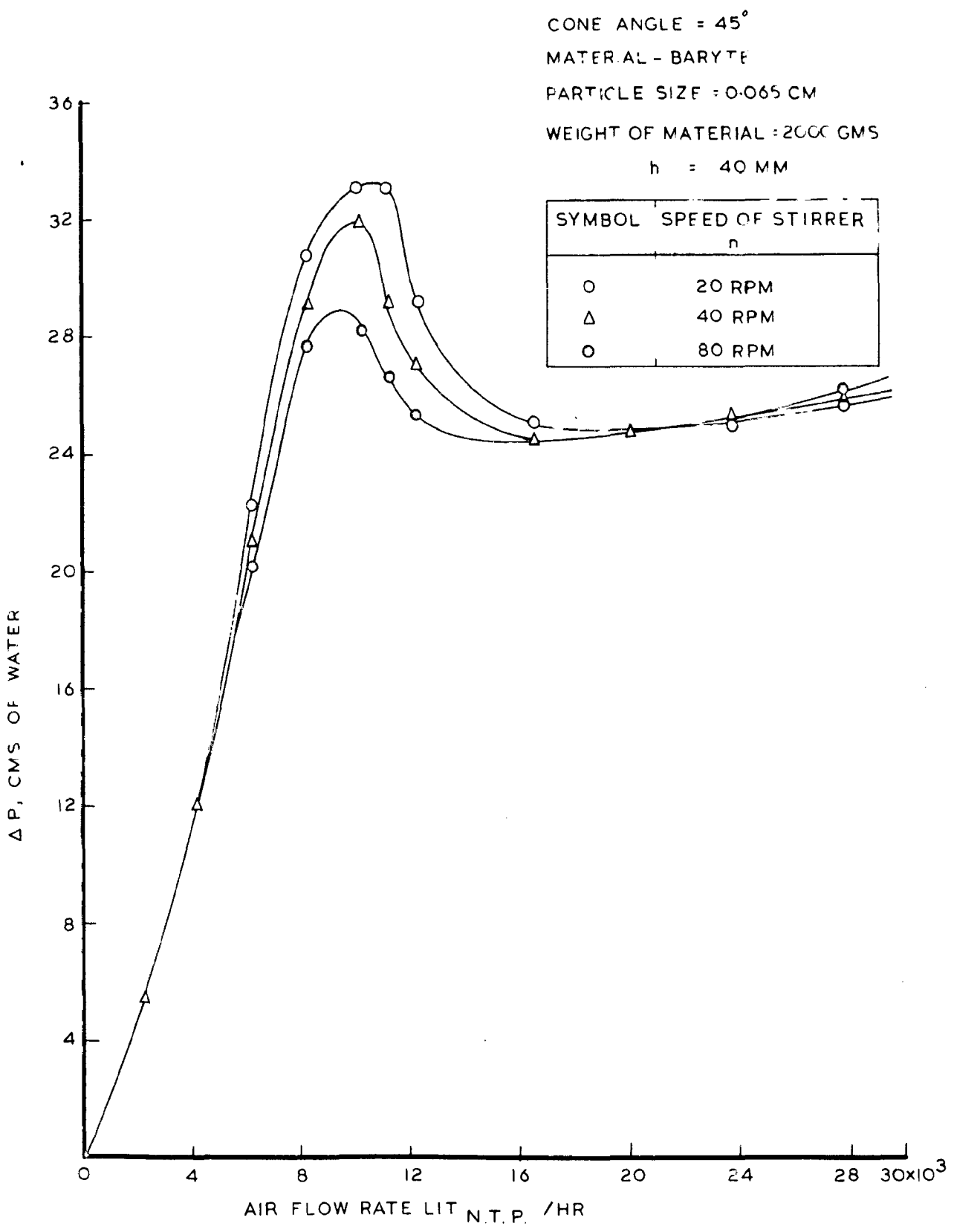

FIG. 4·16 VARIATION OF ΔP WITH AIR FLOW RATE BY VARYING THE SPEED OF STIRRER FOR BARYTE

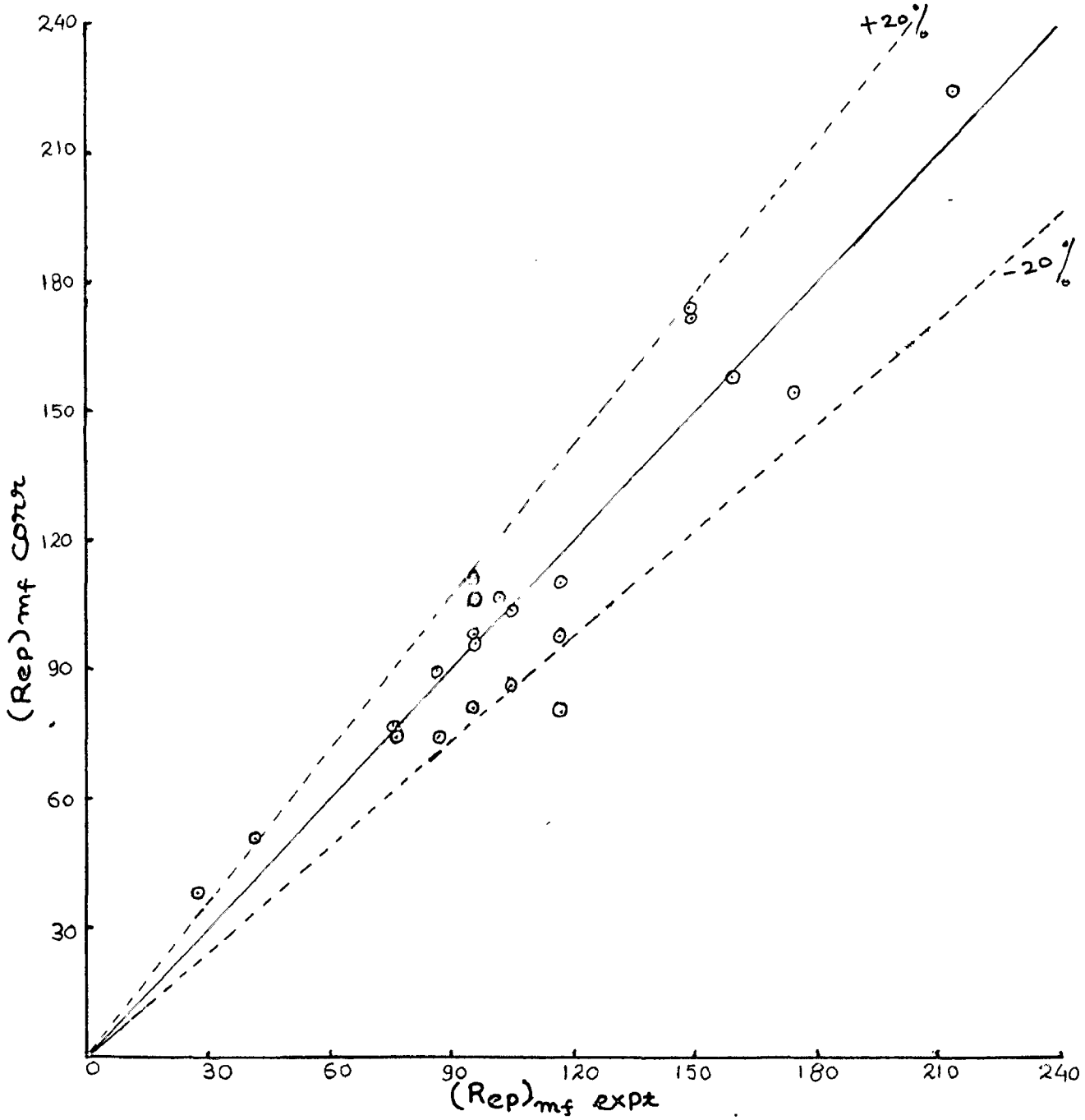

FIG 4.17 PLOT BETWEEN CORRELATED AND EXPEREIMENTAL VALUES OF $(Rep)_{mf}$

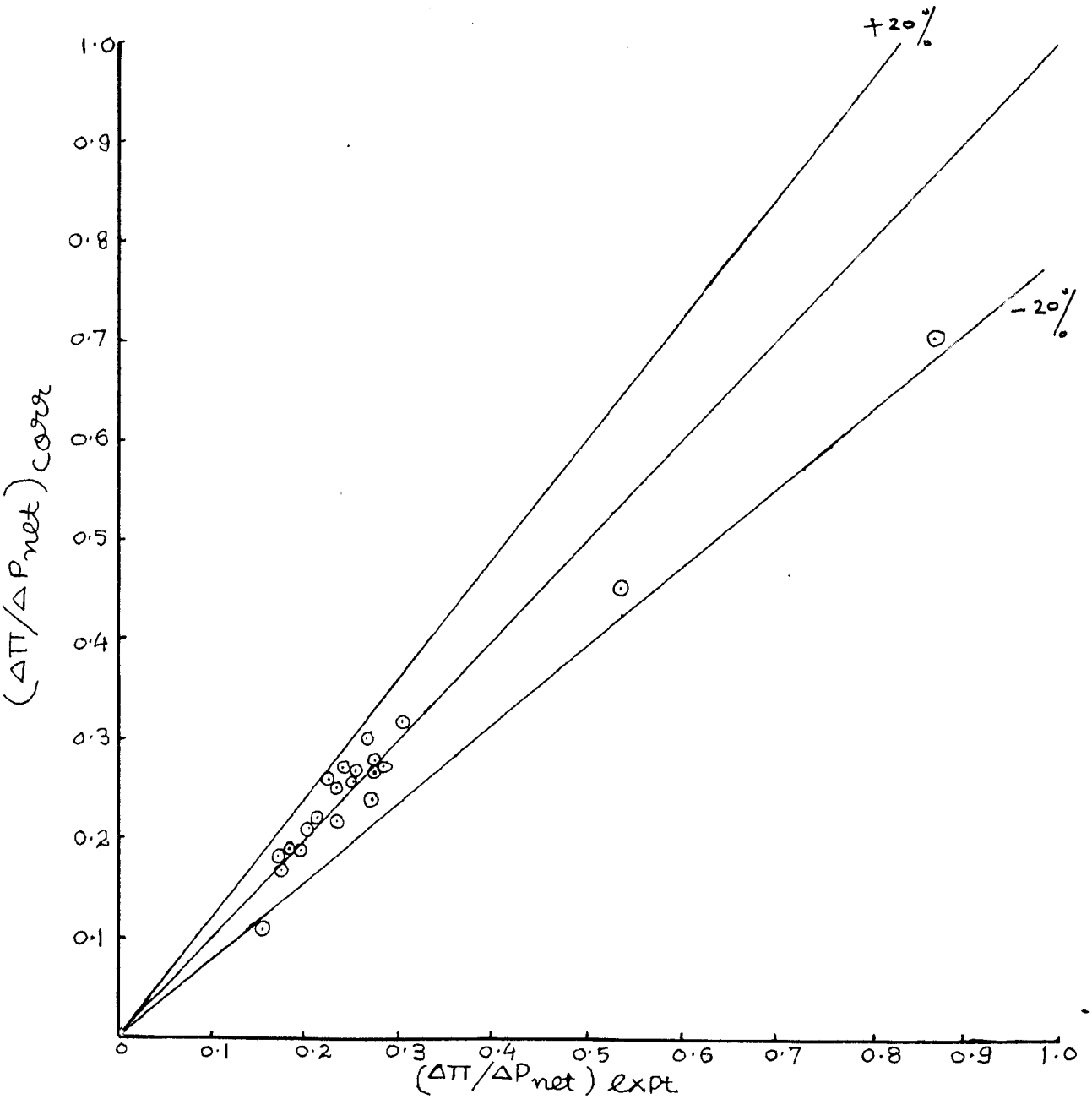

FIG 4.18 PLOT BETWEEN CORRELATED AND EXPERIMENTAL VALUES OF $\left(\frac{\Delta\Pi}{\Delta P_{net}}\right)$

CHAPTER-V

CONCLUSION AND RECOMMENDATIONS

CHAPTER - V

CONCLUSION AND RECOMMENDATIONS

Based on the present studies the following conclusions can be drawn:

1) In the vessels with taper angle more than 45° the fluidized bed tends towards non-uniformity on the walls of the vessel and spouting tendencies are observed at the centre of the bed.

2) Pressure peak values reduce in tapered vessels with large cone-angles which is caused by the fluidization of only a limited part of the bed confined to the central portion of the vessel.

3) Minimum fluidizing velocity and the pressure peak in tapered vessels can be computed using the generalized correlations vide equations 3.2 and 3.3 respectively.

4) The fluidization characteristics such as minimum fluidizing velocity and pressure-peak are observed to be lower in tapered beds when mechanical stirrer was employed as compared to those in the beds without stirrer. However, the trend of variation of pressure drop with air flow rate in beds with stirrer was similar to that of the beds without stirrer.

5) When mechanical stirrer is used in a tapered vessel, the power required for unlocking the particles in the bed is lower than the bed without stirrer.

6) Minimum fluidizing velocity and the pressure peak in tapered vessels can be computed using the generalized correlations vide equations 4.1 and 4.2

Further, work in following areas is recommended to be carried out so as to make the more generalized studies:

1) The size and type of the paddle of stirrer may be varied.

2) Bed expansion characteristics in tapered vessels with stirrer may be studied.

A P P E N D I C E S

APPENDIX- I

TABLE-1

Fluidization Studies in Tapered Vessels

Run No.	1	Cone Angle	= 45°
Material	Glass Beads	Weight of material	= 1 kg
Particle Size	= 0.0977 cm	Speed of stirrer, n	= 40 rpm
Depth of stirrer in the bed, h	= 20 mm	Height of fixed bed,	L, = 78.5 mm

S. No.	Air flow rate LIT N.T.P./HR	△P across bed (cms of water)	△P across bed using stirrer (cms of water)	Power consumed by stirrer (watts)
1.	2100	2.9	2.8	41.3
2.	4160	7.0	6.7	41.2
3.	6170	12.3	11.0	41.1
4.	0150	19.8	18.4	41.1
5.	10200	26.9	20.5✧	40.2
6.	11200✧✧	27.1✧	18.7	39.2
7.	12200✧✧	25.4	14.0	39.2
8.	16600	17.8	14.2	36.3
9.	20000	17.4	15.0	36.2
10.	23700	16.1	15.7	36.2
11.	27700	16.3	16.3	36.2

✧ Pressure peak with and without stirrer

✧✧ Air flow rate for minimum fluidization with and without stirrer.

TABLE-2

Fluidization Studies in Tapered Vessels

Run No.	- 2	Cone angle	= 45°
Material	- Glass Beads	Weight of material	= 1 Kg
Particle Size	- 0.065 cm		
Depth of stirrer in the bed,	h = 20 mm	Speed of stirrer, n	= 40 rpm
Height of fixed bed,	L = 74 mm		

S. No.	Air flow rate LIT/HR N.T.P.	ΔP across bed (cms of water)	ΔP across bed using stirrer (cms of water)	Power consumed by stirrer watts.
1.	2180	4.8	4.8	39.2
2.	4160	11.1	10.5	39.2
3.	6170	18.1	17.0	38.1
4.	8150	21.6	19.8*	37.3
5.	9180**	21.8*	15.1	37.3
6.	10200**	18.0	13.8	36.3
7.	11200	14.2	13.8	36.3
8.	13400	14.2	14.1	34.4
9.	16600	14.4	14.3	34.4
10.	20000	14.4	14.4	33.5
11.	23700	14.5	-	-

* → Pressure peak with and without stirrer

** → Air flow rate for minimum fluidization with and without stirrer.

TABLE-3

Fluidisation Studies in Tapered Vessels

Run No. = 3 Cone angle = 45°

Material = Glass Beads Weight of material = 1 Kg

Particle Size = 0.046 cm Speed of stirrer, n = 40 rpm

Depth of stirrer in the bed, h = 20 mm

Height of fixed bed L = 71.2 mm

S. No.	Air flow rate LIT/HR N.T.P.	ΔP across bed (Cms of water)	ΔP across bed using stirrer (cms of water)	Power consumed by stirrer (watts)
1.	1200	5.4	5.3	39.6
2.	2180	10.6	10.3	39.5
3.	3180	17.5	17.0	39.2
4.	3620	19.1	18.4+	38.8
5.	4160++	19.5+	18.2	38.1
6.	4600++	16.2	12.4	30.0
7.	5130	13.5	12.3	37.7
8.	6170	13.3	12.3	37.5
9.	7200	13.1	12.4	36.8
10.	8150	13.1	12.4	36.3
11.	10200	13.2	12.7	36.3
12.	11200	13.3	13.1	35.4
13.	13400	13.4	13.4	35.4
14.	16600	13.5	-	-

+ Pressure peak with and without stirrer

++ Air flow rate for minimum fluidisation with and without stirrer

TABLE-4

Fluidization Studies in Tapered Vessels

Run No. - 4 Cone-angle = 45°

Material - Baryte Weight of material= 1 Kg

Particle Size 0.0977 cm Speed of stirrer n= 40 rpm

Depth of stirrer in the bed, h = 20 mm

Height of the fixed bed L = 74 mm

S. No.	Air flow rate LIT/HR N.T.P.	Δ P across bed (cms of water)	Δ P across bed using stirrer (cms of water)	Power consumed by stirrer (watts)
1.	2100	2.4	5.3	39.3
2.	4160	6.1	5.6	38.8
3.	6170	11.3	9.7	38.6
4.	8150	18.2	15.3	38.4
5.	10200	27.6	21.2	38.1
6.	11200	30.9	22.8	37.8
7.	12200	33.4+	23.7+	37.3
8.	15000++	30.7	22.6	37.3
9.	16600	28.9	21.2	37.2
10.	20000	25.2	19.0	37.0
11.	23700	21.8	17.7	36.8
12.	27700	19.0	17.8	36.8

+ Pressure peak with and without stirrer.

++ Air flow rate for minimum fluidisation with and without stirrer.

TABLE-5

Fluiddization Studies in Tapered Vessels

Run No.	= 5	Cone angle	= 45°
Material	= Baryte	Weight of material	= 1 Kg
Particle Size	= 0.065 cm	Speed of stirrer, n	= 40 rpm

Depth of stirrer in the bed, h = 20 m.m.

Height of fixed bed, L = 68.5 m.m.

S. No.	Air flow rate LIT/HR. N.T.P.	ΔP across bed (cms of water)	ΔP across bed using stirrer (cms of water)	Power consumed by stirrer (watts)
1.	2180	3.6	3.4	39.2
2.	4160	9.1	7.6	38.9
3.	6170	16.3	13.0	38.6
4.	8150	24.4	19.5	38.4
5.	9180	27.8	21.8*	38.10
6.	10200**	29.9*	20.4	37.70
7.	10800**	28.6	18.3	37.20
8.	11200	26.8	16.8	36.80
9.	12200	25.0	16.2	36.30
10.	15000	19.1	16.4	36.30
11.	16600	17.6	16.6	36.20
12.	20000	17.4	17.2	36.20

* Pressure peak with and without stirrer

** Air flow rate for minimum fluidization with and without stirrer.

TABLE-6

Fluidization Studies in Tapered Vessels

Run No. - 6 Cone angle = 45°

Material - Baryte Weight of material = 1 Kg

Particle Size = 0.046 cm Speed of stirrer, n = 40 rpm

Depth of stirrer in the bed , h = 20 m.m.

Height of fixed bed, L = 65.6 m.m.

S. No.	Air flow rate LIT/HR. N.T.P.	ΔP across the bed (cms of water	ΔP across bed using stirrer (cms of water)	Power consumed by the stirrer (watts)
1.	2180	8.1	8.0	37.00
2.	4160	18.8	18.3	37.00
3.	4660	21.5	19.3	36.80
4.	5130	24.3	21.0	36.80
5.	5660	24.8	21.4*	36.50
6.	6170**	25.4*	21.2	35.90
7.	6720**	22.9	20.1	35.70
8.	7200	21.9	19.0	35.70
9.	8150	19.4	17.0	35.40
10.	10200	17.6	16.0	35.40
11.	12200	16.6	15.9	35.40
12.	15000	16.1	15.8	35.20
13.	20000	16.0	-	35.20

* Pressure peak with and without stirrer

** Air flow rate for minimum fluidization with and without stirrer.

TABLE-7

Fluidization Studies in Tapered Vessels

Run No. - 7 Cone angle = 45°
Material - Bauxite Weight of material= 1 kg
Particle size = 0.065 cm Speed of stirrer,n= 40 rpm
Depth of Stirrer in the bed, h = 20 mm
Height of fixed bed, L = 95.2 mm

S. No.	Air flow rate LIT/HR N.T.P.	ΔP across bed (cms of water)	ΔP across bed using stirrer (cms of water)	Power consumed by stirrer (watts)
1.	2180	5.6	5.4	39.80
2.	4160	12.0	11.3	39.60
3.	6170	19.3	17.8	39.40
4.	7200	21.0+	18.4+	38.20
5.	8150 ++	18.4	15.6	38.10
6.	9180	15.1	13.6	38.10
7.	10200	13.8	13.3	37.70
8.	11200	13.7	13.2	37.70
9.	13400	13.7	13.9	37.30
10.	16600	14.0	13.7	37.10
11.	20000	14.1	14.0	36.80

\+ Pressure peak with and without stirrer

++ Air flow rate for minimum fluidization with and without stirrer.

TABLE-3

Fluidisation Studies in Tapered Vessels

Run No. - 8 Cone angle = 45°

Material - Calcite Weight of material = 1 Kg

Particle size = 0.065 cm Speed of stirrer, n = 40 rpm

Depth of stirrer in the bed, h = 20 mm

Height of fixed bed, L = 68 mm

S. No.	Air flow rate LIT/HR N.T.P.	ΔP across bed (cms of water)	ΔP across bed with stirrer (cms of water)	Power consumed by stirrer (watts)
1.	2180	6.5	6.3	39.3
2.	4160	15.2	13.8	38.8
3.	6170	23.2	20.0	38.8
4.	7200	25.9	22.0*	38.6
5.	8150**	26.0*	21.9	38.4
6.	9180**	24.8	19.4	38.4
7.	10200	19.8	15.8	38.1
8.	11200	15.8	14.8	37.8
9.	13400	14.6	14.3	37.8
10.	16000	14.8	14.6	37.3
11.	20000	15.3	15.0	37.3

* Pressure peak with and without stirrer

** Air flow rate for minimum fluidization with and without stirrer.

TABLE-9

Fluidisation Studies in Tapered Vessels

Run No. = 9 Cone angle = 45°

Material = Glass beads Weight of material = 1.5 Kg

Particle Size = 0.065 cm Speed of stirrer, n = 40 rpm

Depth of stirrer in the bed, h = 20 mm

Height of fixed bed, L = 98 mm

S. No.	Air flow rate LIT/HR N.T.P.	ΔP across bed (cms of water)	ΔP across bed using stirrer (cms of water)	Power consumed by stirrer (watts)
1.	2180	5.4	5.2	37.10
2.	4160	11.8	11.2	36.00
3.	6170	20.0	18.8	36.80
4.	8150	29.9	27.7	36.60
5.	9180	34.5	30.2*	36.60
6.	10200**	36.5*	29.4	36.30
7.	10800**	33.3	26.7	35.90
8.	11200	32.0	22.0	34.90
9.	12200	27.7	20.0	34.70
10.	16600	18.8	17.8	34.40
11.	20000	18.4	18.2	34.40
12.	23700	18.4	18.3	34.20

* Pressure peak with and without stirrer

** Air flow rate for minimum fluidisation with and without stirrer.

TABLE-10

Fluidization Studies in Tapered Vessels

Run No.	= 10	Cone angle	= 45°
Material	= Glassbeads	Weight of material	= 2 Kg
Particle Size	= 0.065 cm	Speed of stirrer, n	= 40 rpm
Depth of stirrer in the bed,		h = 20 mm	
Height of fixed bed,		L = 115 mm	

S. No.	Air flow rate LIT/HR. N.T.P.	ΔP across bed (cms of water)	ΔP across bed using stirrer (cms of water)	Power consumed by stirrer (watts)
1.	2180	5.6	5.4	39.20
2.	4160	12.4	11.8	39.20
3.	6170	21.0	19.4	39.00
4.	8150	30.0	28.2	38.80
5.	9180	35.0	32.0	38.80
6.	10200	37.5	34.0	38.60
7.	11200	39.2✧	35.0✧	37.70
8.	12200✧✧	37.1	30.4	37.70
9.	15000	33.0	25.8	37.00
10.	16600	29.7	24.2	35.90
11.	20000	25.6	21.8	35.20
12.	23700	21.3	20.3	35.20
13.	27700	21.4	20.5	35.20

✧ Pressure peak with and without stirrer

✧✧ Air flow rate for minimum fluidization with and without stirrer.

TABLE-11

Fluidization Studies in Tapered Vessels

Run No.	= 11	Cone angle	= 45°
Material	= Baryte	Weight of material	= 1.5 Kg
Particles Size	= 0.065 cm	Speed of stirrer, n	= 40 rpm

Depth of stirrer in the bed, h = 20 mm

Height of fixed bed, L = 85 mm

S. No.	Air flow rate LIT/HR. N.T.P.	ΔP across bed (cms of water)	ΔP across bed using stirrer (cms of water)	Power consumed by stirrer (watts)
1.	2100	4.0	4.7	39.20
2.	4160	12.2	11.2	38.80
3.	6170	21.9	19.6	38.80
4.	8150	33.9	30.2	38.60
5.	9300	39.9	31.0	38.30
6.	10200	42.0	32.4*	38.10
7.	10000**	42.6*	32.0	37.80
8.	11200**	40.9	31.0	37.50
9.	12200	38.2	23.8	37.20
10.	16600	29.4	21.2	36.50
11.	20000	24.6	21.4	36.10
12.	23700	22.6	21.5	35.90
13.	27700	22.7	21.7	35.70

* Pressure peak with and without stirrer

** Air flow rate for minimum fluidization with and without stirrer.

TABLE-12

Fluidization Studies in Tapered Vessels

Run No. - 12 Cone angle = 45°
Material - Baryte Weight of material = 2.0 Kg
Particle Size- 0.065 cm Speed of stirrer,n = 40 rpm
Depth of stirrer in the bed, h = 20 m.m.
Height of fixed bed, L = 102 m.m.

S. No.	Air flow rate LIT/HR. N.T.P.	ΔP across bed (cms of water)	ΔP across bed using stirrer (cms of water)	Power consumed by stirrer (watts)
1.	2180	6.0	5.8	38.00
2.	4160	13.4	12.4	37.80
3.	6170	24.8	21.6	37.60
4.	8150	37.3	30.4	37.00
5.	10200	43.4	37.6	37.60
6.	11200	44.6	38.6*	37.50
7.	12200**	45.0*	37.4	36.80
8.	16600**	35.6	25.3	36.60
9.	20000	30.0	25.4	36.00
10.	23700	26.6	25.5	35.20
12.	27700	26.8	25.7	34.70

* Pressure peak with and without stirrer

** Air flow rate for minimum fluidization with and without stirrer

TABLE-13

Fluidisation Studies in Tapered Vessels

Run No	13	Cone angle	= 20°
Material	Glass-beads	Weight of material	= 1 Kg
Particle Size	0.0977 cm	Speed of stirrer, n	= 40 rpm

Depth of stirrer in the bed, h = 20 mm

Height of fixed bed, L = 151 mm

S. No.	Air flow rate LIT/HR N.T.P.	ΔP across bed (cms of water)	ΔP across bed using stirrer (cms of water)	Power consumed by stirrer (watts)
1.	2180	28.0	27.0	40.2
2.	4160	61.2	57.2	39.8
3.	6170	75.4	68.0	39.8
4.	8150	76.8✧	68.8✧	39.2
5.	10200✧✧	67.6	60.0	38.4
6.	11200	64.8	58.0	38.0
7.	12200	61.0	57.0	37.6
8.	16600	56.8	55.0	37.0
9.	20000	56.0	55.4	36.2
10.	23700	55.6	55.5	36.2
11.	27700	56.0	56.0	36.2

✧ Pressure peak with and without stirrer

✧✧ Air flow rate for minimum fluidization with and without stirrer.

TABLE-14

Fluidization Studies in Tapered Vessels

Run No. 14 Cone angle = 30°

Material - Glass-beads Weight of material = 1 Kg

Particle Size = 0.0977 cm Speed of stirrer, n = 40 rpm

Depth of stirrer in the bed, h = 20 mm

Height of fixed bed L = 128 mm

S. No.	Air flow rate LIT/H.R. N.T.P.	ΔP across bed (cms of water	ΔP across bed using stirrer (cms of water)	Power consumed by stirrer (watts)
1.	2180	10.2	10.0	39.80
2.	4160	24.4	22.0	39.80
3.	6170	40.4	34.0	39.60
4.	8150	54.5*	42.0*	39.20
5.	10200**	53.0	38.8	38.80
6.	11200	50.4	36.0	38.60
7.	12200	46.0	34.20	37.40
8.	16600	41.0	34.40	37.00
9.	20000	40.8	35.2	36.20
10.	23700	40.0	36.0	36.20
11.	27700	40.2	37.0	36.20

* Pressure peak with and without stirrer

** Air flow rate for minimum fluidization with and without stirrer

TABLE-15

Fluidization Studies in Tapered Vessels

Run No. - 15 Cone angle = 90°

Material - Glass-beads Weight of material = 1 kg

Particle Size = 0.0977 cm Speed of stirrer, n = 40 rpm

Depth of stirrer in the bed, h = 20 mm

Height of fixed bed, L = 62 mm

S. No.	Air flow rate LIT/H.R N.T.P.	ΔP across bed (cms of water)	ΔP across bed using stirrer (cms of water)	Power consumed by stirrer (watts)
1.	2180	1.6	1.5	39.60
2.	4160	4.0	3.7	39.40
3.	6170	6.8	6.2	39.20
4.	8150	8.9	8.1	39.00
5.	10200	12.6	11.3	38.60
6.	11200	13.2	11.8*	38.60
7.	12200**	14.4*	11.6	38.40
8.	16600**	12.2	10.8	38.00
9.	20000	11.4	11.0	37.60
10.	23700	11.8	11.4	37.60
11.	27700	11.6	11.5	37.60

* Pressure peak with and without stirrer

** Air flow rate for minimum fluidization with and without stirrer

TABLE-16

Fluidization Studies in Tapered Vessels

Run No. - 16 Cone angle = 45°

Material - Glass-beads Weight of material= 2 Kg

Particle Size = 0.065 cm Speed of stirrer, n= 40 rpm

Depth of stirrer in the bed, h = 40 mm

Height of fixed bed, L = 115 mm

S. No.	Air flow rate LIT/HR. N.T.P.	ΔP across bed (cms of water)	ΔP across bed using stirrer (cms of water)	Power consumed by stirrer (watts)
1.	2180	5.6	5.4	39.80
2.	4160	12.4	11.8	39.60
3.	6170	21.0	20.8	39.20
4.	8150	30.0	28.6	39.00
5.	9180	35.0	30.4✧	39.00
6.	10200✧✧	37.5	29.2	38.40
7.	11200	39.2✧	26.8	36.80
8.	12200✧✧	37.1	21.2	36.30
9.	15000	33.0	19.4	35.40
10.	16600	29.7	19.6	35.30
11.	20000	25.6	20.0	35.20
12.	23700	21.3	20.4	35.20
13.	27700	21.4	20.4	35.20

✧ Pressure peak with and without stirrer

✧✧ Air flow rate for minimum fluidization with and without stirrer.

TABLE-17

Fluidisation Studies in Tapered Vessels

Run No. - 17 Cone angle = 45°
Material - Glass-beads Weight of material = 2 Kg
Particle Size - 0.065 cm Speed of stirrer, n = 40 rpm
Depth of stirrer in the bed, h = 60 mm
Height of fixed bed, L = 115 mm

S. No.	Air flow rate LIT/HR. N.T.P.	ΔP across bed (cms of water)	ΔP across bed using stirrer (watts)	Power consumed by stirrer (watts)
1.	2180	5.6	5.6	37.90
2.	4160	12.4	12.2	37.70
3.	6170	21.0	20.9	37.50
4.	8150	30.0	27.2	37.10
5.	9180	35.0	27.2*	36.80
6.	10200**	37.5	20.7	36.80
7.	11200	39.2*	19.4	36.10
8.	12200**	37.1	19.4	35.20
9.	15000	33.0	19.4	34.70
10.	16600	29.7	19.6	34.70
11.	20000	25.6	20.0	34.70
12.	23700	21.3	20.4	34.50
13.	27700	21.4	20.5	34.50

* Pressure peak with and without stirrer.
** Air flow rate for minimum fluidisation with and without stirrer.

TABLE-18

Fluidisation Studies in Tapered Vessels

Run No. - 18 Cone angle = 45°
Material - Baryte Weight of material = 2 Kg
Particle Size = 0.065 cm Speed of stirrer, n = 40 rpm
Depth of stirrer in the bed, h = 40 cm
Height of fixed bed, L = 102 mm

S. No.	Air flow rate LIT/HR. N.T.P.	Δ P across bed (cms of water)	Δ P across bed using stirrer (cms of water)	Power consumed by stirrer (watts)
1.	2180	6.0	5.7	38.20
2.	4160	13.4	12.0	38.20
3.	6170	24.8	21.0	38.00
4.	8150	37.3	29.0	37.80
5.	10200	43.4	31.8*	37.60
6.	11200**	44.6	29.2	37.60
7.	12200	45.2*	27.0	37.50
8.	16600**	35.6	24.6	36.60
9.	20000	30.0	24.8	36.00
10.	23700	26.6	25.4	35.20
11.	27700	26.8	26.0	35.20

* Pressure peak with and without stirrer.

** Air flow rate for minimum fluidisation with and without stirrer.

TABLE-19

Fluidisation Studies in Tapered Vessels

Run No. = 19 Cone angle = 45°
Material = Baryte Weight of material = 2 Kg
Particle Size = 0.065 cm Speed of stirrer, n = 40 rpm
Depth of stirrer in the bed, h = 60 mm
Height of fixed bed, L = 102 mm

S.No.	Air flow rate LIT/HR. N.T.P.	ΔP across bed (cms of water)	ΔP across bed using stirrer (cms of water)	Power consumed by stirrer (watts)
1.	2180	6.0	5.6	39.20
2.	4160	13.4	11.8	39.20
3.	6170	24.8	20.9	39.00
4.	8150	37.3	27.0*	38.20
5.	10200**	43.4	27.00	38.20
6.	11200	44.6	24.40	37.60
7.	12200	45.2*	24.20	37.60
8.	16600**	35.6	24.10	37.40
9.	20000	30.0	24.50	36.60
10.	23700	26.6	25.20	36.40
11.	27700	26.8	26.00	36.40

* Pressure peak with and without stirrer

** Air flow rate for minimum fluidization with and without stirrer.

TABLE-20

Fluidisation Studies in Tapered Vessels

Run No. - 20 Cone angle = 45°

Material - Glass beads Weight of material = 2 Kg

Particle Size = 0.065 cm Speed of stirrer, n = 20 rpm

Depth of stirrer in the bed, h = 40 mm

Height of fixed bed, L = 115 mm

S. No.	Air flow rate LIT/HR. N.T.P.	ΔP across bed (cms of water)	ΔP across bed using stirrer (cms of water)	Power consumed by stirrer (watts)
1.	2180	5.6	5.4	39.20
2.	4160	12.4	11.8	39.00
3.	6170	21.0	20.8	39.00
4.	8150	30.0	29.8	38.40
5.	9180	35.0	31.5	37.80
6.	10200	37.5	31.6✧	37.80
7.	11200✧✧	39.2✧	29.2	36.80
8.	12200✧✧	37.1	24.3	35.40
9.	15000	33.0	19.8	35.20
10.	16600	29.7	19.6	34.80
11.	20000	25.6	19.7	34.60
12.	23700	21.3	20.0	34.60
13.	27700	21.4	20.2	34.60

✧ Pressure peak with and without stirrer

✧✧ Air flow rate for minimum fluidization with and without stirrer.

TABLE-21

Fluidization Studies in Tapered Vessels

Run No. - 21 Cone angle = 45°

Material - Glass-beads Weight of material = 2 Kg

Particle Size - 0.065 cm Speed of stirrer, n = 80 rpm

Depth of stirrer in the bed, h = 40 m.m.

Height of fixed bed, L = 115 m.m.

S. No.	Air flow rate LIT/HR. N.T.P.	ΔP across bed (cms of water	ΔP across bed using stirrer (cms of water)	Power consumed by stirrer (watts)
1.	2180	5.6	5.4	40.20
2.	4160	12.4	11.8	39.80
3.	6170	21.0	19.8	39.8
4.	8150	30.0	27.6*	39.60
5.	9180**	35.0	26.0	39.60
6.	10200	37.5	21.7	39.20
7.	11200	39.2**	20.5	39.00
8.	12200**	37.1	20.0	39.00
9.	15000	33.0	19.6	38.40
10.	16600	29.7	19.6	30.00
11.	20000	28.6	19.8	36.80
12.	23700	21.3	20.2	35.40
13.	27700	21.4	20.6	35.40

* Pressure peak with and without stirrer

** Air flow rate for minimum fluidization with and without stirrer.

TABLE-22

Fluidisation Studies in Tapered Vessels

Run No. = 2 Cone angle = 45^0

Material = Baryte Weight of material = 2 Kg

Particle Size = 0.065 cm Speed of stirrer, n = 20 rpm

Depth of stirrer in the bed, h = 70 m.m.

Height of fixed bed, L = 102 m.m.

S. No.	Air flow rate LIT/H.R N.T.P.	ΔP across bed (cms of water)	ΔP across bed using stirrer (cms of water	Power consumed by stirrer (watts)
1.	2180	6.0	5.7	38.00
2.	4160	13.4	12.0	37.80
3.	6170	24.8	22.3	37.60
4.	8150	37.3	30.8	37.40
5.	10200	43.4	33.0	37.20
6.	11200	44.6	33.10+	37.00
7.	12200++	45.2+	29.2	36.40
8.	16600++	35.6	25.0	35.20
9.	20000	30.0	24.0	35.00
10.	23700	26.6	25.4	34.80
11.	27700	26.8	26.0	34.80

+ Preassure peak with and without stirrer.

++ Air flow rate for minimum fluidisation with and without stirrer.

TABLE-23

Fluidisation Studies in Tapered Vessels

Run No. = 23 Cone angle = 45°

Material = Baryte Weight of material = 2 Kg

Particle Size = 0.065 cm Speed of stirrer, n = 80 rpm

Depth of stirrer in the bed, h = 40 m.m.

Height of fixed bed L = 102 m.m.

S. No.	Air flow rate LIT/HR. N.T.P.	Δ P across bed (cms of water)	Δ P across bed using stirrer (cms of water)	Power consumed by stirrer (watts)
1.	2180	6.0	5.7	39.80
2.	4160	13.4	12.0	39.60
3.	6170	24.8	20.20	39.40
4.	8150	37.3	27.80	39.40
5.	10200	43.4	28.20✧	39.20
6.	11200✧	44.6	26.60	39.20
7.	12200	45.2✧	25.30	39.20
8.	16600✧✧	35.6	24.6	38.40
9.	20000	30.0	24.8	38.20
10.	23700	26.6	25.3	37.60
11.	27700	26.8	26.2	37.60

✧ Pressure peak with and without stirrer

✧✧ Air flow rate for minimum fluidication with and without stirrer.

APPENDIX - II

```
C      MAIN PROGRAM FOR LEAST SQUARE  CURVE FITTING
C       M.E.THESIS  ASHOK KUMAR
C      PROGRAM WAS EXECUTED AT THE COMPUTER CENTRE AT SERC ROORKEE
       DIMENSIONA(15,15),X(15,100),XB(15),CO(15),Y(100),ER(100)
     2 READ1,N,M,IM
     1 FORMAT(3I5)
C
C      N IS NO. OF VARIABLES  M IS NO. OF DATA POINTS
C      IM =1 INDICATES RELATIONSHIP OF TYPE Y=A*(X**B)*(Z**C)
C      IM=2 RELATION IS Y=A+B*X+C*Z
C      READING OF DATA POINTS
C
     3 FORMAT(6E12.5)
       DO5 J=1,M
       READ3,(X(I,J),I=1,N)
     5 CONTINUE
C      IF  IM=1 GO TO 10 , IF IM=2 GO TO 20
       IF(IM-1)10,10,20
    10 DO15 I=1,N
       DO 15 J=1,M
    15 X(I,J)=LOGF(X(I,J))
    20 AM=M
       DO 50I=1,N
       SUM=0.0
       DO 40 J=1,M
       SUM=SUM+X(I,J)
    40 CONTINUE
       XB(I)=SUM/AM
    50 CONTINUE
       PUNCH 55
    55 FORMAT( 5X, 11HMEAN VALUES//)
       PUNCH 3,(XB(I),I=1,N)
       DO 60 I=1,N
       DO 60 J=I,M
    60 X(I,J)=X(I,J)-XB(I)
       N1=N-1
       DO 65 I=1,N1
       DO 65 K=I,N
       A(I,K) =0.0
       DO 65 J=1,M
       A(I,K) =A(I,K)+X(I,J)*X(K,J)
    65 CONTINUE
       DO 70 I=2,N1
       I1=I-1
       DO 70 J=1,I1
    70 A(I,J) =A(J,I)
       PUNCH 71
    71 FORMAT( 5X, 24HCOEFFICIENT OF EQUATIONS//)
       DO 80 I=1,N1
       PUNCH 3,(A(I,J),J=1,N)
    80 CONTINUE
       CALL SIMEQ(A,N1,CO)
       CO11 =XB(N)
       Do 82 K = 1, N1
```

```
      COI1 =COI1-CO(K)*XB(K)
   82 CONTINUE
      IF(IM-1)83,83,84
   83 COI =EXPF(COI1)
      GO TO 85
   85 PUNCH 86
   84 COI= COI1
   86 FORMAT (5X,22HCONSTANTS OF RELATION//)
      PUNCH 87 ,COI
   87 FORMAT (5X,2HA=,E12.5)
      PUNCH 88,(CO(K),K=1,N1)
   88 FORMAT (2X,5HB(I)=,6E12.5)
      DO 90 K=1,N
      DO 90 J=1,M
   90 X(K,J) =X(K,J)+XB(K)
      DO 100 J=1,M
      Y(J)=Y(J)+CO(K)*X(K,J)
  100 CONTINUE
      IF(IM-1)105,105,120
  105 DO 115 J=1,M
      DO 110 I=1,N
  110 X(I,J)=EXPF(X(I,J))
      Y(J)=EXPF(Y(J))
  115 CONTINUE
  120 DO 130 I=1,M
      ER(I) =(Y(I)-X(N,I))*100./X(N,I)
  130 CONTINUE
      PUNCH 131
  131 FORMAT (5X,12HFINAL RESULT//)
      PUNCH 132
  132 FORMAT( 40H****************************************,1H*,
     139H****************************************//)
      PUNCH 133
  133 FORMAT(4X,2HX1,10X,2HX2,10X,2HX3,10X,2HX4,10X,2HX5,10X,2HX6)
      PUNCH 132
      DO 140 J=1,M
      PUNCH3,(X(I,J),I=1,N),Y(J),ER(J)
  140 CONTINUE
      PUNCH 132
      GO TO 2
      STOP
      END
```

```
      SUBROUTINE SIMEQ(A,N,X)
      DIMENSION A(15,15),U1(15,15),U(15,15),X(15)
      M=N+1
      DO20IT=1,N
      JT=1
    1 IF(JT-1)3,3,2
    2 J=IT+1
      I=IT
      GO TO 4
    3 I=IT
      J=I^T
    4 U(I,J)=A(I,J)
      IF(IT-1)7,7,5
    5 M1=IT-1
      DO6K=1,M1
    6 U(I,J)=U(I,J)-U(I,K)*U(K,J)
    7 IF(JT-1)8,8,10
    8 I=I+1
      IF(I-N)4,4,9
    9 JT=2
      GO TO 1
   10 U(I,J)=U(I,J)/U(I,T)
      J=J+1
      IF(J-M)4,4,20
   20 CONTINUE
      DO30 I=1,N
      DO30 J=1,M
      IF(I-J)25,27,27
   25 U1(I,J)=U(I,J)
      GO TO 30
   27 U1(I,J)=0.0
   30 CONTINUE
      DO 35J=1,N
   35 X(J)=0.0
      N1=N
   40 I=N1
      X(I)=U1(I,M)
         DO45 J=1,N
   45 X(I)=X(I)-U1(I,J)*X(J)
      N1=N1-1
      IF(N1-1)47,40,40
   47 RETURN
      END
```

REFERENCES

1. Brotz, W., Chem. Engg. Tech, 24, 60 (1952).
2. Roman, G.H., Chem. and Ind. (Rev.), P. 46 (1955).
3. Levoy, R.P., et al, 'Fluid bed Conversion of UO_3 to UF_4' Chem. Eng. Progr, 56(3), 43-48 (1960).
4. MacMullin, R.B., and Weber, M., Trans. A.I.Ch.E.Jl, 31, 409 (1935).
5. Omae, T., and Furukawa, J.J. Chem. Soc Japan, Ind. Chem.Section, 56 (12), 824 (1953).
6. Romero, J.B., and Johanson, L.N., Chem. Eng. Progr Symp. Ser, 58 (38), (Oct 1962).
7. Sutherland, K.S., 'Solids Mixing Studies in the Gas Fluidized Beds Part I, A Preliminary Comparison of Tapered and Non-tapered Beds', Trans. Inst. Chem. Engrs., 39, 189-194 (1961).
8. Sutherland, K.S., and Rowe, P.N., Trans. Inst.Chem. Engrs., 42, 55 (1964).
9. Littman, H., 'Solids Mixing in Straight and Tapered Fluidized Beds', A.I.Ch.E.Jl., 10(6), 924-929 (1964).
10. Gel'perin, et al, Khim.i Tekhnol Topliv i Masel 5(8), 51-57 (1960).
11. Bacakov, A.P., Gel'perin, L.G., Inzh Fiz. Zh., 9(2), 217-222 (1965).
12. Farkas, E.J., and Koloini, T., 'Fixed Bed Pressure Drop and Liquid Fluidization in Tapered or Conical Vessels', Can. J. Chem. Eng., 51, 499-502 (1973).
13. Singh, R., 'M.E.Dissertation on Fluidization in Tapered Vessels (Air Solid System)', (1973).
14. Chandra, I., 'M.E.Dissertation on Liquid Fluidization in Tapered Vessels', (1974).
15. Sharma, D., 'M.E.Dissertation on Gas-Solid Fluidization in Tapered Vessels', (1974).

16. Coulson, J.M. and Richardson, J.F., 'Chem.Engg.', Pergamon Press, London, 2, 286, (1955).

17. Kunii, D., and Levenspiel, O., John Wiley and Sons, Inc., (1969).

18. Zabrodsky, S.S., 'Hydrodynamics and Heat Transfer in Fluidized Beds', M.I.T. Press (1966).